FENG YUNXUAN BACHELOR OF MECHANICAL ENGINEERING WITH HONOURS 2022

Effect of Opening Size for Building Natural Ventilation in Urban Airflow Environment

FENG YUNXUAN

FACULTY OF ENGINEERING, BUILT ENVIRONMENT

AND INFORMATION TECHNOLOGY

SEGI UNIVERSITY

2022

Effect of Opening Size for Building Natural Ventilation in Urban Airflow Environment

FENG YUNXUAN

A final year project report submitted in partial fulfilment

of the regulations for the award of Bachelor of Mechanical Engineering with honours at the SEGi University

2022

DECLARATION

I hereby declare that this report, submitted to SEGi University, Malaysia as a partial fulfilment of the requirements for the Bachelor of Mechanical Engineering has not been submitted as an exercise for a degree at any other university.

I also certify that the work described here is entirely my own except for excerpts and summaries whose sources are appropriately cited in the references. This report may be made available within the university library and may be photocopied or loaned to other libraries for the purposes of consultation.

5 December 2022 _____

FENG YUNXUAN

(EB8982109)

APPROVAL SHEET

This thesis entitled:

"Effect of Opening Size for Building Natural Ventilation in Urban Airflow Environment"

Submitted by: Feng YunXuan

FENG YUNXUAN (EB8982109)

In requirement for the degree of Bachelor of Mechanical Engineering, SEGi University, Malaysia has been accepted.

Supervisor:	**Ir. Dr. Moey Lip Kean**
Signature:	**_____**
Date:	**5 December 2022**

Module Leader:	**Ms. Phoon Sin Ye**
Signature:	**_____**
Date:	**5 December 2022**

Acknowledgements

Praise and thanks to God first and foremost whose blessing enabled me to accomplish this project.

I wish to express my deepest appreciation to my supervisor Ir. Dr. Moey Lip Kean for relentless guidance, helpful suggestion, close supervision and moral encouragement to complete this task. Lecturer's personal five-star rating is the limit of the rating system, but it is not the limit of Ir. Dr. Moey Lip Kean. With a good learning environment and professional faculty, I am extremely proud and honored to be studying at SEGi University.

A special thank to my parents, my parents provided strong guarantees for my schooling and life and established the correct direction of life for me. and thanks to all my lecturers the careful explanation and enthusiastic guidance effectively helped me solve the difficulties encountered in my study. Thanks to Fang Yanmin for her suggestions on the picture structure and writing ideas of the article. Talking with her has benefited me a lot.

My sincerely thanks to all those whom directly or indirectly help me to complete this project.

Abstract

Air circulation is closely related to quality of life. Good ventilation performance for building can effectively improve the indoor air quality without using electrical appliances. Natural ventilation not only saves power resources, but also improves indoor ventilation. This study uses CFD simulation to analyze the airflow under different building layout. This study includes (i) one building (ii) two buildings with opening for the front building, (iii) two buildings without opening for the front building (iv) nine buildings with opening around buildings (v) nine buildings without opening around buildings, with the building opening ratio of 4:1, 2:1, 1:1, 1:2, 1:4. ANSYS 2021 R2 was selected as the simulation software, and the standard k-ε (SKE) was selected for this study. From the simulation results, all building layout cases reflect a common feature: as the outlet opening area increases, the internal air velocity of the building becomes faster, while the air velocity at the outlet opening location slows down. Another aspect, as the building layout changes, the airflow inside the target building also changes. For the cases of two buildings, the air flows into the target building decreases and the age of air (AOA) becomes longer as compared to cases with one building. In the case of the same opening ratio, the overall ventilation rate for the target building around nine buildings is lower than that of one building, but better than that of target building for the two buildings. The reason for this phenomenon is due to the characteristics of the nine buildings arrangement, which has a relatively fast air velocity around the target building. The opening ratio of a building is therefore important for ventilation in an urban environment.

TABLE OF CONTENT

Chapter Page

LIST OF TABLES

TABLE **PAGE**

LIST OF FIGURES

FIGURE **TITLE** **PAGE**

LIST OF SYMBOLS

BES	Building Energy Simulation
ACE	Change effectiveness
V	Velocity
Cd	Drag coefficient
ACH	Air exchange rate
UTZ	Urban Terrain Zones
HCRs	Horizontal convective rolls
zi	The boundary-layer depth
L	The Monin–Obukhov length
K	Dimensionless concentration
2D-LDA	A two-component laser Doppler anemometer
LES	Large eddy simulation
Q	Volume flow rate
RH	Relative humidity
Sk- ε	Standard k- ε model
UCL	Urban canopy layers
AOA	Age-of-air
VR	Ventilation rate
SST k- ω	Shear-stress transport k- ω model
C	Flow coefficient
cp	Pressure coefficient
B/H	Aspect ratio
IAQ	Indoor air quality
μt	Turbulence viscosity
PIV	Particle Image Velocimetry
k	Turbulent kinetic energy
Sk- ε	Standard k- ε model
Rk- ε	Realizable k- ε model
RNG k- ε	Renormalization Group k- ε model
Sk- ω	Standard k- ω model
RLZ	realizable k − ε

RSM	Reynolds Stress Model
CFX	Ansys software
e	The relative error

LIST OF EQUATION

EQUATION **PAGE**

CHAPTER 1

INTRODUCTION

1.1 Background

From villages and towns to developed cities and then to world-famous super cities. The development of the city shows that people yearn for a more convenient and comfortable living environment. However, with the development of urbanization, the population is becoming more and more dense. The problem of urban ventilation is getting bigger and bigger. Air pollution is becoming more and more serious with the urban heat island effect. Epidemic diseases are also spread widely in cities. It is very important to improve urban ventilation (Bady et al. 2011).

1.2 Ventilation

The core of ventilation is air flow, and the efficiency of ventilation influences the air purity and living satisfaction of urban areas to some degree. The ventilation efficiency may be evaluated. In 1981, some researchers did numerous investigations on airflow performance and concluded that ventilation effectiveness may be estimated. The gradient of the tracer gas, the

proportion of concentrations, or the area under the curve may all be used to assess the airflow effectiveness of a specific region (Sandberg 1981).

Ventilation, as one of the major techniques of improving the living environment, can cause heat, humid air, or germs in the living environment to travel from one place to another. Clean air enters the room after effectively replacing with outdoor air, and the interior air is released from the room and naturally degraded by sunlight, plants, and so on, which can be transformed back into fresh air to accomplish effective and sustainable development.

1.3 Mechanical Ventilation

Mechanical ventilation is the method that replace the air in an open or closed space with ambient air by using equipment or modules to change the air flow in the environment. For example, air conditioners, fans, exhaust fan piping systems are devices that need to be driven by energy in order to move the air flow from original area and discharge to the other end. By using mechanical ventilation, energy consumption such as electricity is needed in order to achieve ventilation efficiency of the space in the area and the environment will be more comfortable (Livada et al. 2005).

1.4 Natural Ventilation

Natural ventilation happens when natural flow of air having air replacement between interior and exterior space under natural condition. Natural ventilation considers as a passive ventilation since the ventilation cannot be controlled but can be influenced. The factors that can influence the natural ventilation includes layout of the city, geographical location, temperature, air pressure and season. Effectively using natural ventilation can achieve a good ventilation without using any energy, thus improving the living quality of the occupants without any effort (Livada et al. 2005).

1.4.1 Single-sided Ventilation

Single-sided ventilation is mainly used in apartments, which mainly shows that there are one or more openings on the single plane inside the space. Single-sided ventilation will affect the air flow through vents with excessive air volume in a single wall, which will generate

pressure difference between indoor and outdoor. For example. Windows, doors and openings in single wall. Figure 1.1 shows that the air flow in a single-sided ventilation case (Allocca et al. 2003).

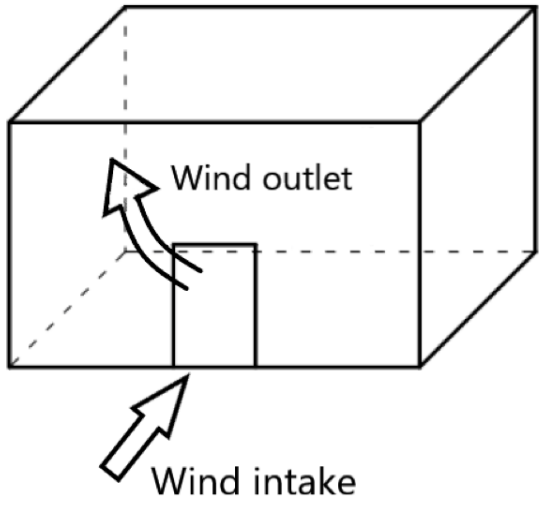

Figure 1.1: Working process of single-sided ventilation

1.4.2 Cross Ventilation

In the cross ventilation, the air flow in interior room is generated by the geometric wind that created by one or more openings of different facades. This is because the pressure difference between the openings will cause the air pass through the room, thus completing the air replacement between the room and the outdoors. Figure 1.2 shows that the air flow through cross ventilation (Stavrakakis et al. 2008).

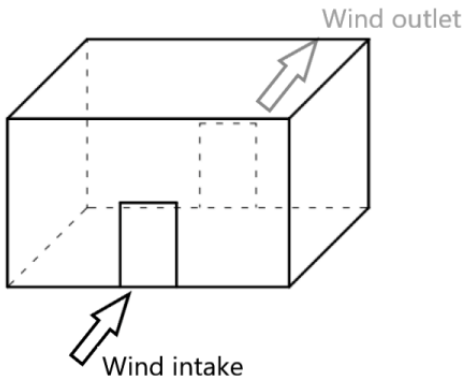

Figure 1.2: Working process of cross ventilation

1.4.3 Stack Ventilation

There are two openings in chimney ventilation, which the air flow through height difference. The air enters one of the openings, then the air is discharged from the another opening. Under natural conditions, the main factors affecting this ventilation are air density, pressure, and the difference between indoor and outdoor temperatures. (Hawendi & Gao 2016). Figure 1.3 shows the air flow through two openings in stack ventilation.

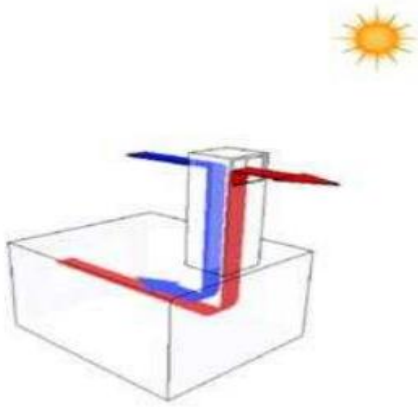

Figure 1.3: Working process of stack ventilation (Jomehzadeh et al. 2017).

1.5 Urban Airflow

A city refers to a human settlement dominated by non-agricultural activities and population. City has a large area, population, and high density when comparing with rural area. For example, city has residential areas, streets, hospitals, schools, office buildings, commercial stores, squares, parks and other public facilities. With the development of social economies and the acceleration of urbanization, cities have become one of the important spatial carriers, the air flows through these complex structures to form a special urban air flow state, which has both natural phenomena and artificial properties. For example, there are obvious differences between buildings; the temperature difference inside or outside the building is large, the height difference of houses is relatively small, and the road slope changes drastically. In modern urban construction, occupants have higher expectations toward living environment and living quality. Hence, study of rational planning of urban layout is a realistic and arduous task (Yazid et al. 2017).

Different structural characteristics of buildings will affect the state of air flow, such as triangular spire building roofs, circular arc curved building structures and flat roof building structures. In practical engineering, special wind tunnel tests were studied in order to influence of the wind environment on the movement of objects as the airflow around the building will form a very complex flow field composed of a three-dimensional turbulent vortex structure due to different building structures. The building structures were characterized by stagnation, separation, circulation, and instability (Song & He 1993).

Macroscopically, urban ventilation efficiency was inverted proportional to urban density. For example, the denser the city, the lower the efficiency of urban air circulation. The suburbs have a great a great ventilation efficiency when comparing to city as the urban density is relevantly less. As the central area of the city has a great influence on indoor thermal comfort, the higher building density or favorable enclosure structures need to be adopted in order to improve the thermal comfort of the city. The building layout, structure and science of urban planning works have a direct effect on the living environment of residents (Hang et al. 2013).

1.6 Opening Size

Indoor air in an urban residential environment will pass through opening size in order to improve air quality. The better the air quality, the better the health of residents. The air passes through the opening structure such as window, will form airflow without direct contact with the surrounding environment. The importance of designing and use this structure reasonably is to improve the air ventilation of buildings. The research was made pertain various openings and strips of the window that will affect the ventilation of the environment (Varela-Boydo et al. 2021).

In current urban buildings, windows are the openings that make the indoor space directly contact with outside air. The factor that influences the air flow includes the size ratio between openings and the ratio of opening size to room area. For example, open houses, that has a larger window has a lower wind resistance, which lead to a higher wind pressure coefficient, hence the air circulation increased. The benefit of installing opening in a open house can improve the indoor ventilation conditions and thermal environment, thus reducing air conditioning load, which is environmental friendly, save electricity and improve the energy utilization rate. Therefore, it is necessary to optimize the design of the window frame structure (Moey et al. 2021).

The combination of large opening size and small opening size can increase the ventilation rate and air flow efficiency of the building. For example, living space that use different types of window fans can improve the indoor air quality, which plays a key role in creating a comfortable indoor climate. Ventilation effects are closely related to windows, which will help to improve the indoor thermal environment in modern residential design. In practice, air flow performance can be improved by reducing the opening of doors, walls and shortening the opening distance.

1.7 Computational Fluid Dynamics

Computational fluid dynamics (CFD) is widely used in building ventilation, air flow changes in building, and urban physics. CFD is a very common and efficient software to carry out simulation calculations. For meshing resolution in CFD example, the higher the mesh resolution of the 3D modeling surface, the higher the mesh resolution, the more accurate the simulation results, but there will be a great computational pressure applied on the computer. Scholars from all sides can adjust the accuracy of computer simulation calculations according to experimental needs (Gousseau et al. 2011). CFD calculation can get results similar to those of traditional wind tunnel experiments at a lower cost when comparing to physically experiment (Ramponi & Blocken 2012).

The reason why it is difficult to be exactly the same is that the principle of CFD modeling and simulation calculation is that the whole air flow system is divided into many independent sub-individuals, and the mass equation, momentum equation, capacity conservation and other formulas are used to calculate each sub-individual to predict the velocity, quality and other states of air flow. In this case, some complex workpieces may not be simulated directly by traditional mathematical software, and the final results can only be obtained through physical experiments or human-computer interaction. But now, with the improvement of science and technology, more and more enterprises are beginning to use large-scale virtual prototype systems for product design and research and development. As a new information technology, simulation computing technology has been widely used (Ramponi & Blocken 2012).

1.8 Malaysia Standard

MS1525:2014 is the strategic standard of green building design in Malaysia. This set of guidelines covers architectural design, lighting, electricity, mechanical ventilation, and so on. MS1525:2014 proved that energy waste can be reduced without restricting the architectural design and occupant comfort, while maintaining the health and safety of the occupants and is encourage the use of renewable energy and green energy. This standard provides standards and guidance for the concept of energy-saving design, including the reference to prove the minimum standard of professional judgment. The standard also discusses various factors that affect the comfort of the room, including air temperature, average temperature, radiation temperature, humidity, clothing insulation, metabolic rate, air flow, and residents' preferences. These factors will be included in the evaluation process and take into account the actual situation (Department of standards Malaysia. 2014).

Good air effects give people a fresh feeling in a certain space by lowering their skin temperature. The greater the change in the speed and direction of air flow, the better the convection effect of air flow on skin. Similarly, a good outdoor environment can also promote blood circulation and eliminate fatigue. In addition, due to the difference in outdoor weather, the choice of air conditioning system and heat pump should be different according to specific scenes. For example, in summer, when the direct sunlight point is north or south, the flow rate of cooling water in air conditioning is much smaller than that in normal working conditions, resulting in higher energy consumption, but all these will increase indoor pollutant emissions (Hu et al. 2016).

1.9 12th Malaysia Plan

The 12th Malaysia Plan (12MP) is a document for drafting the five-year outlook from 2021 to 2025. The Ministry of Economy (2019) announced that the 12MP covers three development levels, namely, economic empowerment, environmentally sustainable development and social reconstruction. The strategy is based on six strategic priorities: (1) strengthening inclusiveness and building a fair society; (2) Improve the well-being of all people; (3) Accelerate the development of human capital in advanced countries; (4) Pursuing green growth to achieve sustainability and resilience; (5) Strengthening infrastructure to support economic expansion; And (6) redesign economic growth to achieve greater prosperity. The strategic plan is made to solve the current challenges (Mahadi et al. 2021).

The 12th Malaysia Plan (12MP) is consistent with the vision of common prosperity in 2030 (SPV2030) and the sustainable development goals of the United Nations (SDGs) in order to finally realize the foundation of economic power, environmental sustainability, and social improvement of social reconstruction.

Environmental protection provides an opportunity to promote the balanced development of economy and environment. The climate problem is one of the greatest threats facing mankind in the 21st century with the increasing world population, acceleration of industrialization and global carbon dioxide emissions are rising sharply. In the past few years, global warming has led to frequent extreme weather events and serious consequences. In order to cope with climate change, many countries have taken positive actions, such as reducing greenhouse gas emissions, limiting fossil energy consumption and improving energy efficiency. These measures have achieved certain results (Wang et al. 2020).

Therefore, sustainable development is important and scientific. Natural ventilation is very important for maintaining ecosystem health and protecting biodiversity. It can effectively improve indoor air quality and reduce pollution. Compared with mechanical ventilation, natural ventilation, as a passive ventilation method, can achieve good indoor air quality and reduce carbon dioxide emissions without consuming energy. Therefore, it is of great significance to achieve the goals of energy conservation, emission reduction and ecological environment protection. With the acceleration of urbanization and the improvement of people's living standards, the problem of urban air pollution has become increasingly prominent, and the traditional natural ventilation methods can no longer meet the current environmental needs, so we must seek new natural ventilation methods. This paper aims to introduce the research of natural ventilation strategy under the background of sustainable development.

1.10 Problem Statement

The use of mechanical ventilation equipment, such as an air conditioning system in the room, provides a comfortable environment for the occupants but will cause energy consumption and a large amount of greenhouse gas emissions. With the extensive use of air conditioners further increasing the greenhouse effect of the natural environment, the use of air conditioners will be further increased, forming a vicious circle, which will not only consume a lot of energy, but also bring great damage to the environment (Zhao et al. 2015). This is not conducive to the green and sustainable development of society. Today, with global carbon dioxide emissions increasing, it is of great significance to find other ways of indoor ventilation to reduce the frequency of indoor air-conditioning systems and even replace the use of mechanical equipment such as air-conditioning fans for the green growth of the economy. Natural ventilation, as a passive ventilation method, can improve indoor air quality and enhance living comfort by making full use of natural conditions without consuming any other energy or generating excess carbon emissions. So, natural ventilation is a great alternative to air conditioners, fans, and other mechanical ventilation systems.

Indoor natural ventilation. Previous study has analysed the influence of the size of the opening inlet and the size of the opening outlet on the airflow in the cross-ventilated room and found that the airflow is largely depends on the opening ratio. It is therefore important to consider the size of openings for better ventilation in a building (Moey et al. 2022).

When the air flows into the urban environment, the blocking of buildings in the urban will change the movement of the air. Literature found that the leeward vortex formed by the target building and airflow changes inside the building are different in an urban environment (Shirzadi et al, 2019). People's life is closely related to the urban environment. the structure and arrangement of the city has a certain degree of influence on the airflow flow into the interior of the building. However, to the knowledge of the author, there is no study from the literature that analyze the natural ventilation in buildings with opening size in the urban environment. Therefore, understanding the flow of air in the urban environment is important for analyzing the airflow inside the building for better ventilation performance.

1.11 Objective

1. To validate the simulation results with the reference model by van Hooff et al (2017).
2. To investigate the changes in airflow pattern in a building for urban airflow based on various opening sizes.
3. To investigate the effect of opening configurations on the internal velocity, pressure coefficient, age of air and air ventilation rate within a building.

1.12 Scope of Study

In this study, two openings are considered on both windward and leeward side of the building. Few parameters were kept constant throughout the study in order to evaluate the airflow in urban environment.

1. Building model used for simulation is based on the reference of the study by van Hoofs (van Hooff et al. 2017). The model had the dimension of 0.16 m height, 0.2 m width and length equipped with two openings at opposing walls with dimension of 0.036 m height and 0.092 m length (van Hooff et al. 2017).
2. The building model walls had a thickness of 3mm (van Hooff et al. 2017).
3. Incoming wind angle was set to be 0^o (van Hooff et al. 2017).

CHAPTER 2

LITERATURE REVIEW

2.1 Background

In this chapter, the existing relevant literature was reviewed, and the findings from the literature were summarized at the end of each subsection. The single-sided ventilation, cross ventilation, urban airflow, wind tunnel experiment, computational fluid dynamics were discussed. At last, the "gap identified" table of the literature on urban ventilation was presented.

2.2 Single-sided Ventilation

Single-sided ventilation, as a ventilation system, its opening only appears on the single facade of the wall of a building or structure. The flow reason of air flow in unilateral ventilation mainly depends on buoyancy and pressure (Daish et al. 2016). Buoyancy effect mainly involves density difference caused by temperature difference between air layers, while pressure factors are mainly reflected in wind effect, such as fluctuation and incident angle. Additionally, there are two types of airflow on one side: single opening and numerous openings. In the research of Daish et al, it is found that the ventilation performance is better when there are two or more openings for air exchange than when the air exchange occurs at the same opening.

In 1995, There are researchers tested 52 kinds of single-sided natural ventilation configurations in full-scale buildings of Institute of Meteorology and Atmospheric Environmental Physics (IMPAE) to study the airflow field of buildings and repeated 49 experiments to obtain more accurate results. Then, the measured data are compared with the predicted results of six different network ventilation models, and some suggestions for improving the modeling process of single-sided natural ventilation experimental configuration are put forward. Not only that, Dascalaki proposed a correction factor considering the inertia force will affect the total air volume inside the building, which will enhance the network model's ability to forecast airflow on single-sided ventilation (Dascalaki et al. 1995).

In 2003, Jiang & Chen proposed a new empirical model to calculate and analyze the ventilation volume driven by unidirectional wind. The indoor and outdoor air flow characteristics and ventilation rate were measured in detail. The computational modelling of the air flow field at different wind speeds in the laboratory is carried out, and the results are compared with those of wind tunnel experiments and other related research results. The LES turbulence model, RANS model, standard K-ε model and large eddy simulation are used to analyze the ventilation air flow of indoor unilateral ventilation. It is found that the low-frequency area contains natural air flow, and the high-frequency area contains mechanical ventilation. In this kind of natural ventilation driven by unilateral buoyancy, the average flow field plays an important role. This is why the average air exchange rate is almost the same as the average instantaneous air exchange rate (Jiang & Chen 2003).

Cho et al proved in research that properly changing the window area and partition/position can improve the ventilation efficiency of single-sided ventilation, while properly changing the conditions of building structure can promote the natural ventilation efficiency of single-sided ventilation. Eight hundred airflow statistics was used. Finally, through the network air flow simulation method, these data are obtained by changing the unit position, adjusting the height, and adjusting the window area. This study is about one-way ventilation, considering single or multiple openings on a single surface. There are five options for wind tunnel simulation based on cfd. Compared with the simulation results of network ventilation, it is found that the natural ventilation efficiency of unilateral ventilation is lower than that of cross ventilation. From the results of indoor air velocity distribution, the case of dividing the window into two smaller windows and placing them on one side has better ventilation efficiency than the case of placing a larger single window on one side (Cho et al. 2012).

In recent years, due to cross ventilation has a higher air exchange rate than single-sided ventilation, so cross ventilation is often more popular. However, in most cases, due to internal partitions, obstacles and thickness, few buildings can achieve cross ventilation. Therefore, unilateral ventilation is still of great significance in architectural design (Wang & Chen 2012).

2.3 Cross Ventilation

Cross ventilation has been studied since the beginning of the 20th century, and it exists as a form of natural ventilation. In the middle of the 20th century, people studied and developed other methods to replace mechanical ventilation, considering environmental pollution, greenhouse effect and oil consumption. Naturally, passive ventilation became a reliable way to implement this idea, and its advantages were recognized and developed rapidly. The most effective mode to drive natural ventilation by wind is horizontal cross ventilation (Zhang et al. 2022). The external opening and internal layout will have a great influence on cross ventilation. The ideal opening position and internal structure will not only effectively improve the ventilation efficiency of cross ventilation, but also effectively reduce the air pollution and internal temperature in the building and improve the living comfort of the occupants (Fan et al. 2022).

With further study of the effects of natural cross-ventilation, a more accurate description of flow characteristics was obtained using the RANS equation turbulence model based on previous methods (Endo et al. 2006; Hu et al. 2005). Comparing the results of simplified models with experimental analyses shows good agreement, but only if the turbulence model selected is suitable for boundary conditions and grid resolution levels. Additionally, these approaches fall short if focused in analytical explanations of variable velocities. So, in 2008 Hu et al, used the LES method in research experiments to study the velocity of wind-induced fluctuations, whose CFD code can generate time-dependent and unstable inflows. Two experimental cases were presented: perpendicular to the opening (case 1) and parallel to the opening (case 2). Based on the flow observed during the experiment, case 1 was stable flow and case 2 was unstable flow. The outcome of the experiment demonstrates that the flow pattern surrounding the structure has a substantial impact on the ventilation rate. Because of wind disturbance and boundary layers instability in the airflow division zone, the ventilation air close to the opening is unstable when the wind direction is perpendicular to the building (instance 1). The energy stored in the upstream air flow has been exhausted by the splitting of

the near air flow at the front edge of the building sidewall for wind directions parallel to the building (instance 2). As a result, energy is transferred to smaller vortices, which are more frequent and unstable, and which become the primary factor in air exchange. Last but not least, the outcome of (instance 2) demonstrates that the deviation of changing ventilation rate is significantly higher than the average air flow speed (Hu et al. 2008).

Advances in measurement techniques and stability have led to better studies of cross-ventilation in real-world buildings. Ramponi & Blocken conducted a detailed review of cross-ventilation literature in 2012, Ramponi and Blocken proposed a series of coupled 3D stable RANS simulations, mainly for the research of commonly used independent buildings. The purpose is to help improve the accuracy, reliability, and evaluation of coupled CFD simulation for cross ventilation evaluation. (Ramponi and Blocken 2012) However, in practice, this study is suitable for idealized case reference, in which two opposite open openings are used less in actual architectural design considering the influence of more complicated factors. For this reason, Bangalee conducted cross ventilation research on three full-scale buildings with different open positions in 2014. With the help of computational fluid dynamics (CFD), each case is analyzed and calculated. Through the comparative analysis of experimental results, it is found that the ventilation angle, the number and location of windows will all affect the ventilation rate in the structure. This is a more comprehensive analysis of cross ventilation and provides a strong contribution for follow-up research (Bangalee et al. 2014).

In Karava research examines and presents experimental data on the porosity, intake to output proportion, opening position, and occlusion of large facade openings on opposing or neighbouring walls. To increase the experiment's precision, data from a number of internal pressure suction nozzles are used throughout. The average and maximum values of internal pressure are found to be significantly influenced by the internal ventilation pattern, although the effect on structures with walls that are more porous than 10% and walls that have openings is quite uneven. For designs with wall porosity of greater than 10% and openings on adjacent walls, values and peaks have a significant but non-uniform effect. (1) Exceeded ASCE 7–10 recommendations for internal pressure coefficient peaks. Wind tunnel testing is simply one aspect of ASCE 49, which primarily addresses wind tunnel testing. (Simiu et al. 2013) applies to all configurations with entrances above the middle height of the building, particularly the ratio of entrances to exits equals one configuration, and (2) Structures with huge open positions through which air flows internally are highly likely to open during air flow, such as factory structures with transport entrances, for which recommended design values are given, setups

with open positions above the middle height of the building, leeward. Future updates of the standard should include variables that describe the wind-induced internal pressure of a structure, such as walls porous, entrance positioning, inlet/exit proportion, and internal blockage (Karava & Stathopoulos 2012).

According to earlier study, "the entrance dimension is vital to the airflow of buildings because different entrance dimensions affect the structure's airflow. As a result, a highly thorough research on the impact of various opening widths on cross airflow was carried out in year 2021. To investigate the impact of the entrance dimension of a natural airflow structure design on the features of internal airflow, Moey et al. in 2021 conducted this investigation. The constant RANS equation was simulated numerically throughout the experiment. There are six alternative aperture ratios: 4: 1, 2: 1, 1: 1, 1: 2, 4: 9, and 1: 4. The outcomes of the grid independence research and model validation are also in line with earlier investigations. The outcomes of the simulation demonstrate a strong correlation between the pumping rate and the velocity, pressure, and ventilation of indoor air as well as the pressure coefficient. Additionally, the velocity and pressure distribution graphic demonstrate that the building's internal velocity and pressure decrease as the aperture decreases. Additionally, the pressure factor and airflow rates will rise with a decrease in opening rate. Additionally, the ventilation percentage of the openings of 4: 1 and 2: 1, 2: 1 and 1: 1, and 1: 1 and 1: 2 is higher than that of 1: 2 and 4: 9, 4: 9, and 1: 4. It has been discovered that using a combination of a large exit and a tiny entry can increase the ventilation of buildings. (Moey et al. 2021).

The computational simulations depending on the three-dimensional stable RANS equations was then finished in March 2022. This study examined the ventilation performance of five alternative opening ratios for the inlet and outlet, namely, 1: 4, 1: 2, 1: 1, 2: 1, and 9: 4, which are more intuitive. The outcomes of the grid independence study and models confirmation are in line with those of the earlier studies. On the basis of velocity vector, velocity and pressure, pressure drop, and air flow, the simulated conclusions of this research are further explored. The findings unequivocally demonstrate that the aperture proportion has a significant impact on the velocity vector, velocity and pressure, pressure drop, and airflow. The experiment revealed that the air in the building model will circulate at the top and bottom of the airflow when it goes through. Additionally, the relationship between pressure and velocity demonstrates that the pressure in the building model will decrease when the room opening ratio decreases and air flow velocity increases. In terms of pressure drop amplitude, the findings indicate that the pressure drop amplitude increases with decreasing room structure

aperture proportion. Additionally, the air flow in the room improves when the entrance proportion is lower than 1, but it starts to decline when the opening ratio is larger than 1. As a result, the change in inlet size ratio is one of the key elements affecting ventilation rate performance.

Zhang et al. A study conducted in 2022 looked more closely at the connection between cross airflow and structure interiors. In this study, we looked into the impact of apertures on the general four-wall space's cross airflow. The participating buildings had one to four external openings of various sizes, and computational fluid dynamics (CFD) modelling was used in the study. Additionally, different arrangements of vertical and horizontal walls are made in that research object, and the inside of the room's blocking rate is changed from 5% to 20%. Experiments have shown that the building's double-hole structure is particularly good for cross ventilation. The airflow rate of the double openings of the single opening scheme in a building is typically half that of the opening scheme, assuming that all of the openings are roughly the same size. In comparison to three or four openings, using wide open positions on the windward or leeward side of structures can improve the internal air exchange rate and speed of air flow. The air flow is always lower than it would be without an inside wall because it raises the internal blockage rate. The ventilation rate and the interior obstruction rate are inversely related. The loss of ventilation efficiency can be minimised by positioning the horizontal walls above the height of the opening and using multiple small inside walls instead of wide vertical walls in the room (Zhang et al. 2022).

2.4 Urban Airflow

With the improvement of people's living quality, cities are developing faster and more densely, air pollution in urban areas has caused serious damage to urban environment, quality of life and physical and mental health of urban residents (Hachem et al. 2019). According to the theory of aerodynamics, airflow movement is a complex process formed by the dynamic action caused by the mutual contact and energy exchange between components in the atmosphere. In this flow process, there are various interactions among the constituent gases. The research on vehicle exhaust pollutants and urban street canyon ventilation shows that good urban and architectural design can improve the air circulation of urban canopy, thus reducing air pollution and urban heat island intensity (He et al. 2020).

In order to express the interaction and influence of many components in the city, Cionco and ellefsen used structure, plants, detail elements, and changing terrain in 1998. They also added a local high-resolution wind field and temperature field into the analytic approach. It is suggested that high-resolution morphological databases combined with modelling and simulation processes can give crucial input data for the study and evaluation of connected urban applications and challenges after the comparison and investigation of multi-party data. Additionally, it can be utilised in urban planning and other areas (Cionco & Ellefsen 1998).

In the experiment, the formation of horizontal convection rolls (HCRs) in urban areas was studied by observation and fine-scale numerical simulation. The experiment was conducted around noon in Beijing. From the observation of Fengyun-2C satellite images, we can see that the direction of air flow is the wind parallel to the average boundary layer (a manifestation of HCRs). The vertical velocity and horizontal wind field were observed in the urban airflow, which indicates that there are alternating updrafts and downdrafts in the boundary layer, and the updrafts and downdrafts have observable lengths. Through analysis and comparison, it is found that the alternating time of updraft and downdraft is about 30 minutes, and the length of downdraft and updraft is about 9 kilometers (Miao & Chen 2008).

Finally, through the analysis of numerical simulation, it is found that most HCR occurs in urban areas, and the zi/l is less than 25. Through the sensitivity test, it is found that the urban space is dense, so HCR is very common in the urban boundary layer, while the open terrain in rural areas is more common with round cellular convection air. The landscape of the city and the details of the city have no significant influence on the aspect ratio of HCR diffusion in the city (Miao & Chen 2008).

In the tests of Huang et al., the air flow in a canyon similar to this one, made up of urban streets and high-rise structures, was evaluated using a thorough understanding of the relationship between air flow and urban structure. A two-dimensional computational fluid dynamics (CFD) model was created using the FLUENT programme prior to the experiment. This CFD simulation was tested in a wind tunnel and used to assess the circulation of air in a canyon made up of different buildings as well as the dispersion of air contaminants. The outcomes demonstrate that the model has high computation accuracy, quick analysis speed, and good outcomes. Following the development of the method, a total of 16 unique wedge roofs were simulated in accordance with the air flow and contaminant dispersion in urban street canyons. Finally, it can be deduced from the experiment that the wedge roof's form has an

impact on the canyon's vortex dynamics and pollution distribution. (1) The wedge-shaped roof is located on top of the canyon, and its peak height determines the structure of the vortex in downwind conditions; (2) When the wedge roof is positioned against the wind, the roof will separate the airflow, and its downstream corner height determines the vortex in the canyon; (3) When the front of the wedge-shaped roof is downwind, its upstream corner altitude determines the state of the air flow in the canyon. (4) The pollution level of the entire air circulation travelling below the canyon is significantly greater than that of the urban canyon air flow with "flat trend" and "upward trend" for different pollutant diffusion characteristics (Huang et al. 2009).

Wen et al in 2017, considered the influence of the structure and the air flow behavior around the building for the ideal street canyon. During the experiment, according to the height of the building, the width of the canyon, and the height and width of the independent building, 17 numerical simulation models with arcade or semi-open street roofs were designed and compared with the wind tunnel experimental data of (Brown et al 2001). The accuracy of CFD simulation was verified, and it was found that the adoption of arcade structure increased the hourly air exchange rate (ACH) of buildings without arcade design by 60%, and the existence of Urban canopy layers (UCL) had little effect on ACH. By comparing the building height, canyon width, wind tunnel test results, numerical simulation results of individual buildings, can be found that the stable wind environment around the building can be effectively implemented through the arcade design, and the air flow rate in the urban street canyon area can be increased (Wen et al. 2017).

T The wind flow pattern surrounding urban buildings always affects the internal and outdoor air circulation, which has a substantial impact on living comfort and air quality, according to extensive research of urban ventilation. However, as the population increases, the density of the city's façade and the design of its buildings also increase. Pasdarshahri & Hadavi, Such questions have objective responses in 2020, along with justifications and analyses. Based on the experimental data verification and simulation results, the K-omega SST turbulence model is presented to simulate the outside airflow. CFD was used during the experiment to experimentally compute the permeability of the ground floor residential buildings. The parallel and vertical wind circulation in street canyons is simulated using four common urban patterns and three densities of urban design areas. The analysis of the entire urban layout system's data indicates that when the density of urban buildings rises, the negative pressure gradient will do

likewise. Additionally, the leaking rates is essentially unrelated to the air flow speed if the leakage area is parallel to the main air flow (Song et al. 2018).

The wind flow pattern surrounding urban buildings always affects the internal and outdoor air circulation, which has a substantial impact on living comfort and air quality, according to extensive research of urban ventilation. However, as the population increases, the density of the city's façade and the design of its buildings also increase. Pasdarshahri & Hadavi, Such questions have objective responses in 2020, along with justifications and analyses. Based on the experimental data verification and simulation results, the K-omega SST turbulence model is presented to simulate the outside airflow. CFD was used during the experiment to experimentally compute the permeability of the ground floor residential buildings. The parallel and vertical wind circulation in street canyons is simulated using four common urban patterns and three densities of urban design areas. The analysis of the entire urban layout system's data indicates that when the density of urban buildings rises, the negative pressure gradient will do likewise. Additionally, the leaking rates is essentially unrelated to the air flow speed if the leakage area is parallel to the main air flow (Hadavi et al. 2020).

In the 2020s, Shirzadi et al studied and introduced the The outcome of the trial of cross airflow of moderate buildings in high-density cities. During the experiment, models with different structures representing high-density urban areas and different angles of air flow were selected to enter the model. By using a smoke generator to generate a certain amount of smoke, the change of airflow in the research process can be visualized, allowing researchers to study the characteristics of ventilation patterns in and around cross-ventilation structures. During the experiment, the distribution of wind pressure coefficient on the windward surface and leeward surface of the target building was measured, and the pressure suction system was used to participate in the measurement process. In addition, the velocity of air flowing through the building opening was measured by the tracer gas method. The outcome of the trial shows that the mechanism of cross ventilation in the layout of medium-density and high-density buildings is obviously different. The leeward vortex formed by the target and downstream buildings can be observed by visible smoke. Through observation, it is found that the leeward vortex has a highly transient, transparent leeward jet.

This research is accompanied by another new discovery. Cross-ventilation happens very briefly in urban regions with a dense population and the indoor and outdoor air exchange rates are frequently and suddenly increased through windward and leeward openings. That is to say,

indoor and outdoor air has the characteristics of periodic fresh air intake under these conditions (Shirzadi et al. 2020).

Surrounding conditions are also important for cross-ventilation in buildings, especially in high-density urban areas. Some scholars in a 2021 study. Mirzaei & Tominaga. Large eddy simulation method is used to study this situation, and computational fluid dynamics (CFD) model is used to study cross ventilation in high-density urban configuration. In the experiment, the general building model was densely installed by nine identical building models, and the turbulence statistics, wind pressure changes and air flow velocity of different plane area ratios and wind from different angles were compared. Based on different air flow definitions of time average and fluctuating velocity decomposition, the research conclusion considers the transient air flow velocity in air flow.In the crowded urban structure where the overall airflow velocity is poor but the direction and angle of the airflow fluctuate substantially, it is discovered that there are obvious disparities between the instantaneous average velocity and the instantaneous airflow velocity. The research's findings also indicate that it is not possible to forecast the cross ventilation of covered buildings in medium- and high-density urban structures using the calculation of air velocity per unit time. This is so that the air flow variation caused by the opening's opening and the periodic air flow can be balanced by the averaging process. Additionally, because they take into account instantaneous airflow exchange, using the cumulative instantaneous ventilation rate when calculating ventilation rate is preferable (Shirzadi et al. 2021).

Table 2.1 : Review of research on urban airflow.

Author (Year)	Modelling approach	Findings	Parameters
(Sandberg 1981)	Tracer gas	The definition of ventilation efficiency can be based on the slope of trace gas curve, the ratio between concentrations or the area under the curve.	VR
(Song & He 1993)	Smagorinsky's subgrid-scale turbulent model.	On the present basis, the large-scale vortex structure of turbulent shear flow around high-rise buildings is analyzed.	V, (*Cr and Cd)*

(Cionco & Ellefsen 1998)	High-resolution simulation of local wind field and temperature field	Using detailed morphological data to simulate high-resolution wind and temperature inside and outside the urban area, other obstacles can be defined and quantified to improve airflow ventilation and similar processes.	UTZ
(Chang & Meroney 2003)	LES	The diffusion of gas in the urban environment is basically unstable, and it is not always possible to predict them well by using the steady-state prediction method.	(B/H), K
(Miao & Chen 2008)	Fengyun -2C satellite image	Finally, through numerical simulation analysis, it is found that most HCRs occurs in urban areas, while the open terrain in rural areas often sees circular convective air.	V，zi/L
(Huang et al. 2009)	PHOENICS code	The velocity field and concentration contour obtained from the experiment show that the vortex dynamics and pollutant distribution in the canyon are closely related to the wedge roof configuration.	*K, RH, Q*
(Hang et al. 2013)	Sk- ε	A larger city size includes a larger UCL volume, and it takes longer to ventilate.	ACH, AOA
(Wen et al. 2017)	RANS, Sk-ε	The results show that the arcade design can effectively maintain a stable wind environment and improve the flow aeration in urban street canyons.	VR, Q, ACH,
(Shirzadi et al. 2018)	Sk- ε and k-ω SST	The cross-ventilation performance of highly congested urban areas with buildings arranged in regular and staggered sequences of different urban densities is studied using a stable RANS model. A series of new closure coefficients were found at urban densities between 0.25-0.4. The calculation	C_p, V

		accuracy can be effectively improved by setting these closure coefficients in the calculation module.	
(Shirzadi et al. 2020)	Tracer gas	The leeward vortex formed by the sample and the downstream buildings can be observed by visible smoke, and the cross ventilation mechanism in the layout of medium-density buildings and high-density buildings is obviously different.	Q, c_p
(Hadavi & Pasdarshahr 2020)	SST k- ω model	The analysis results of the whole urban layout system show that the negative pressure gradient will increase with the increase of the density of urban buildings.In addition, if the leakage area is parallel to the main air flow, the leakage rate has almost nothing to do with the flow speed of air flow	Q, C, c_p
(He et al. 2020)	RANS, Sk-ε	Shallow streets experience better indoor and outdoor ventilation. In deep canyons, ACH becomes smaller. Smaller window size reduces indoor ACH but hardly affects outdoor ventilation.	ACH
(Shirzadi & Tominaga 2022)	Sk- ε， RLZ, k-ω SST, RNG k-ε and LES	A simulation study was carried out using the steady-state Reynolds-averaged Navier-Stokes equation (RANS) model and large eddy simulation (LES), and the simulation results were compared with the measurement results obtained from wind tunnel experiments. In urban environments, the performance of both LES and RANS degrades, indicating the complexity of predicting flow around tall buildings through simulation.	V, k

Building Energy Simulation(BES), Change effectiveness(ACE), Velocity(V), Drag coefficient(Cd), Air exchange rate (ACH), Urban Terrain Zones (UTZ), Horizontal convective rolls (HCRs), The boundary-layer depth (zi), The Monin–Obukhov length(L), Dimensionless concentration (K), A two-component laser Doppler anemometer (2D-LDA), Large eddy simulation (LES), Volume flow rate (Q), Relative humidity(RH), Standard k- ε model(Sk- ε), Urban canopy layers (UCL), Age-of-air (AoA), Ventilation rate(VR), Shear-stress transport k- ω model (SST k- ω), Flow coefficient (C), Pressure coefficient (cp), Aspect ratio (B/H), Indoor air quality (IAQ) Turbulent kinetic energy (k).

2.5 Wind Tunnel Experiment

Wind tunnel is a kind of experimental equipment that can produce artificial controlled airflow in the pipe. Wind tunnels work in a similar way to various aerodynamic experiments and are commonly used to study interactions between spacecraft and aerodynamics (Hongshan, et al. 2015).

Wind tunnel test is based on the principle of kinematics similarity, the subject (aircraft, large buildings, structures, etc.) is modeled or placed directly in a wind tunnel pipe. By means of a drive device, the wind tunnel produces an artificial, controllable air flow, simulates the behavior of the subject under the action of air flow, and then obtains relevant parameters to determine the stability and safety of the subject (Moonen et al. 2007). The first experiments to determine wind power were carried out by John Smeaton in the 18th century, and his theoretical basis was used until the 20th century. Wind tunnel theory was first developed in the 1890s to study the lift and drag of aircraft. Wind tunnels have been in existence since the late 1800s, creating favorable test conditions for wind effects research. By the mid-1960s, British engineer Alan Davenport began studying the effects of wind on buildings (Addis 2020).

As the study progresses in 2009 (Heist et al. 2009) people will be directly affected by the airflow caused by road structures when they walk or are exposed to road, highway, and other environments. There have been many previous wind tunnel studies of urban street canyons and air-flow junctions (Hayden et al. 2002; Kastner-Klein & Plate 1999) but these studies have been vague in their consideration of road configurations and surrounding structures, Considering (Zhu et al. 2002) that the downwind direction of the road is inversely proportional

to the concentration of traffic-related pollutants with the acceleration of air flow speed, and the decrease rate of pollution concentration will be significantly different due to the change of road structure.

Therefore, different road configurations are considered, including concave roads leading to the surrounding terrain, roadside devices, and convex roads with a relative height higher than the terrain. The influence of vertical wind and parallel wind on pollutant diffusion is studied. According to the conditions of the system composition, the wind tunnel simulation experiment was carried out with 12 different configurations to study the diffusion flow field and concentration distribution of simulated vehicle emissions on the six-lane highway. Compared with the flat and barrier-free roads, all the configurations examined here are characterized by low concentration in the downwind and near the ground; However, the specific degree of reduction varies from case to case.

In this study, the case of considering the ground concentration data of each shows that a constant shear rate can be used downwind of any initial disturbance caused by road configuration (for example, the area behind road obstacles with multiple cycles), and at least extend to the end point measured in the experiment. For a single road obstacle on the downwind side of the road, this area extends from about 4 barrier obstacle heights to 40 barrier obstacle heights on the downwind side of the road. The concept of virtual origin used in the experiment is also considered to be helpful to describe the initial air flow mixing caused by the specific road configuration. To effectively express the influence of simulated road configuration on dispersion, the combination of virtual origin and time segment analysis may be an effective scheme to improve the experimental accuracy. The specific road configuration seems to determine the size of the virtual origin offset. These results show that considering the road configuration in the system during the experiment is beneficial to improve the simulation results of verifying the air quality of simulated urban roads (Heist et al.2009).

With the increasing density of big cities, more and more people live in them, and the utilization rate of air-conditioned and vehicles is increasing, the diffusion of air pollutants has become a problem. Liu et al. Investigated the diffusion of indoor air pollutants and possible cross-regional pollution, and the survey object was mainly the design of typical high-rise residential buildings in Hong Kong. During the experiment, the model with the target building of 1: 30 scale was tested in the boundary layer wind tunnel. In the experiment, the indoor air flow from three different floors was simulated. Through the detector, the gas concentration of

the adjacent wall and the opposite wall is continuously measured, and the pressure distribution of the facade inside the room during typical air intake is measured and determined. The risk of cross-contamination of air in both directions was assessed by analysing the pressure and concentration distribution. Experimental results show that in so-called reentry spaces, pollutants can be dispersed in two vertical directions, not only upward, as detected by buoyancy, but also downwards. In addition, horizontal direction may also be dispersed, indicating the potential for cross-contamination of flats adjacent to the horizontal level. The study of this natural phenomenon can not only be used to control the spread of bacteria and viruses, but also be of great significance to indoor airflow and living comfort. Through a lot of literature review and comparison, I quite agree with this point: in the long run, the development of calculation tools depends on wind tunnel test data, both of which contribute to building design and regional planning (Liu et al. 2010).

The tenants of buildings, as well as other living things in nature, benefit from improved indoor air quality. In order to successfully design the passive airflow of the building structure and maintain the aim of sustainable development, the problem must be solved. In 2013, Tecle et al. performed a wind turbine simulation on the natural airflow layout of a shorter building, modelling the structure at a scale of 1: 20. A single wall's air flow status in relation to a side wall and adjacent side walls with various-sized holes was evaluated during the experiment. Additionally, it takes into account the conditions of air flow inside the space with and without a dividing wall, with and without an open barrier, and under 36 different air input angles. According to the experimental findings, it is crucial to increase the detection precision by adjusting the interior volume by altering the speed scaling. This standard can also be used to correctly regulate the cross ventilation of openings with relative elevations in the opposite rooms. The pressure drop in the room increases with decreasing the opening proportion, or the ratio of outflow to input, according to an analysis of the experimental results. The pressure drop of the opening in the wall will be greater than the pressure drop of the opening in the neighbouring wall for the same inlet-outlet ratio. Room partition has a significant impact on the internal pressure distribution range, therefore each room's ventilation benefits from well-designed room partition (Tecle et al. 2013).

The total flow coefficient and ventilation rate decrease with the decrease of the opening rate in the room. The inlet emission coefficient obtained in this test ranges from 0.65 to 1.08, and the results are similar to those of various early studies. (Sharma RN 2007; Sharma & Richards 2005; Wong & Loke 2001).

The cross ventilation generated by the large opening of the building is formed by the interaction between the external airflow around the building and the airflow flowing inside the building. The movement of the cross-ventilation airflow is three-dimensional, unstable and diverse. Tominaga and Blocken in 2015, this natural phenomenon was analyzed experimentally, and the changes of airflow velocity and pollutant concentration in a fixed area were measured and studied. Firstly, the basic characteristics of the concentration field and airflow velocity in the ventilation airflow in the unobstructed building interior are determined. Then, the flux distribution law of turbulent scalar in the ventilation air flow in the region is measured effectively, and the transfer principle of turbulent scalar in the ventilation air flow inside the room is analyzed. Finally, the flow of cross ventilation around buildings is studied. The results show that different environmental conditions will produce different turbulence velocity fluctuations and concentration fluctuations, and the wind speed of sheltered buildings is 70% lower than that of buildings without shelter. The experimental results can be used to compile the CFD method verification database, and the CFD methods of ventilation flow field and concentration field can be effectively verified by the results of this study (Tominaga et al. 2015).

The detailed experimental data of cross ventilation was determined by using wind tunnel experimental technology, and the experiment of recording the characteristics of gas flow and dispersion was completed by Tominaga and Blocken in May 2016. Five isolated single-zone building structures with different opening positions were used in this experiment. Ethylene (C2H4) with a density similar to that of air was used as a tracer gas to perform visualization of air flow. By comparing and observing the processes of highly transient flow and divergence of the experimental airflow in time segments, it is found that the spurting jet is dominated by obvious Kelvin-Helmholtz instability in the experimental process. With the experiment, the movement changes of the average concentration field, concentration fluctuation field, average velocity field, and turbulence kinetic energy field are presented and analyzed. Finally, the total time of instantaneous concentration change in buildings is summarized. According to the whole experiment, it is concluded that the position of the outlet opening does not seem to be particularly important for the dispersion of pollutants in the cross-ventilation flow, but the position of the inlet opening has a more important influence on this situation. These results provide new insights into the processes of flow and divergence in cross-ventilated buildings. This experimental result can be used to verify the CFD simulation of cross-ventilation air flow and divergence, and then a new CFD best practice guide can be made based on that (Tominaga et al. 2016)

Fan et al conducted a field study in London, and the research target was a naturally ventilated office. Evaluate the natural ventilation model in the office, including unilateral ventilation and cross ventilation. A 1: 200 scale model was built in the wind tunnel environment, and the urban area within 300 meters was selected in the model. In the field environment under study, CO tracer gas technology was used to observe the ventilation of the target office under natural ventilation. At the same time, vertical temperature array is used to judge the influence of temperature change on flowing air. Through the data measured by the nearby weather station, we can get the air velocity and air flow angle closer to the natural conditions. In addition, the pressure coefficient within the experimental sample range under natural ventilation was obtained through wind tunnel experiment. In the experiment, the wind data measured from Heathrow Airport and the pressure coefficient data proposed in the literature are used. The air flow data measured by the weather station and the data measured by the wind tunnel experiment are also used. From the whole experiment, no matter which input data source is selected, the experiment of cross ventilation model can give a reasonable prediction on the whole. For the experiment of one-sided ventilation, although many models are used for the experiment, the prediction is still poor. Conducted a field study in London, and the research target was a naturally ventilated office. Evaluate the natural ventilation model in the office, including unilateral ventilation and cross ventilation. A 1: 200 scale model was built in the wind tunnel environment, and the urban area within 300 meters was selected in the model. In the field environment under study, CO tracer gas technology was used to observe the ventilation of the target office under natural ventilation. At the same time, vertical temperature array is used to judge the influence of temperature change on flowing air. Through the data measured by the nearby weather station, we can get the air velocity and air flow angle closer to the natural conditions. In addition, the pressure coefficient within the experimental sample range under natural ventilation was obtained through wind tunnel experiment. In the experiment, the wind data measured from Heathrow Airport and the pressure coefficient data proposed in the literature are used. The air flow data measured by the weather station and the data measured by the wind tunnel experiment are also used. From the whole experiment, no matter which input data source is selected, the experiment of cross ventilation model can give a reasonable prediction on the whole. For the experiment of one-sided ventilation, although many models are used for the experiment, the prediction is still poor. conducted a field study in London, and the research target was a naturally ventilated office. Evaluate the natural ventilation model in the office, including unilateral ventilation and cross ventilation. A 1: 200 scale model was built in the wind tunnel environment, and the urban area within 300 meters was selected in the model.

In the field environment under study, CO tracer gas technology was used to observe the ventilation of the target office under natural ventilation. At the same time, vertical temperature array is used to judge the influence of temperature change on flowing air. Through the data measured by the nearby weather station, we can get the air velocity and air flow angle closer to the natural conditions. In addition, the pressure coefficient within the experimental sample range under natural ventilation was obtained through wind tunnel experiment. In the experiment, the wind data measured from Heathrow Airport and the pressure coefficient data proposed in the literature are used. The air flow data measured by the weather station and the data measured by the wind tunnel experiment are also used. From the whole experiment, no matter which input data source is selected, the experiment of cross ventilation model can give a reasonable prediction overall. For the experiment of one-sided ventilation, although many models are used for the experiment, the prediction is still poor (Fan et al. 2021).

Finally, here is a conclusion. The wind tunnel experiment takes a long time, costs a lot, and requires individuals with professional knowledge to operate. Only by using different types of measuring instruments on the physical model, and so on, can the experiment be successfully completed. However, the use of wind tunnel can often produce high-precision results and clearly observe the changes in the experiment. Therefore, with the invention and wide application of CFD, the research on wind tunnel is gradually reduced, but the wind tunnel experimental results are still used as reference for verification.

2.6 Computational Fluid Dynamics

Ohba et al used CFD technology to study the influence of building arrangement on natural ventilation rate and adopted the standard two-equation k-epsilon turbulence model to determine the air exchange rate of apartment models under cross ventilation under isothermal conditions. Observe the influence of these variables on ventilation rate by changing the direction of air intake, the location of buildings, and adjusting the distance between buildings. By comparing the simulated airflow model with the wind tunnel test results, it is verified that the k-epsilon turbulence model is correct in predicting the upward accelerating airflow after the exit. Although the similarity is high, there are still errors. The error is mainly reflected in the fact that the windward direction of the building's roof is overestimated, but the windward direction of the building close to the ground is accurately predicted. Systematic analysis shows that five times the width of each building is the best distance between buildings for natural ventilation.

This distance can be cut down to three times the width of each building with the right adjustments, so it can be said that building layout can effectively increase ventilation (Ohba et al. 2001).

Numerical simulation (DNS), large eddy simulation (LES), and Reynolds Average Naville-Stroke (RANS) modeling are commonly used calculation methods in CFD software. According to the corresponding calculation requirements and use environment, the appropriate method should be selected for simulation calculation. The DNS method is rarely used in natural ventilation simulation, and under this condition, the simulation calculation requires high software and hardware requirements. The most commonly used method for natural ventilation or other industrial applications is to use the RANS method for research. When we need to calculate the time average flow parameters and the average air speed, the RANS model uses the characteristics of a turbulence model to accomplish the simulation experiment objectives. Compared with large eddy simulation, the RANS model needs more calculation time because it not only solves the average flow parameters, but also correctly solves the airflow around the building, which the RANS model can't accomplish. In the LES modeling calculation, the large eddy is solved by three-dimensional and time correlation methods, while the small eddy is calculated by a sub-grid model, which can effectively distinguish the large eddy. The calculation of the small eddy can improve the calculation efficiency and save time (Jiang & Chen 2002).

Chang and Meroney presented fresh concepts based on their prior research experiences. The purpose of the research in 2003 was to examine how air movement and pollution dispersion move throughout the ideal urban setting. The experiment examines the behaviour of natural air circulation and diffusion in a street canyon arrangement made up of several forms of construction. Different aspect ratios in the street canyon problem were set, and various experiments were carried out, in order to assess the correctness of the desired result generated by the street canyon model. Additionally, it attempts to restore as much of the roughness in both urban and rural settings. The gas flow and diffusion between two buildings in a street canyon made up of urban buildings were calculated using FLUENT, the prediction models using four different RANS turbulence, and the model using the large eddy simulation approach. The fluid model used in Colorado State University's industrial meteorological wind tunnel is compared to these findings. In this study, the structure of Texas Tech University's Wind Engineering Research Field Laboratory (WERFL) was utilised. There was no model of an exact size surrounding the urban street canyon in the experiment; instead, it was represented by a

WERFL model at a scale of 1: 50. These structures are positioned in different states with varying upwind building densities and distances. Calculations and measurements lead to the conclusion that the steady-state prediction approach frequently fails to correctly anticipate the air flow in metropolitan environments because the gas diffusion there is visibly unstable (Chang & Meroney 2003).

The whole air flow field has been reproduced in the CFD program and the observation in the measurement process by comparing the data of wind tunnel experiment with the data of numerical simulation in detail, but the intermittent feature of air flow penetrating into the canyon has not been reproduced by the steady-state calculation of air flow, which ultimately leads to the poor prediction of the relationship between CFD concentration and canyon wall. We also found that the wall size is sensitive to the rough boundary conditions set in the CFD (Chang & Meroney 2003).

Nikas et al used a numerical method to study the distribution of air flow velocity and induced velocity in buildings in 2010, taking into account the inlet windows of air flow velocity distribution at different incident angles and natural conditions, so as to better understand the needs of the natural ventilation mechanism in buildings. In this study, the inside and outside of natural cross-ventilation buildings were modeled, and the flow pattern of air flow in buildings was predicted by a three-dimensional numerical method. The RANS model is used to calculate the air exchange rate and wind speed in the building at different incident angles, and the columnar obstacles with geometric shapes are set in the room so as to be closer to the real layout of room facilities. Finally, the collected data is compared with the wind tunnel experiments of Larsen and Heisenberg (Larsen & Heisenberg, 2008), to verify the accuracy of the numerical results. It is considered that the wind speed has a great influence on the volume flow velocity of the air inlet and then influences the air exchange rate inside the building. As an older document, it led to later research on the position of the opening and the angle of air flow (Nikas et al. 2010).

Li, et al relate to the comparison between wind tunnel experimental data and numerical simulation of airflow in buildings with openings. In the part of numerical simulation, in order to simulate the flow area close to the natural environment, large eddy simulation is chosen instead of RANS. This is because large eddy simulation can simulate large eddy and small eddy, and then different methods are used to calculate the two kinds of vortices. The method

of three-dimensional change is used for the large eddy, and the sub-grid model is used to figure out the data for the small eddy.

Although the RANS model is weak in the calculation of large vortices and small vortices, it can calculate the whole system in a shorter time, but later Li et al shows that it is difficult to predict the airflow around buildings effectively and correctly. During the experiment, the boundary layer wind tunnel was used, and two unilateral ventilation situations and one lateral ventilation situation were deduced. The anemometer was used to capture the average velocity and pressure changes of air flow indoors. The results of all three experiments are basically consistent with the predictions of large eddy simulation. Therefore, LES prediction of wind-driven ventilation has been proven to be able to achieve high-precision prediction results (Li et a.l 2012).

The problem is that in all three cases, LES underestimated the speed in front of the building. It really caused new thinking and analyzed how to reduce the error by changing the grid resolution. The calculation results show that as the mesh of the network model becomes finer, the experimental error becomes smaller and smaller. Nevertheless, the coarse grid model agrees to correctly calculate the ventilation volume of natural ventilation, and the results are still of reference value. In the summary of the experiment, it is pointed out that LES, as a prediction model, can predict the average velocity and fluctuation velocity with high accuracy under high calculation pressure, and the grid roughness determines the experimental error, which is of research value as a whole. In the future research, the opening position can be included in the research scope, to investigate the ventilation volume under different air flow conditions and different opening positions (Li et al. 2012).

Some scholars believes that the design and evaluation of accurate natural ventilation strategy of buildings need to rely on CFD simulation of outdoor wind and indoor air. Therefore, in 2012, extensive universal research on three-dimensional steady-state RANS simulation of natural ventilation was put forward, and an isolated building model was used for modeling. The effects of parameters such as computational domain size, computational grid resolution and turbulence model are studied. It fills in the extensive general sensitivity research on CFD simulation of natural cross ventilation. A detailed wind tunnel experiment based on particle image velocimetry (PIV) (Karava et al. 2011) erifies the CFD simulation and considers the relationship between the accuracy of natural ventilation flow analysis and input parameters. A remarkable feature of the comparison between CFD and PIV results is that there are obvious

differences between the two groups of results near the room opening. The sensitivity study of CFD shows that this is the area where CFD results are least sensitive to the selection of calculation parameters. On the other hand, this is also the area with the biggest difference from PIV results. Considering the good consistency between computational fluid dynamics and particle image velocimetry, this may be due to Karava's mention that PIV calculation is not accurate enough, and the instability in some areas leads to a certain degree of error through the expansion of space under the shadow effect and reflection effect. The comparison between the two methods in the prediction of airflow velocity in indoor and outdoor situations shows that they are consistent. The influence of the size of the calculation domain shows that the air velocity ratio decreases with the increase in the area size. The shear stress transport k- model provides good prediction results and stability for the turbulence model, followed by the renormalization group k- model to provide accurate ventilation performance results. To sum up, the air flow in the cross-ventilation air flow mode of a room is complicated, and the parameters such as wall porosity, hole location, and hole ratio will have a great influence on the cross-ventilation flow state (Ramponi & Blocken 2012).

Then, Ramponi and Blocken published a new research paper on this basis, which verified the results of wind tunnel experiments and the principles that influenced the physical and numerical diffusion of cross-ventilation airflow. Continue to compare. Karava's wind tunnel experiment (Karava et al. 2011). By comparing the results of eight different experiments from wind tunnel experiments and CFD simulations, this method is verified to be effective. It is found that RANS, which uses shear stress transport k-ω model, has the best effect in simulating indoor and outdoor airflow, followed by RNG k- ε model. The change of the entrance profile of turbulence kinetic energy affects the physical diffusion, and the grid resolution affects the numerical diffusion. In addition, three configurations have good consistency in the research process, but the simulation effect of four configurations is poor. It is considered that the key transmission mechanism of diffusion should be paid attention to in order to realize accurate cross ventilation simulation. Through the experiment, it is suggested to add obstacles in the building structure to obtain the ventilation rate under the influence of obstacles (Ramponi & Blocken 2012).

Tominaga et al Based on the steady Reynolds-Flat NaviereStokes equation (RANS) model, the airflow around the top of double-slope buildings with different pitched roofs was studied. The pitch of roof is defined as three different experimental samples of 3:10, 5:10 and 7.5:10. Firstly, wind tunnel experiments are carried out on the three samples to obtain the data of the

average flow velocity, turbulent momentum and pressure coefficient of the air around the samples, and the database is established through the wind tunnel data. Then CFD simulation experiments are carried out on the 5:10 roof model, and the sensitivity of grid resolution and turbulence model is analyzed. By comparing the wind tunnel experimental data with CFD simulation data, the grid resolution and turbulence model of CFD are verified. Generally speaking, the experimental results are in good agreement with the measured values, and the average deviation is less than 0.15, resulting in an error of 0.3 for the airflow behind the building. This is because the steady RANS simulation used in this study can't effectively calculate the fluctuation caused by air when solving the calculation caused by vortex shedding around buildings. Through CFD simulation, the influence of roof slope on the flow field around the building is studied. It is found that the error ratio of the experimental results of the flow field of 3:10 and 5:10 roofs is larger than that of 5:10 and 7.5:10 (Tominaga et al. 2015).

Van Hooff et al in 2017. Based on the experimental results of previous wind tunnel experiments, the numerical differences between different models using specific computational fluid dynamics (CFD) simulations were studied to improve the future simulation. In this experiment, the experimental object is the building structure with general isolation shell, and the stable RANS simulation and large eddy current simulation (LES) are used to evaluate the three-dimensional cross ventilation of the experimental building structure. There are five parameters involved in the experimental evaluation, which are: the average velocity of air flow, the turbulence kinetic energy of air flow, the ventilation velocity, the angle of air entry and the jet diffusion width of air entering and shooting into the room (van Hooff et al. 2017).

In this experiment, RANS simulation is carried out by using standard k-ε(SKE), RNG k-ε, realizable k-ε(RLZ), SST k-ω and RSM turbulence models. The LES simulation calculation is carried out by using the dynamic Smagorinsky sub-grid scale model. Finally, by comparing the experimental data of wind tunnel experiment with the experimental data of numerical simulation, the results of numerical simulation experiment are verified. The numerical simulation results prove that the numerical simulation results of RANS can't show the turbulence simulation obviously because the turbulence kinetic energy is too low, and because of the characteristics of the stable RNS simulation, it can't capture the up-and-down flapping of the jet after it enters the opening. Among them, RNG k-ε model, SST k-ω and RSM turbulence model can simulate the air flow direction in the wind tunnel experiment well. Regarding the LES experiment, the LES model shows the air flow velocity, the turbulence kinetic energy produced by the air flow in the room, and the volume flow rate of the air flow.

By comparing the numerical simulation of LES and RANS, it is found that the appropriate numerical simulation method should be selected according to the experimental requirements in the experimental process. When LES is used, attention should be paid to increasing the requirement of calculation factor, and the set value of factor should be 80~100 (Tominaga et al. 2017).

Most of the time, we live in urban areas. Understanding the influence of large-scale dense urban layout on ventilation is helpful to improve the design of building structures and maximize the comfort of living. Hadavi and Pasdarshahri put forward 12 urban layouts in 2020, and made CFD simulation predictions with three wind speeds, which made up 36 different situations. Considering the eddy viscosity caused by turbulence fluctuation, a K-Ω SST turbulence model is proposed to simulate and predict the air flow state and permeability in dense cities according to the experimental data verification results. The simulation results show that the air retention rate has no great influence on the phenomenon of air infiltrating into or seeping out of the city but can only increase or decrease its change rate. Decreasing the compactness of buildings will increase the air flow speed inside the city (Hadavi et al. 2020).

Table 2.2: Review of computational fluid dynamics research.

(Author, Year)	Modelling approach	Findings	Parameters
(Ohba & Kurabuchi 2001)	Sk- ε	Proper building layout can effectively increase ventilation.	Q, VR
(Jiang & Chen 2003)	LES, SST *k–ω*	It is found that most of the energy is contained in the low frequency region, and the average flow field plays an important role.	Q，ACH
(Chang & Meroney 2003)	RANS, Sk-ε, RNG k-ε, Rk-ε and RSM	When the air flow is in the urban environment, the gas diffusion is obviously unstable, and the steady-state prediction method may not be able to accurately predict the air flow in the urban environment.	K

(Nikas et al. 2010)	RANS, k–ω	It is considered that the wind speed has a great influence on the volume flow velocity of the air inlet, and then affects the number of air changes inside the building.	ACH, V
(Gousseau et al. 2011)	Sk- ε, LES	LES with dynamic sub-grid scale model shows better performance without any parameter input to solve the dispersion equation.	V, e
(Cho et al. 2012)	Sk- ε	The influence of wind can reinforce or oppose each other.	V, ACH
(Li et al. 2012)	LES	As a prediction model, LES can predict the average velocity and fluctuation velocity with high accuracy under high computational pressure, and the roughness of the grid determines the experimental error.	V, μt
(Ramponi & Blocken 2012)	SST *k–ω*	It has a strong influence on turbulence kinetic energy convergence and results.	V, VR
(Ramponi, & Blocken, 2012)	SST *k–ω*	It is an important transmission mechanism in cross ventilation of diffusion buildings, so special attention should be paid to selecting proper physical diffusion and reducing numerical diffusion, using high-resolution grid and at least second-order accurate discretization scheme.	V, VR
(Tominaga et al. 2015)	RNG k-ε, Sk- ε, Rk-ε, and SST *k–ω*	The steady-state RANS simulation used in this study will not reproduce the transient fluctuations caused by vortex shedding around buildings.	k, c_p
(van Hooff et al. 2017)	SST *k-ω* RNG k-ε RSM, Sk-ε and LES	The LES simulation reproduces the transient flow characteristics, and all RANS simulations underestimate the turbulence kinetic energy inside the room.	Q, V

(Sacht & Lukiantchuki. 2017)	CFX	The modification of the opening size and the change of the wind incidence angle change the natural ventilation conditions, and at the same time affect the average indoor pressure coefficient and the air change rate.	c_p, Q
(Shirzadi et al. 2017)	Sk- ε	By proposing a set of systematic methods, relevant reference values are proposed after adjustment and verification, which effectively improves the calculation accuracy and reduces the error of simulation results.	V, k, T
(Tominaga & Stathopoulos 2018)	Sk- ε, RLZ, k-ω SST, RNG k-ε and LES	Steady-state RANS calculations often also reproduce the effect of plume buoyancy on mean concentrations in experimental results, Buoyancy modeling in the ε equation has a negligible effect on the results.	C, F_{rd}
(Shirzadi et al. 2018)	Sk- ε and k-ω SST	During simulation validation for urban densities between 0.25 and 0.4, a series of new closure coefficients were found	c_p, V
(Shirzadi et al. 2020)	Sk- ε and calibrated k – ε model	Based on the Reynolds Averaged Navier-Stokes (RANS) Computational Fluid Dynamics model, there is a method to improve the accuracy of urban airflow simulation is proposed, and high-quality data are used to define verification indicators, Finally, the best value for improving the closure coefficients of the RANS turbulence model is obtained	V, c_p
(Hadavi & Pasdarshahri 2020)	k-ω SST	The results of urban layout show that reducing the compactness of buildings will	c_p, AoA

		increase ventilation performance and improve negative pressure.	
(Shirzadi & Tominaga 2022)	Sk- ε， RLZ, k-ω SST, RNG k- ε and LES	The error between the simulation results of urban building ventilation using the correction coefficient and the experimental results is less than 8%, and the error of other RANS models reaches 70%.	V

Turbulence viscosity (μt), Particle Image Velocimetry (PIV), Turbulent kinetic energy (k), Standard k- ε model (Sk- ε), Realizable k- ε model (Rk- ε), Renormalization Group k- ε model (RNG k- ε), Standard k- ω model (Sk- ω), Shear-stress transport k- ω model (SST k- ω), Reynolds Stress Model (RSM), Ansys software (CFX). The relative error (e). Realizable k – ε (RLZ). Reynolds-averaged Navier-Stokes (RANS). Concentration (C). Plume buoyancies (F_{rd}). Turbulent kinetic energy(k). Temperature(T)

2.7 Summary

Through many literature searches on cross ventilation, it can be seen that wind CFD technology is a powerful tool for fluid mechanics calculation, but there is still a distance for complete accuracy. The final result of CFD needs to be referenced with the experimental data of wind tunnel experiment to ensure the accuracy of CFD prediction. The wind tunnel experiment is reliable through manual testing, but the complexity of time and equipment increases the cost of a single experiment, which makes CFD technology still one of the popular fluid detection methods at present. Compared with wind tunnel experiments, CFD technology is simple and fast to solve, and the trend of proportional relationship is roughly consistent. Large or small experiments can use CFD technology to quickly understand and obtain the influence relationship between environment and air flow. With the call of low-carbon life and the view of sustainable development, more and more researchers have recognized that natural ventilation has become an effective alternative to mechanically ventilated buildings.

Table 2.3: Research from literature with gap identified

Author (Year)	Findings	Gap Identified

(Nikas et al. 2010)	It is considered that the wind speed has a great influence on the volume flow velocity of the air inlet, and then affects the number of air changes inside the building.	Only the relationship between wind speed and ventilation rate is concerned, and the relationship between opening ratio and ventilation rate can be considered by extending the concept.
(Tominaga 2015)	The wake flow behind the building is analyzed, and different calculation modules are used to obtain more accurate simulation results	Only studied the wake of the building. Suggest to include the impact of the wake behind the building by considering the size of the opening and the surrounding building structure
(Hadavi & Pasdarshahri 2020)	The analysis results of the whole urban layout system show that the negative pressure gradient will increase with the increase of the density of urban buildings.In addition, if the leakage area is parallel to the main air flow, the leakage rate has almost nothing to do with the flow speed of air flow	Only studied the state of urban air flow. Suggest to consider changing the opening of building inside to check the state of air flow.
(Hadavi & Pasdarshahri 2020).	The results of urban layout show that reducing the compactness of buildings will increase ventilation performance and improve negative pressure.	Only the urban layout problem is considered, and there is a lack of research on the effect of changing the opening ratio on air flow
(Moey et al. 2021)	The opening ratio has a great influence on the internal airflow.	Only the effect of building opening size on indoor ventilation performance was studied. Suggest to bring this feature into urban environments
(Zhang et al. 2022)	The internal blockage rate is inversely proportional to the ventilation rate. Using several narrow interior walls instead of wide vertical walls in the room and placing	Only focuses on the interior of buildings. Suggest to placed in an urban environment to consider the relationship between urban ventilation and internal structure

	the horizontal walls above the height of the opening can minimize ventilation.	
(Moey et al. 2022)	When the opening ratio in the room is less than 1, the ventilation volume in the room increases, but when the opening ratio in the room is greater than 1, the ventilation volume in the room begins to decrease.	Only indoor airflow changes were observed. Suggest to consider other influencing factors such as urban building layout and surrounding building openings
(Shirzadi & Tominaga 2022)	Air flow conditions around tall buildings surrounded by low street canyons are simulated. And compared the results with the results of wind tunnel experiments, the comparison results are good	Only focus on the ventilation performance in the urban street environment. Suggest to include opening size for urban buildings and the air flow inside the room can be studied.

CHAPTER 3

METHODOLOGY

3.1 Background

This chapter introduces different building geometries that used in the simulation. Moreover, the numerical and solver setting, grid convergence index, and model validation were be discussed in detail. In addition, the simulation batches and cases was presented.

3.2 Flowchart

Figure 3.1 shows the simulation flowchart. Completing simulation studies through scientifically rigorous steps helps reduce research loopholes.

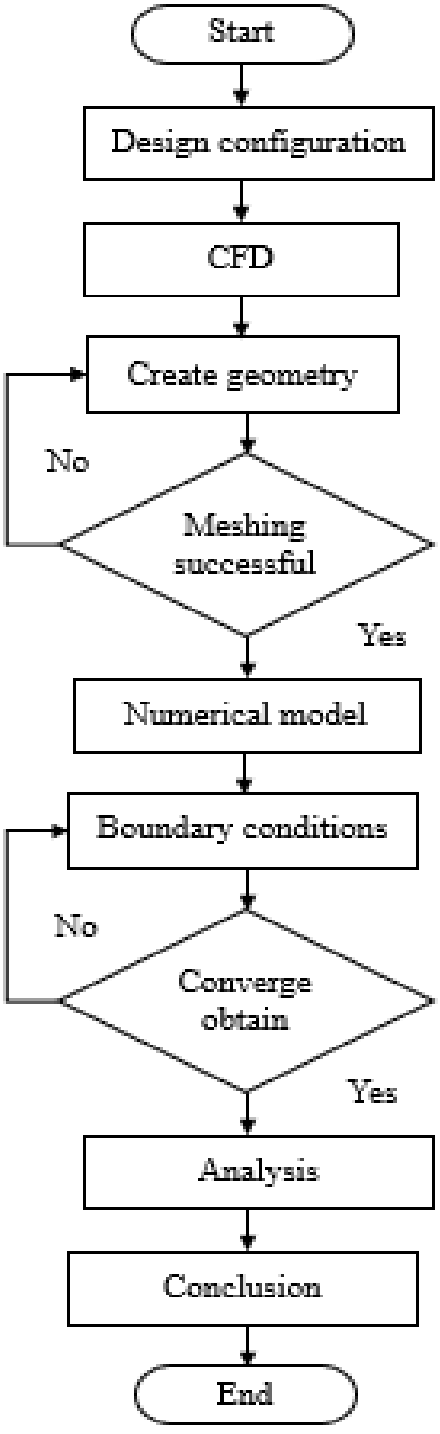

Figure 3.1: Simulation Flowchart.

3.3 Model Geometry

The reference model selected in this numerical study is a stand alone building model which is based on the model demonstrated by van Hooff (van Hooff et al. 2017). The reference model is shown in Figure 3.2. The building has a dimension of 0.2 m × 0.2 m × 0.16 m (L × W × H). Two openings are included in the building model which are opposite to each other at the center of the wall. The dimensions of the two openings are 0.092 m × 0.036 m (W × H) and the thickness of the wall is 0.03 m (van Hooff et al. 2017).

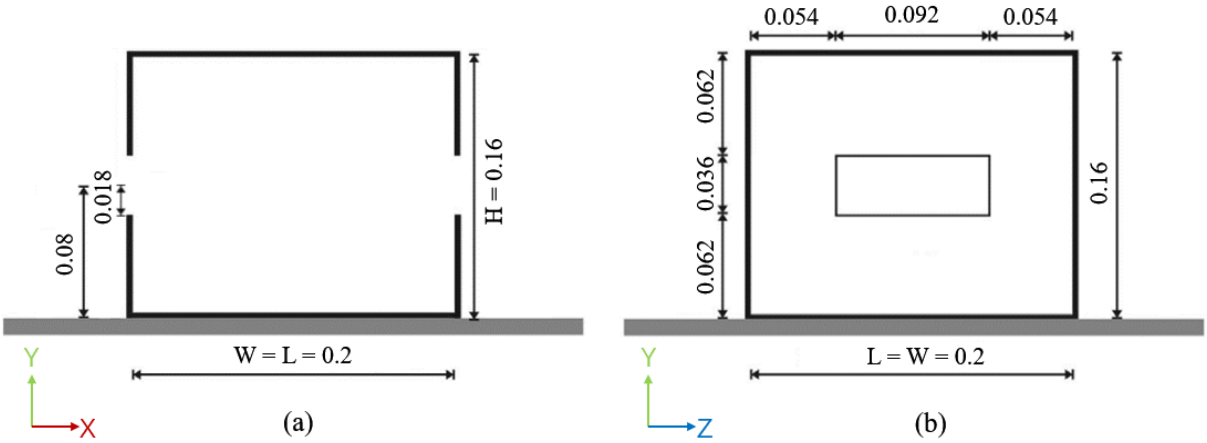

Figure 3.2 : Building geometry (a) Front view (b) Side view dimensions in m.

3.4 Computational Domain and Grid

The computational domain used in this study is based on the parameters recommended by Franke et al, Tominaga et al, and Blocken with certain adjustments. As shown in Figure 3.3, the distance from inlet to model windward wall the was set to be five times the model height, 5H which is 0.8 m to restrict the chances of unintended streamwise gradients to develop (H is the height of the building). The distance from the outlet to model leeward wall was set to be 15H, which is 2.4 m. When the lateral side and top of the domain was set 5H which is 0.8 m, the overall dimensions of the computational domain were 3.4 m × 1.8 m × 0.96 m (L × W × H). Figure 3.3 shows the dimensions of computational domain (Franke et al. 2007; Tominaga et al. 2008; Blocken 2015).

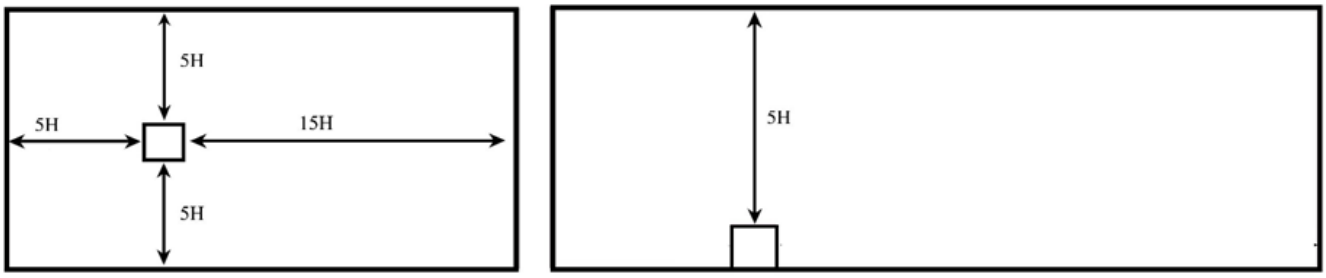

(a) (b)

Figure 3.3: Dimension of the computational domain (a) Top view (b) Front view.

Figure 3.4 shows the isometric view and symmetrical plan of the computational domain (Ramponi & Blocken, 2017). In addition, the simulation cases were further modified on the basis of reference model.

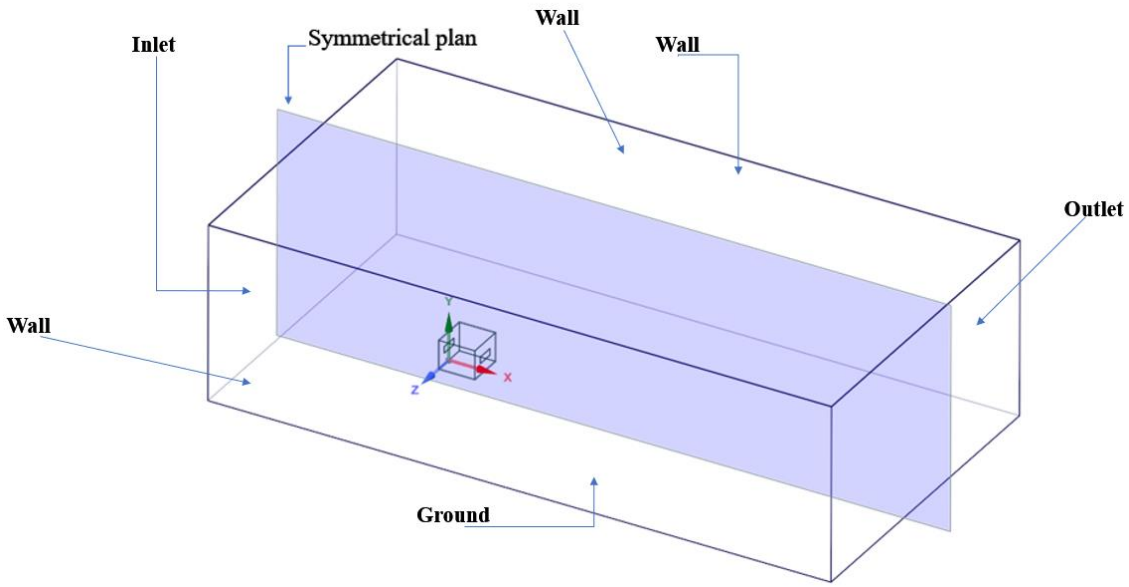

Figure 3.4: The isometric view and symmetrical plan of the computational domain.

3.4.1 Model Body of Influence of Single Building (BOI)

A domain called the body of influence (BOI) wrapped the geometry (van Hooff & Blocken 2010; Moey et al. 2021). Figure 3.5(a) shows the front view of the flow domain. Similarly Figure 3.5(b) and Figure 3.5(c) show the side view and the isometric view of the flow domain. Furthermore, as a second BOI, a far BOI was placed to capture the approaching flow and separation flow outside of the building as shown in Figure 3.5(C)(2). The near BOI has a

160 mm offset distance from the top and side walls of the building, as shown in Figure 3.5(c)(3). The fourth BOI named house BOI enclosed the building itself as illustrated in Figure 3.5(C)(4). The fifth and sixth BOI named windward BOI and leeward BOI were placed at the windward and leeward openings to accurately capture the flow through the opening as shown in Figure 3.5(c)(5) and (6) respectively. Meanwhile, Figure 3.5(d) shows the windward and leeward BOI, and the thickness of the wall is symbolized as ζ which is 3 mm.

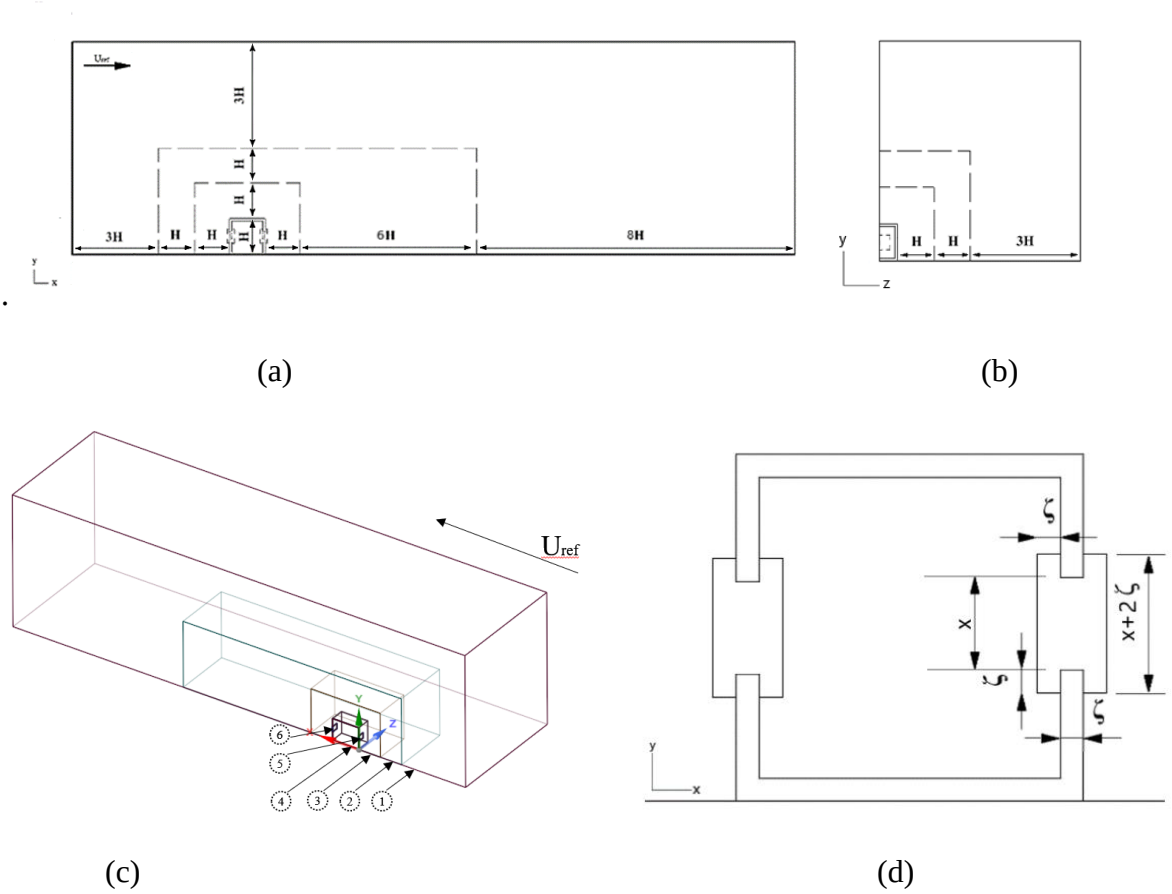

Figure 3.5: (a) Front view of flow domain (b) Side view of flow domain (c) Isometric view of flow domain (d) Windward and leeward BOI.

3.5 Meshing

In this simulation, a grid independence study was performed to eliminate discretization errors. Three different numbers of cells representing coarse, medium, and fine grid were selected. There were 1,162,978 cells (coarse), 2,327,525 cells (medium), and 3,336,968 cells (fine) used in this study. Subsequent grid convergence research was carried out on these three grids.

3.5.3 Meshing of Coarse Case

The local and global scope sizing for the coarse grid meshed can be summarised in the Table 3.1. In the local and global scope sizing ANSYS Fluent console. the unspecified variables meant that they were left by default according to the values proposed by the software.

Table 3.1: Setting for the coarse meshing.

A. Local Sizing	
1.BOI-far	
Type	BOI
Target Mesh Size	0.012
2.BOI-near	
Type	BOI
Target Mesh Size	0.006
3.BOI-House	
Type	BOI
Target Mesh Size	0.003
4.BOI-opening	
Type	BOI
Target Mesh Size	0.0015
5.Curvature-House	
Type	Curvature
Local Min Size (m)	0.003
Max Size (m)	0.06
Scope to	Edges
B. Surface Mesh	
Min Size (m)	0.003
Max Size (m)	0.06
Growth Rate	1.05
Size Functions	Curvature & Proximity
Curvature Normal Angle	10
Cell Per Gap	2
C. Geometry Descripition	
Geometry Type	Fluid regions with no voids
Change fluid-fluid boundary types from wall to internal	No
Share topology	No
D. Boundary Layers	
Frist height(μm)	350
Offset method	Last ratio
No.of layers	12
Grow on	Selected labels:House
E. Volume Mesh	
Fill with	Poly-hexcore
Peel layers	1
Min cell length	0.0015
Max cell length	0.192
F.Improve Volume Mesh	
Cell quality limit	0.3

Figure 3.6 shows the coarse grid, also known as Grid A with 1,162,978 cells. The final grid information can be checked from the information bar as follows; minimum volume: 8.213365e-11; maximum volume: 4.203282e-04.

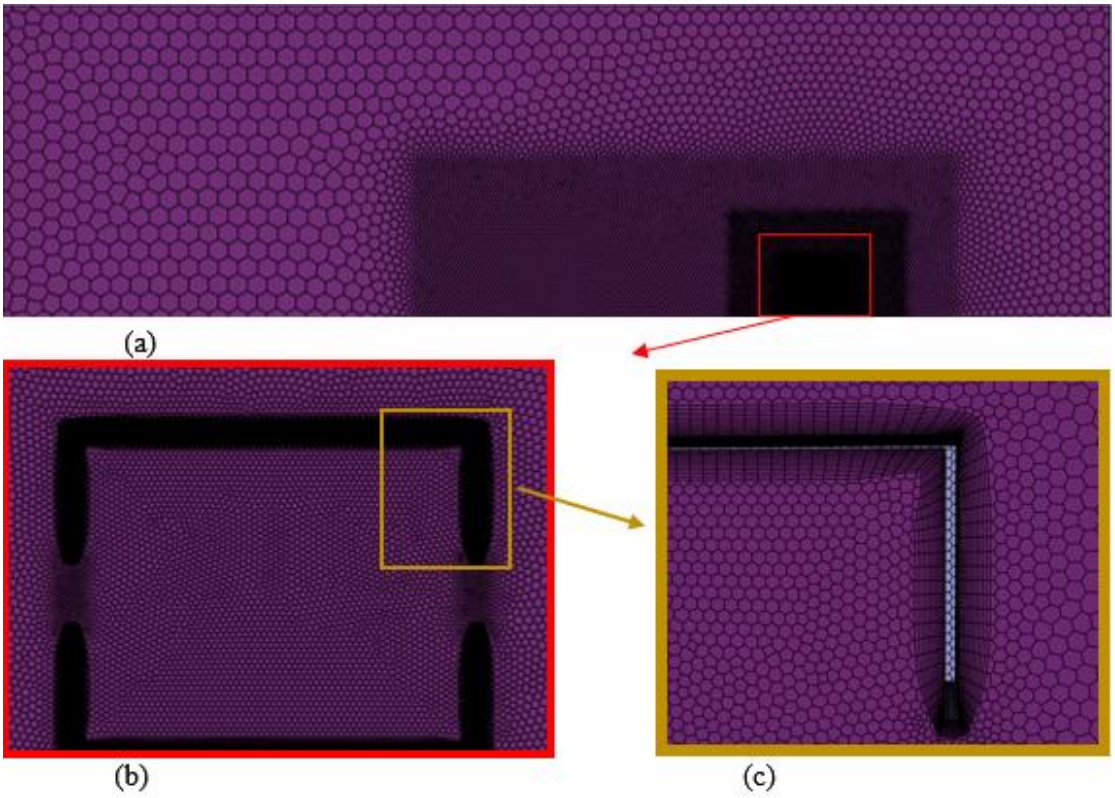

Figure 3.6: Results for the coarse mesh (a) Computational grid on ground and target building surfaces for fine grid (b) Computational grid on target building surface details (c) Computational grid on edge details of target building surface structure.

3.5.2 Meshing of Medium Case

The local and global scope sizing for the medium grid meshed can be summarised in the Table 3.2. In the local and global scope sizing ANSYS Fluent console, the unspecified variables meant that they were left by default according to the values proposed by the software.

Table 3.2: Setting for the medium meshing

A. Local Sizing	
1.BOI-far	
Type	BOI
Target Mesh Size	0.01
2.BOI-near	
Type	BOI
Target Mesh Size	0.005
3.BOI-House	
Type	BOI
Target Mesh Size	0.0025
4.BOI-opening	
Type	BOI
Target Mesh Size	0.00125
5.Curvature-House	
Type	Curvature
Local Min Size (m)	0.0025
Max Size (m)	0.05
Scope to	Edges
B. Surface Mesh	
Min Size (m)	0.0025
Max Size (m)	0.05
Growth Rate	1.05
Size Functions	Curvature & Proximity
Curvature Normal Angle	10
Cell Per Gap	2
C. Geometry Descripition	
Geometry Type	Fluid regions with no voids
Change fluid-fluid boundary types from wall to internal	No
Share topology	No
D. Boundary Layers	
Frist height(μm)	350
Offset method	Last ratio
No.of layers	14
Grow on	Selected labels:House
E. Volume Mesh	
Fill with	Poly-hexcore
Peel layers	1
Min cell length	0.001
Max cell length	0.128
F.Improve Volume Mesh	
Cell quality limit	0.3

Figure 3.7 below shows the medium grid, also known as Grid B with 2,327,525 cells. The final gridding information can be checked from the information bar as follows Minimum volume: 3.170025e-11; Maximum volume: 2.663156e-04.

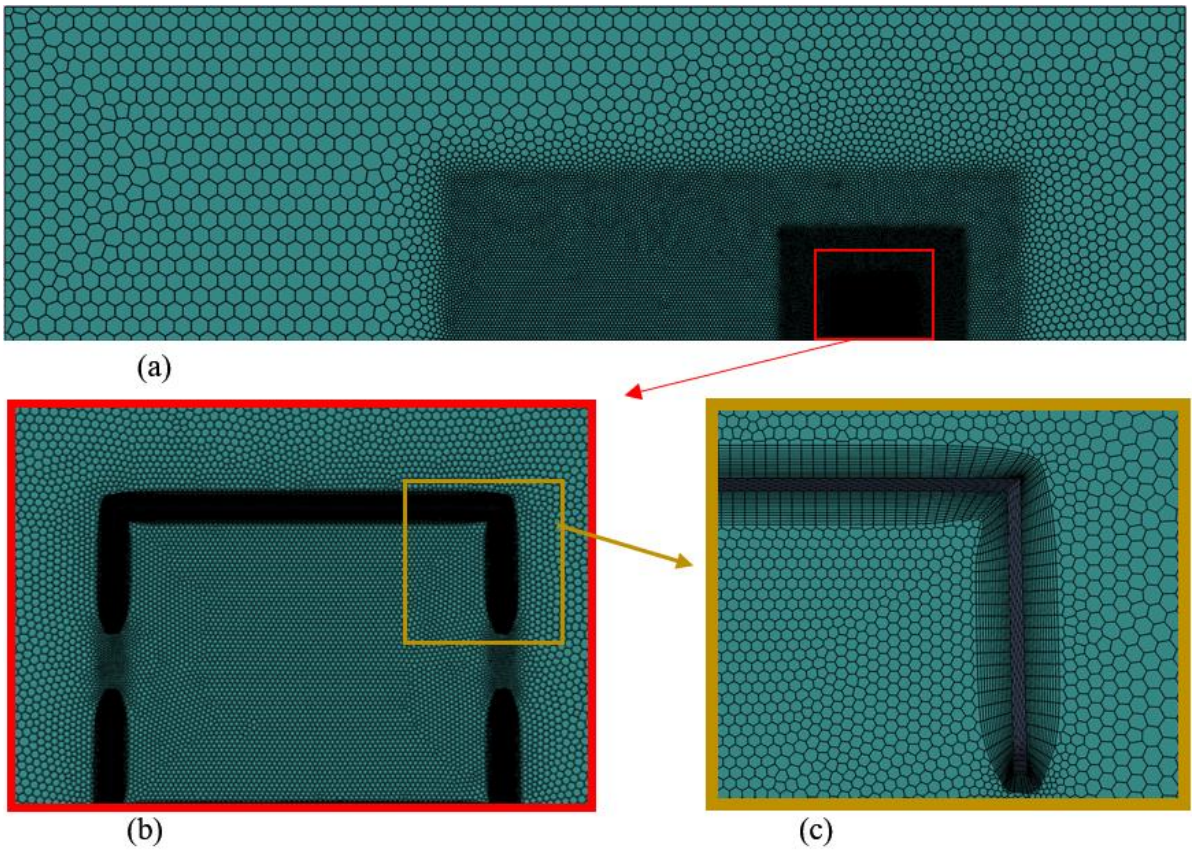

Figure 3.7: Results for the medium mesh (a) Computational grid on ground and target building surfaces for fine grid (b) Computational grid on target building surface details (c) Computational grid on edge details of target building surface structure.

3.5.3 Meshing of Fine Case

The local and global scope sizing for the fine grid meshed can be summarised in the Table 3.3. In the local and global scope sizing ANSYS Fluent console, the unspecified variables meant that they were left by default according to the values proposed by the software.

Table 3.3: Setting for the fine meshing.

A. Local Sizing	
1.BOI-far	
Type	BOI
Target Mesh Size	0.008
2.BOI-near	
Type	BOI
Target Mesh Size	0.004
3.BOI-House	
Type	BOI
Target Mesh Size	0.002
4.BOI-opening	
Type	BOI
Target Mesh Size	0.001
5.Curvature-House	
Type	Curvature
Local Min Size (m)	0.002
Max Size (m)	0.04
Scope to	Edges
B. Surface Mesh	
Min Size (m)	0.002
Max Size (m)	0.04
Growth Rate	1.05
Size Functions	Curvature & Proximity
Curvature Normal Angle	10
Cell Per Gap	2
C. Geometry Descripition	
Geometry Type	Fluid regions with no voids
Change fluid-fluid boundary types from wall to internal	No
Share topology	No
D. Boundary Layers	
Frist height(μm)	350
Offset method	Last ratio
No.of layers	16
Grow on	Selected labels:House
E. Volume Mesh	
Fill with	Poly-hexcore
Peel layers	1
Min cell length	0.001
Max cell length	0.128
F.Improve Volume Mesh	
Cell quality limit	0.3

Figure 3.8 below shows the fine grid, also known as Grid C with 3,336,968 cells. The final gridding information can be checked from the information bar as follows minimum volume: 4.613011e-12; Maximum volume: 2.621440e-04.

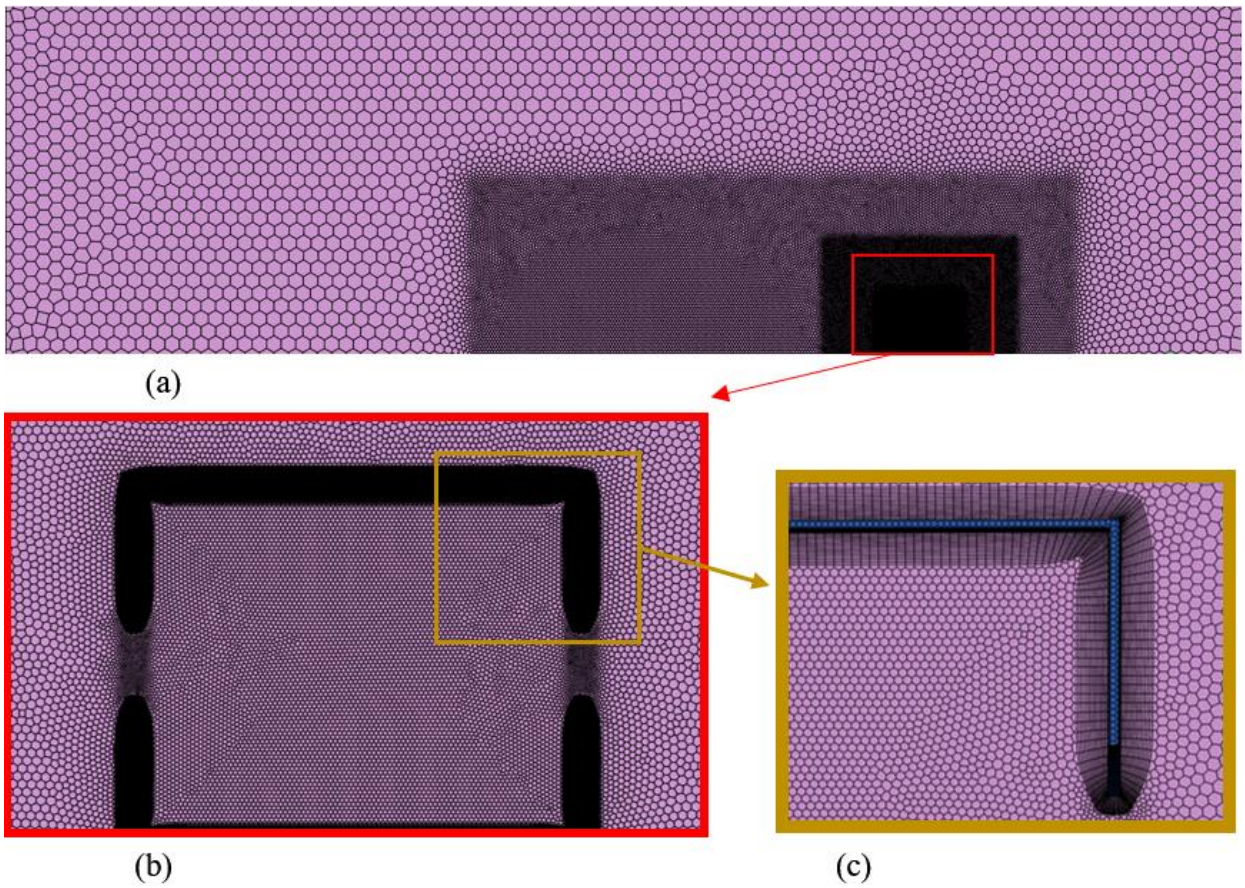

Figure 3.8: Fine meshing results (a) Computational grid on ground and target building surfaces for fine grid (b) Computational grid on target surface details (c) Computational grid on edge details of target surface structure.

3.6 Atmospheric Boundary Layer (ABL)

The ABL friction velocity, U*ABL is calculated using Equation (1) with a reference velocity, Uref of 4.3 m/s and a reference height, Zref of 0.16 m. Additionally, the Von Karman constant, κ of 0.42 with an aerodynamic roughness height, Z_0 of 0.0009 m are used.

$$U^*_{ABL} = \frac{U_{ref} \times \kappa}{log(\frac{Z_{ref}+Z_0}{Z_0})}$$ Equation 1: ABL friction velocity.

The top and side walls are defined for the flow domain to have zero particular shear stress. The outlet is designated as the outlet, the building walls and the ground are subject to a no-slip boundary condition, and symmetry is applied to the vertical centre plane in the direction of the wind. The ABL file generates values for the inlet's magnitude of velocity, turbulent kinetic energy, and turbulence dissipation rate. Turbulence kinetic energy, k was obtained from equation (2) with empirical constant C_MU=0.09 and turbulence dissipation rate was calculated from equation (3).

$$k = \frac{(U^*_{ABL})^2}{\sqrt{C_{MU}}}$$ Equation 2: Turbulence kinetic energy.

$$\varepsilon = \frac{(U^*_{ABL})^3}{\kappa(Z_{ref}+Z_0)}$$ Equation 3: Turbulence dissipation.

3.7 Slover Setting

The approved numerical geometry's boundary conditions are summarised in Table 3.4 below. A user-defined function was uploaded to the ANSYS Fluent 2021 R2 software. This is shown in subsection A-3 in the row of Table 3.4 below. In the research, we will compare the calculation of Standard model and RNG model in K-ε model under different grid conditions, so as to choose the outstanding calculation model as the whole simulation.

Table 3.4: Boundary conditions setting

A. Set up	
1.General	
Gravity	-9.81 (Y-direction)
User defined	Interpreted
2.Models	
Viscous laminar	
-Model	Stand k-e, Enhanced Wall Fn
3.Boundary Conditions	
House	Wall
Ground	Wall
Inlet	Velocity_inlet
-Velocity magnitude	UDF: velocity_profile
-Specification method	k and Epssilon
-Turbulent kinetic ener	UDF: k_profile
-Specific dissipation rat	1
Outlet	Pressure-out
Side & Top	Symmetry_wall
Symmetry	Symmetry
B. Solution	
4. Methods	
Scheme	SIMPLE
Gradient	least squares cell based
Pressue	Second order
Momentum	Second order upwind
Turbulent kinetic energ	Second order upwind
Turbulent dissipation ra	Second order upwind
Offset method	Last ratio
5. Monitors	
Continuity	1×10^-4
X-velocity	1×10^-5
Y-velocity	1×10^-5
Z-velocity	1×10^-5
k	1×10^-5
epsilon	1×10^-5
6. Initialization	Hybrid initialization
7. Run calculation	
Iterations	10000

3.8 Grid Convergence Index (GCI)

The number of cells used the whole simulation was medium case, which is also known as reference grid. The Grid Convergence Index (GCI), as indicated in Equation (4), was used to define the reference grid through a grid independence research (Gilani et al. 2013; Hooff et al. 2017; Kosutova et al. 2019; Ramponi and Blocken 2012).

$$GCI = SF \left| \frac{r^{p} \frac{U_{coarse} - U_{fine}}{U_{coarse}}}{r^{p} - 1} \right| = 4.26777 \left| \frac{U_{coarse} - U_{fine}}{U_{coarse}} \right|$$ Equation 4: Grid convergence index (GCI).

For evaluating indoor natural ventilation performance, the RNG k-ε and standard k-ε (SKE) turbulence models have higher accuracy compared to others. In order to make rational use of the computing efficiency of the computer, it is necessary to compare the results of GCI to choose a better model. (Tominaga et al. 2017).The cell counts for Grids A, B, and C were 1,162,978, 2,327,525 and 3,336,968, respectively.In the process of verification, three positions in the model will be selected, with the same interval, where x is the distance from the value position to the air inlet opening and D is the distance from the air inlet to the air outlet. The positions are expressed as (a), (b) and (c) respectively, which means X/D = 0.125, X/D = 0.500 and X/D = 0.875. Along three vertical lines inside the building in the vertical center plane is shown in Figure 3.9.

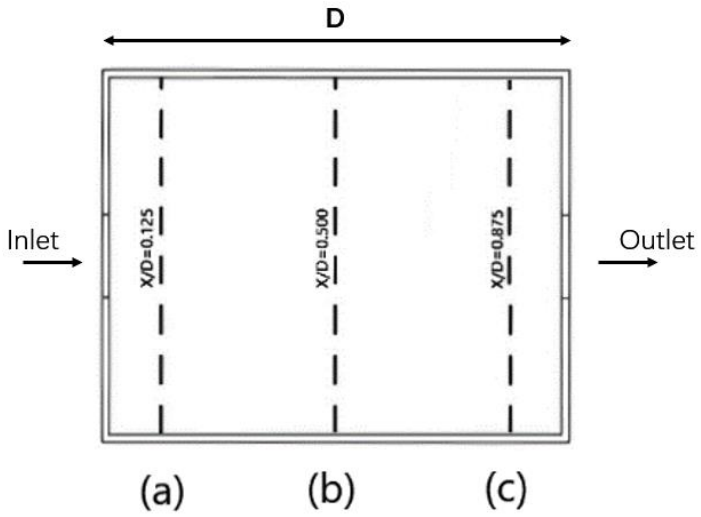

Figure 3.9: Along three vertical lines inside the building in the vertical center plane (a) X/D = 0.125 (b) X/D = 0.500 (c) X/D = 0.875.

3.8.1 GCI Result

Under the condition of using RNG and SKE model, the comparison diagram of simulation results of positions (a), (b) and (c) is shown in Figure 3.10.

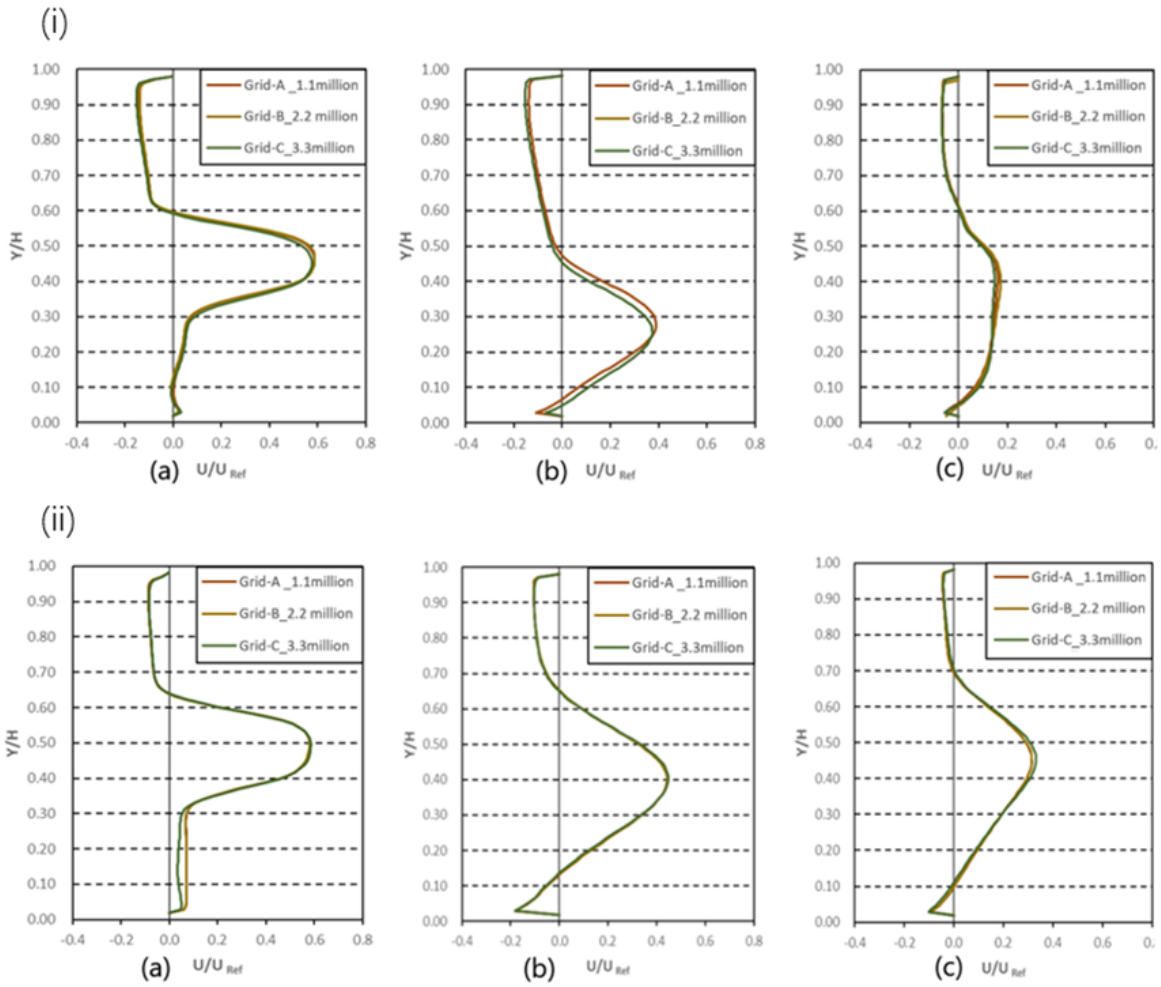

Figure 3.10: Comparison of numerical simulation (i) Results of RNG model. (ii) Result of SKE model. (a) X/D = 0.125; (b) X/D = 0.500; (c) X/D = 0.875.

The GCI results and average values of each position with RNG and SKE model are shown in Tables 3.5 and 3.6, respectively.

Table 3.5: GCI result for RNG turbulence model.

Location	GCI-(RNG)	
	Coarse vs Fine	Medium vs Fine
x/D = 0.125	2.4661	1.6248
x/D = 0.500	5.9994	4.1095
x/D = 0.875	1.7536	1.2212
Average	3.4064	2.3185

Table 3.6: GCI result for SKE turbulence model.

Location	GCI-(SKE)	
	Coarse vs Fine	Medium vs Fine
x/D = 0.125	2.7069	0.1486
x/D = 0.500	1.1241	0.2161
x/D = 0.875	2.0517	0.1973
Average	1.9609	0.1873

By comparing the GCI results of RNG and SKE model, the results of RNG show that the average GCI results are 3.4064% for coarse case and 2.3185% for medium case. The results of SKE show that the average GCI results are 1.9609% for coarse case and 0.1873% for medium case. SKE showed excellent GCI results, so medium case combined with SKE turbulence model was selected as this calculation method in this study.

3.9 Model Validation

Model validation are required for the results generated by the CFD simulation settings to ensure that the simulation results are as accurate as possible. The validation methods include factor of two of observation (FAC2), comparison result contour, Root mean square error (RMSE).

3.9.1 Factor of Two of Observation (FAC2)

The factor of two of observation (FAC2) is a robust model validation approach for computational fluid dynamics (CFD) with regards to the occurrence of sporadic occuring high

or low observations and predictions. Schatzmann et al initially suggested it in 2010 and several authors have since embraced it (van Hooff et al 2017; Kosutova et al. 2019; Shirzadi et al. 2020). To ensure the accuracy of the data, FAC2 was chosen to be used in this study. (Schatzmann, Olesen, and Franke 2010). FAC2 is obtained using Equation (5).

$$FAC2 = \frac{1}{n}\sum_{i=1}^{n} N_i$$

$$N_i = \begin{cases} 1 & if\ 0.5 \le \frac{P_i}{O_i} \le 2 \\ 0; & otherwise \end{cases}$$

Equation 5: Factor of two of observation (FAC2).

Whereby, Pi is the velocity profile value obtained from the reference grid, and Oi is the data obtained from van Hooff et al through observation in 2017. The data content includes wind tunnel test data and data obtained through SKE turbulence model numerical simulation. It is appropriate when the observed value is less than the compared value but still falls within the lower limit threshold. In a similar vein, it is acceptable when the observed value is more than the compared value but still falls within the higher limit threshold. Data was obtained from seven equally spaced positions in target building, and the FAC2 results are shown in Figure 3.11.

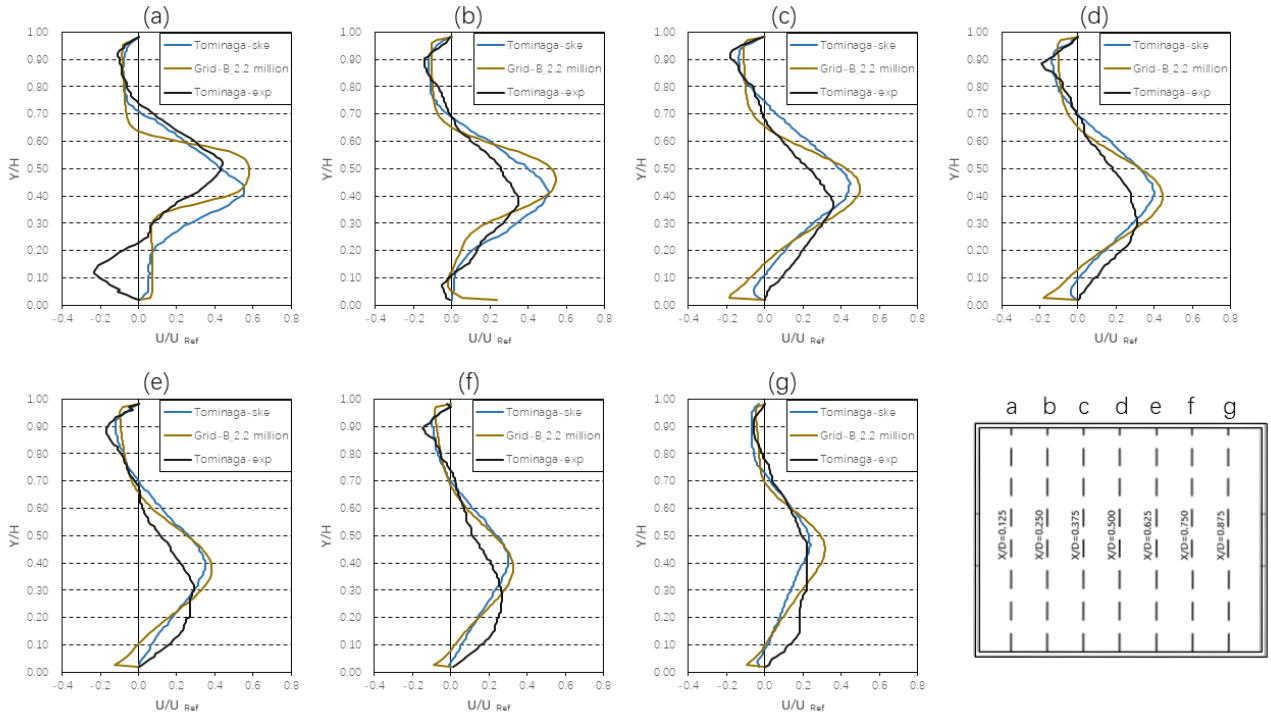

Figure 3.11: The FAC2 data of SKE comparison chart (a) X/D = 0.125 (b) X/D = 0.250 (c) X/D = 0.375 (d) X/D = 0.500 (e) X/D = 0.675 (f) X/D = 0.750 (g) X/D = 0.875.

Comparison and integration of FAC2 data are shown in Table 3.7. the average FAC2 results of SKE and Tominaga data are 0.9, and SKE and experimental data are 0.70. The FAC2 validation result of SKE is great.

Table 3.7: FAC2 data comparison for simulation results (SKE) with van Hooff (SKE) results and Experiment data (van Hooff et al. 2017).

Simulation result (SKE) vs simulation result (SKE) from van Hooff		**Simulation result (SKE) vs experiment data from van Hooff**	
Position	FAC2	Position	FAC2
X/D=0.125	0.99	X/D=0.125	0.61
X/D=0.250	0.86	X/D=0.250	0.71
X/D=0.375	0.87	X/D=0.375	0.72
X/D=0.500	0.88	X/D=0.500	0.73
X/D=0.625	0.99	X/D=0.625	0.68
X/D=0.750	0.88	X/D=0.750	0.74
X/D=0.875	0.87	X/D=0.875	0.73
Average	**0.90**	**Average**	**0.70**

3.9.2 Root Mean Square Error (RMSE)

Another validation indicator in this study, the root mean square error (RMSE) is regularly employed in model validation studies (Willmott & Matsuura, 2005). RMSE is obtained using Equation (6).

$$RMSE = [n^{-1} \sum_{i=1}^{n} (P_i - Q_i)^2]^{1/2}$$ Equation 6: Root mean square error (RMSE).

The RMSE results calculated at each location are shown in Table 3.8. Average RMSE result is 0.058766.

Table 3.8: RMSE result of reference model.

RMSE result of reference model	
Location	**RMSE**
X/D=0.125	0.103072
X/D=0.250	0.075677
X/D=0.375	0.066971
X/D=0.500	0.049009
X/D=0.625	0.041359
X/D=0.750	0.029807
X/D=0.875	0.045464
Average	**0.058766**

3.9.3 Comparison Result Contour

The results obtained for medium mesh with SKE turbulence model then compared with the simulation results obtained by van Hooff (van Hooff et al. 2017). The accuracy of the findings from the CFD simulation was verified by this comparison. As shown in Figure 3.12, the validation was performed using the contours by van hooff. The contour from the CFD simulation is shown to mirror the one from van Hooff through the model validation. This means that the results of the SKE turbulence model case simulation may be applied to simulation investigations.

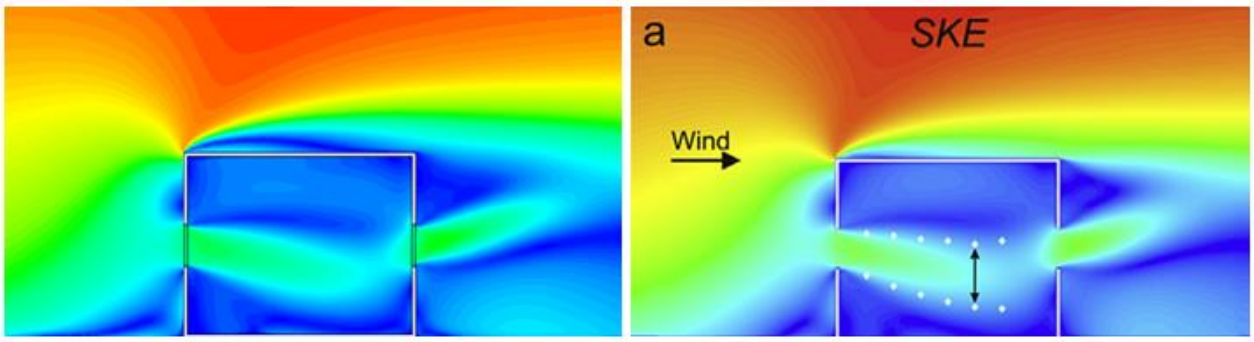

(a) (b)

Figure 3.12: Validation based on velocity contour (a) Simulation result of medium mesh with SKE turbulence model case (b) Result by van Hooff (van Hooff et al. 2017).

3.10 Simulation Cases

The three-dimensional view of each sample in the experiment is shown in Figure 3.13. The opening ratio relationship is calculated by the inlet over outlet opening method, and the size of the inlet opening remains unchanged. The dimensions of each case for the simulation is shown in Table 3.9.

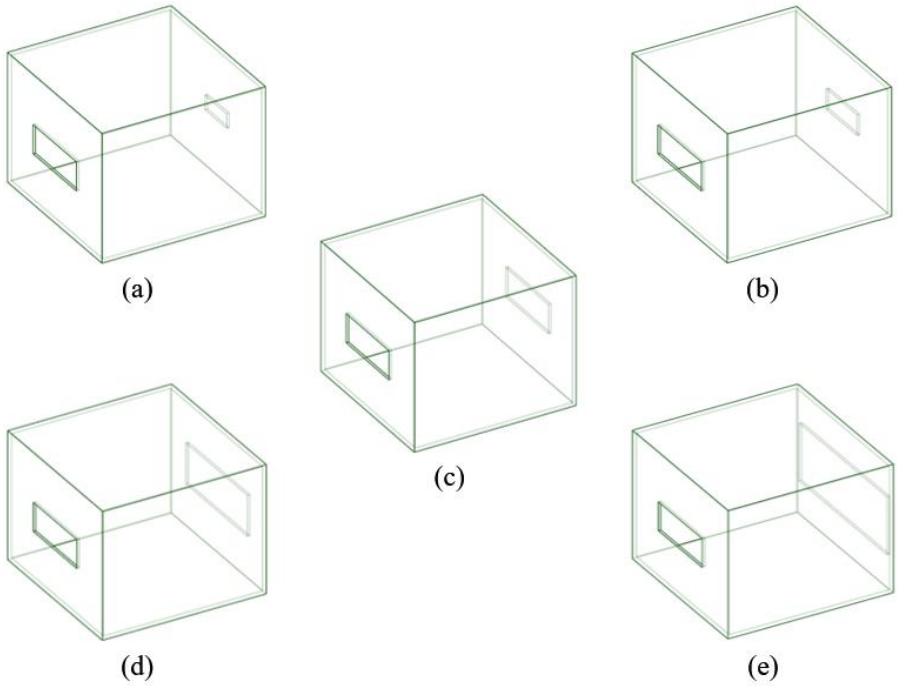

Figure 3.13: Isometric view of all five different cases with opening ratio of (a) 4:1 (b) 2:1 (c) 1:1 (d) 1:2 (e) 1:4.

Table 3.9: Dimension of openings for the five different cases.

Opening Ratio (Inlet to Outlet ratio)	Inlet Opening Size, mm (Width×Height)	Outlet Opening Size, mm (Width×Height)
4∶1	92×36	46×18
2∶1	92×36	65.05×25.46
1∶1	92×36	92×36
1∶2	92×36	130.11×50.91
1∶4	92×36	184×72

3.10.1 Simulation Batches

The purpose of this study is to understand the influence of different opening sizes on natural cross ventilation. Therefore, in the first batch, the configuration of the opposite openings of the house with the same opening size will be checked to understand how the natural cross ventilation airflow passes through the room when the shapes and sizes of the openings on the windward side and the leeward side are in the same configuration. Table 3.10 shows the simulation cases considered in batches.

Table 3.10: Simulation cases in batches.

Batch	Case	Number of buliding	Targeted buliding	Around buliding
			Opening ratio	Opening ratio
Batch 1	1	1	1∶4	None
	2		1∶2	
	3		1∶1	
	4		2∶1	
	5		4∶1	
Batch 2	6	2	1∶4	1∶1
	7		1∶2	
	8		1∶1	
	9		2∶1	
	10		4∶1	
Batch 3	11	2	1∶4	None
	12		1∶2	
	13		1∶1	
	14		2∶1	
	15		4∶1	
Batch 4	16	9	1∶4	1∶1
	17		1∶2	
	18		1∶1	
	19		2∶1	
	20		4∶1	
Batch 5	21	9	1∶4	None
	22		1∶2	
	23		1∶1	
	24		2∶1	
	25		4∶1	

3.11 Body of Influence (BOI) for Two Buildings

Body of influence (BOI) of two buildings case is shows in Figure 3.14. The building of the same size was added at 1H in front of the target building to simulation the urban airflow for the two buildings.

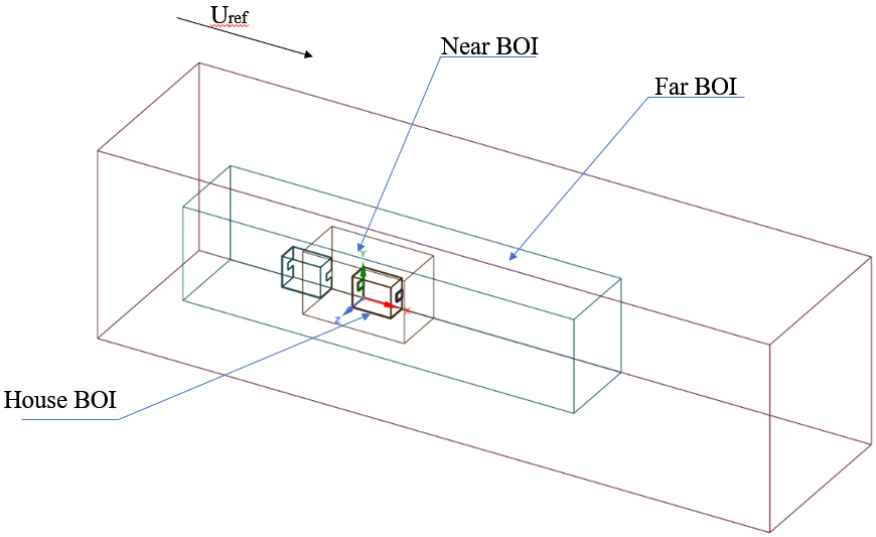

Figure 3.14: Body of influence (BOI) for the two buildings.

3.12 Body of Influence (BOI) for Nine Buildings

Body of influence (BOI) of nine buildings case is shown in Figure 3.15. A total of nine buildings with 1H apart in an arrangement of 3 × 3 with the target building in the centre to simulation the urban airflow for the nine buildings.

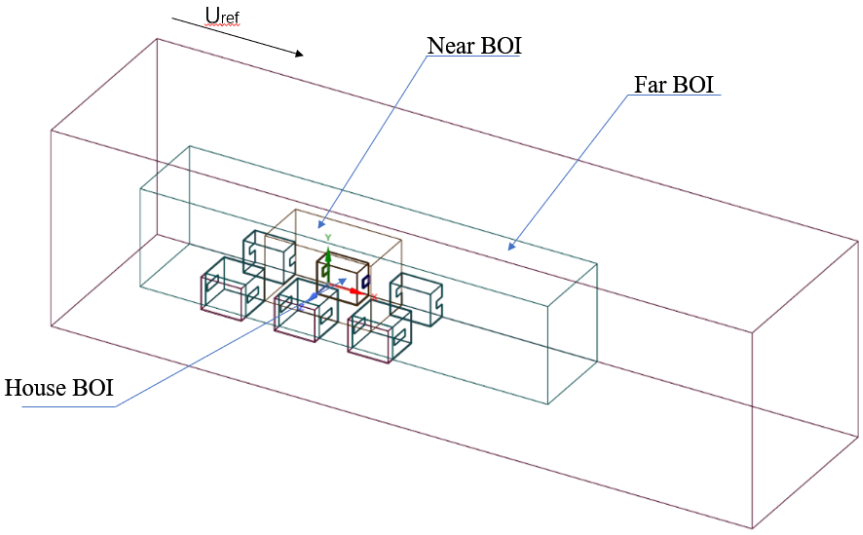

Figure 3.15: Body of influence (BOI) for the nine buildings.

3.12.1 Model Verification – Nine Buildings

In this numerical simulation study, the final calculation result is the reference case of 3 × 3 placement specifications. Before analyzing the results, this study will be compared with Shirzadi (Shirzadi & Tominaga 2022), which will be easier to confirm in whether the air status operation in all twenty five cases is successful. Figure 3.16 shows the simulation result for SKE and realizable k − ε (RLZ) result by Shirzadi (Shirzadi & Tominaga 2022).

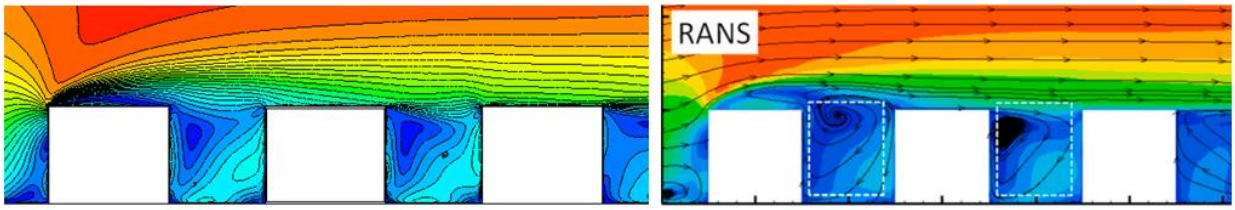

Figure 3.16: Verification based on velocity contour (a) Simulation result of medium mesh with SKE (b) Result by Shirzadi (Shirzadi & Tominaga 2022).

Because the interval selection of geometric modelling is similar in size and quantity, the cyclone negative pressure areas can be observed when the airflow moves through the building. The time and location of these negative pressure areas are roughly the same, indicating that the air state is stable and correct during the simulation process. This also implies that the airflow behaviour in this simulation study under different structural states is meaningful.

CHAPTER 4

RESULTS AND DISCUSSION

4.1 Background

A total of twenty-five different cases were investigated using CFD simulation combined with SKE turbulence model. The results obtained from the simulation were discussed in this chapter. The simulation results were discussed based on velocity, pressure coefficient, age of air, ventilation rate and ventilation contours in different building layout schemes.

4.2 Dimensionless (U/U_{ref})

In Equation (7), the equation for dimensionless U/Uref is displayed. This equation is created by dividing the mean streamwise velocity, U, by the reference velocity, Uref, which is 4.3 m/s.

$$U/U_{ref} = \frac{U}{U_{ref}} \; [-]$$ Equation 7: Dimensionless U/U_{ref}.

Equation (7) is used to determine the dimensionless U/U_{ref} contours as shown in Table 4.1. Referring to Table 4.1, there are differences in the state of air movement in the case of different opening ratios, these contours clearly show that as the leeward opening is increased,

the internal air flow speed gets higher and the affected area of air flow within the building grows larger.

In the cases of one building, as the opening area of the outlet increases, the wind speed at the inlet opening increases and the wind speed at the outlet opening decreases. And the air flow speed at outlet opening position is faster than that at inlet opening position, but with the gradual increase of outlet opening area, the air flow speed at outlet opening position is gradually slower than that at inlet opening position. And nearly the same opening air velocity is achieved when the opening ratio is 1:1. Get a conclusion similar to the literature from the case of one building; the lower velocity is on the side with bigger opening size (Moey et al. 2021).

In the cases of two buildings with openings for the front building, as the opening area of the air outlet opening increases, the wind speed at the intlet opening increases and the wind speed at the outlet opening decreases. In comparison to the cases of one building, the interior airflow speed is influenced by windward-side obstacles with opening, and the air flow speed at the inlet and outlet is slower.

In the cases of two buildings without openings for the front building, as the opening area of the outlet increases, the wind speed at the inlet opening increases and outlet opening decreases. When compared to the case of one building, the interior airflow speed is influenced by the presence of opening obstacles on the windward side, the internal airflow speed becomes slower, and the indoor air flow moves in the opposite direction as the outside air.

In the cases of nine buildings with openings around buildings, increasing the outlet opening area causes increased in wind speed at the inlet and decreased at the outlet. Because there are obstacles with openings around the target building, the air flow velocity inside the building is affected, and the inlet and outlet opening air velocities are slower than in the case of one building.

In the cases of nine buildings without openings around buildings, increasing the opening area at the outlet causes air flow to increase at the inlet. Contrasting to decrease at the air outlet. Because there are obstacles without openings around the target building, the air flow velocity within the building is affected, and the inlet and outlet opening air flow velocities are slower than in the case of one building. Compared with the case of nine buildings without openings for the surrounding buildings, the speed of internal air flow with obstacles without openings around them is lower.

In all cases above, the lowest case of internal air flow is two buildings without openings for the front building with opening ratio of 4:1 case and the fastest internal air flow rate is one building with opening ratio of 1:4 case. It can be seen that as the size of the opening increases, the velocity of the air inside the room increases. In terms of air speed inside the building, one building cases is the fastest, followed by nine building cases, and two building cases is the slowest.

Table 4.1: Dimensionless U/U_{ref} contours for one building, two buildings with/without opening for the front building, and nine buildings with/without opening around buildings with opening ratio of 4:1. 2:1, 1:1, 1:2, and 1:4.

opening ratio	Legend	One building	Two buildings with openings for the front building	Two buildings without openings for the front building	Nine buildings with openings around buildings	Nine buildings without openings around buildings
4 : 1	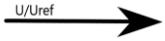	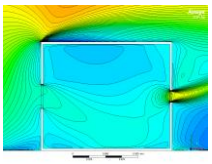	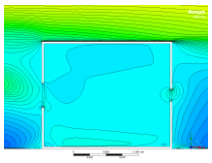	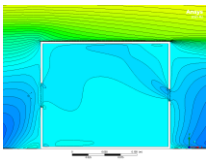	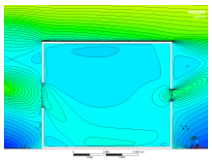	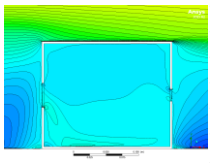
2 : 1	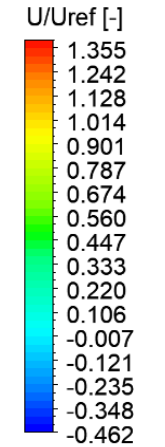	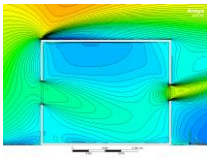	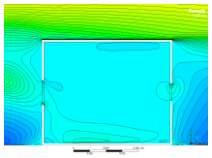	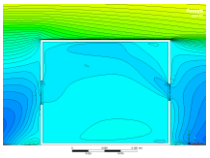	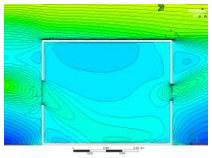	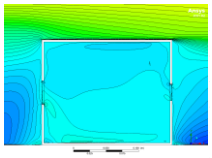
1 : 1		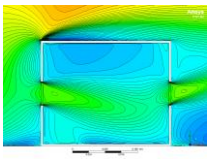	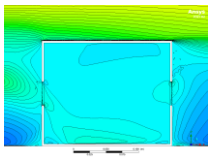	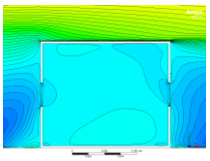	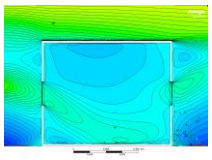	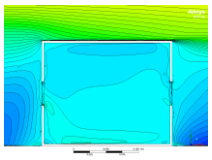
1 : 2		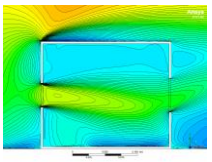	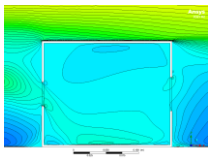	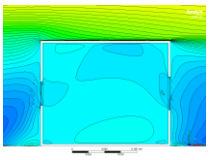	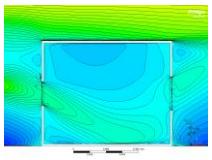	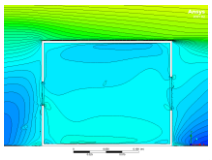
1 : 4		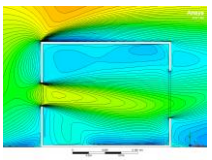	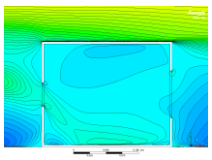	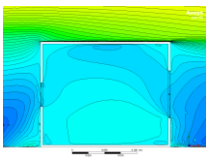	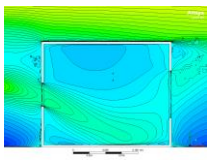	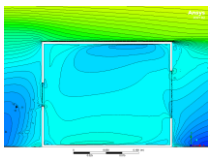

4.3 Pressure Coefficient (ΔCp)

Equation (8) may be used to get the Cp when the air density, ρ is equal to 1.225 kg/m3, the reference velocity, Vref, is equal to 4.3 m/s, the local building pressure, P, and the reference pressure, Pr. The building model's Cp may then be determined (Swami & Chandra 1987).

$$C_p = \frac{P - P_r}{\frac{1}{2}\rho V_{ref}^2}$$ Equation 8: Pressure coefficient.

Referring to Table 4.2, the air movement state differs when various opening ratios are used. These contours clearly show that as the outlet opening area increases, the internal pressure and the inlet opening pressure increase, the outlet opening pressure decrease. Pressure performance varies greatly between simulation cases with different placement structures.

In the cases of one building, as the outlet opening area increases, the indoor pressure of the building decreases. The air enters from inlet opening, and the pressure difference between inside and outside of the building is caused by the continuous air flow and the wall structure. In addition, as the outlet opening area gradually increases, the pressure at the outlet opening decreases, and the pressure is smaller than that at the inlet opening position. Which is similar to that result obtained by Moey (Moey et al. 2021).

In the cases of two buildings with openings for the front building, as the outlet opening area increases, the pressure interior pressure at the building decreases. Due to the characteristics of the building layout structure, a building with opening is placed at the front of the target building. Compared with the one building case, the pressure inside the building is much lower, and the reduction range is smaller. In addition, as the outlet opening area gradually increases, the pressure at the outlet opening decreases, and the pressure is smaller than that at the inlet opening position.

In the cases of two buildings without openings for the front building, as the opening area of the outlet increases, the interior pressure of the building decreases. Due to the characteristics of the building layout structure, a building without opening is placed at the windward region of the target building. Compared with the two buildings with openings for the front building case, the pressure inside the building is much lower, and the reduction range is smaller. And, from the Cp contour map, in this scenario, the pressure at the inlet is larger than the pressure at the outlet opening. With increasing outlet opening area, the pressure differential between inlet and outlet opening becomes more apparent.

In the cases of nine buildings with openings for the front building, as the opening area of the air outlet increases, the interior pressure of the building decreases. Because there are obstacles with openings surrounding by the target building, it blocks the movement of airflow to some extent. Compared with the case of one building, the interior pressure in this case is relatively low. In addition, as the outlet opening area gradually increases, the pressure at the outlet opening decreases, and the pressure is smaller than that at the inlet opening position.

In the cases of nine buildings without openings for the around buildings, as the opening area of the outlet opening increases, the pressure interior the room decreases. Because there are obstacles with openings around the target building, it blocks the movement of airflow to some extent. Compared with the case of one building, the interior pressure in this case is relatively low, this is very consistent with the literature (Shirzadi et al. 2019). In addition, as the outlet opening area gradually increases, the pressure at the outlet opening decreases, and the pressure is smaller than that at the inlet opening position. The interior pressure is lower in this case compared to the case of nine buildings with openings for the front building.

Considering all the situations, the interior pressure is the largest in the case of one building with opening ratio of 4:1. In the case of nine buildings without openings for the around buildings and the ratio 1:4, the interior pressure is the lowest. The size of the outlet opening area affects the internal pressure coefficient. Table 4.2 shows that the lower the opening rate, the lower the pressure in the building, that is to say, the inlet opening remains unchanged, while the outlet opening area increases, and the pressure in the building decreases, which is consistent with the findings of Tecle et al (Tecle et al. 2013).

Table 4.2: Pressure coefficient contours for one building, two buildings with/without opening for the front building, and nine buildings with/without opening around buildings with opening ratio of 4:1. 2:1, 1:1, 1:2, and 1:4.

opening ratio	Legend	One building	Two buildings with openings for the front building	Two buildings without openings for the front building	Nine buildings with openings around buildings	Nine buildings without openings around buildings
4 : 1	U/Uref	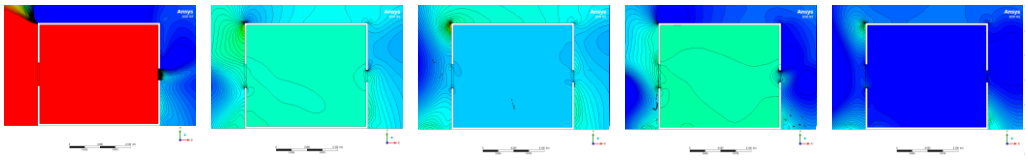				
2 : 1	Cp [-] 0.250 0.219 0.188 0.156 0.125 0.094 0.063 0.031 0.000 -0.031 -0.063 -0.094 -0.125 -0.156 -0.188 -0.219 -0.250	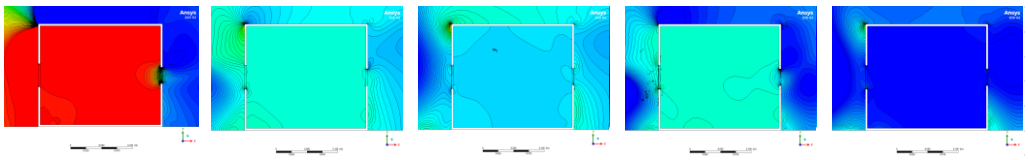				
1 : 1		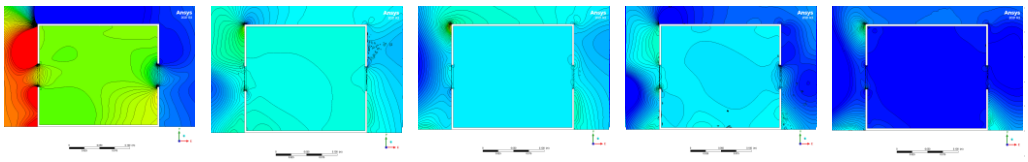				
1 : 2		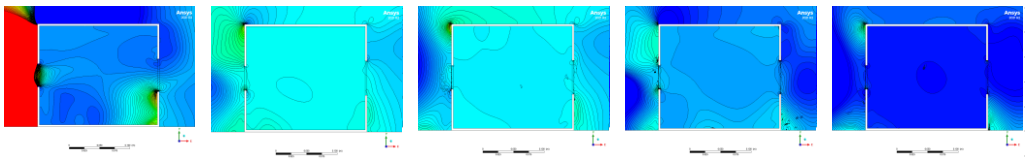				
1 : 4		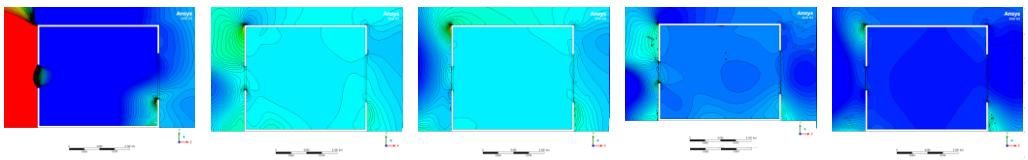				

Combining the results of demensionless and pressure coefficient, the simulation results conform to Bernoulli's law, the faster the fluid velocity, the smaller the pressure generated by the fluid. This point explains how the air flows in the building; In the case of one building, air flows freely move into the building through the inlet opening and exit through the outlet opening. The airflow is subjected to resistance between the wall and the airflow throughout this process, and as a result, the building's internal pressure rises. At this time, the outlet opening is equivalent to the whole building's pressure relief port. Because the air is being obstructed at the inlet opening, the pressure at this position increases. More air can move through the entire room in a unit period by extending the area of the outlet opening, and the airflow could be increased. The most obvious performance is that the air flow speed in the

space increases as the outlet opening area increases. This is consistent with the literature (Moey et al. 2021).

In the cases of two buildings with openings for the front building, as there is an obstacle with a window in the inlet opening direction of target building. Combining table 4.1 and table 4.2, we can see that the air flow speed is very low, and the air enters the building through inlet opening. The pressure of inlet opening and outlet opening position reduces as the outlet opening area increases, and the pressure of inlet opening falls noticeably. In this case, it can be understood that by increasing outlet opening area, The air flow speed of inlet opening is increased, but the speed of outlet opening also increased but not obvious, and it can be seen intuitively that the interior air flow speed has increased to some extent.

In the cases of two buildings without openings for the front building, due to a barrier without an opening in the target building's inlet opening direction, it prevents more air from entering the target building than the obstacle with an opening. Combining table 4.1 and table 4.2, we can see that the pressure at the outlet opening will be slightly higher than that at the inlet opening, which means that the air enters and exit from the outlet opening, which is different from that two buildings with openings for the front building enter from the inlet opening and flow out from the outlet opening. The air velocity is quite sluggish in this air flow condition. The interior air velocity increases as the outlet opening area increases, as do the outlet inflow and inlet outflow speeds, however the air velocity at the inlet opening position is quicker than that at the outlet opening. It can be shown that increasing the outlet opening area increases the internal air velocity to some amount, but in the opposite direction as in all other cases.

In the cases of nine buildings with openings for the around buildings, there are multiple obstacles with openings surrounding the target building, this prevent air from entering that target build, combining table 4.1 and table 4.2 that the pressure at the inlet opening will be higher than at the outlet opening. This means that air enters through the inlet opening and exits through the outlet opening, which corresponds to the corresponding speed change. Compared with the current situation of one building, the interior speed is lower, and the internal wind speed is faster than that of Two Buildings with openings for the front building. This is because the pressure difference between inlet and outlet in this case, and the air is squeezed inside the inlet and the room. With the increase of outlet opening, the air inside the room is released by outlet opening due to the higher pressure of inlet opening, and the air passes through outlet

opening. With the gradual increase of outlet opening area, the pressure inside the room decreases rapidly, and the air flow speed inside the room increases.

In the case of nine buildings without openings for the around building, there are multiple obstacles with no openings surrounding the target building, this prevent more air from entering that target build, Because the inlet opening pressure is only slightly greater than the outlet opening pressure, the air circulation in the room is slow. The pressure of inlet opening is greater than that of outlet opening, which means that air enters from inlet opening and flows out from outlet opening. With the outlet opening area gradually increasing, the pressure at the outlet opening position increases slightly as the outlet opening area increases, and the intlet pressure remains essentially unchanged, implying that when the outlet opening area rises, the air flow speed in the building increased little.

By integrating the information in Tables 4.1 and 4.2, it is discovered that the Coanda effect resurfaced in the study, in which the airflow deviated from the initial flow direction and began to flow along the surface of the protruding object. Horseshoe-shaped vortex exists in the bottom area where air enters. Horseshoe-shaped vortex exists in the bottom area where air enters. As reported by several studies, this recirculation region is attributed to the incoming flow at the air enter wall ,the airflow enters the space and spreads along the building structure, eventually attaching to the room bottom. (Meroney 2009; King et al. 2017; Moey et al. 2022). However, this phenomenon is opposite in the case of two buildings without openings for the front building. Horseshoe-shaped vortex appears on the ceiling of the room after the air enters from the outlet opening. In each case, with the gradual increase of outlet opening area, the Coanda effect becomes more obvious. In addition, in the case of one building, the Coanda effect is weak.

4.4 Age of Air (AOA)

In this study, the fresh air entering into the building and the air staying duration in the building are judged by measuring the age of air (AOA) contours, which impacts the air quality in the building. Table 4.3 shows age of air (AOA) contour in various opening size cases. The air in the room is squeezed out while the airflow continues to enter the space. The time when the room air flows and exits a specific location is recorded, and the images below are generated

In the case of one building, with the movement of airflow, the air in the building quickly moves to the outside, and the residence time of outlet opening is longer than that of inlet opening, and the residence time of air in the moving path of airflow can be seen to be shorter. The air flow speed within and outside the building is improved with the steady increase of the outlet opening area, residence time of air in the room is shortened, which is intuitively shown by the reduction of air AOA parameters inside the room, implying that the air retention period is shortened. When the opening ratio reaches 1∶4, the AOA reaches the minimum value, and the air retention time reaches the best statete.

In the cases of two buildings with openings for the front building, due to the characteristics of the building layout structure, a building with opening is placed in the inlet opening direction of target building. The air flow retention time is obviously affected. As the air flow speed slows down, the AOA value of the air inside the building become higher, which means that the air retention time becomes longer. The air flow speed within and outside the building is improved with the steady increase of the outlet opening area, residence time of air in the building is shortened, which is intuitively shown by the reduction of air AOA parameters inside the building, implying that the air retention period is shortened. When the opening ratio reaches 1:4, the AOA reaches the minimum value, and the air retention time reaches the best state.

In the cases of two buildings without openings for the front building, due to the characteristics of the building layout structure, a building without opening is placed in the inlet opening direction of target building. The air flow retention time is obviously affected. As the air flow speed slows down, the AOA value of the air inside the building become higher, which means that the air retention time becomes longer. The AOA parameter of outlet opening position is lower than inlet opening position due to the air flow entering position. This means that the air retention time of outlet opening is shorter. The air flow speed within and outside the building is improved with the steady increase of the outlet opening area, residence time of air in the building is shortened, which is intuitively shown by the reduction of air AOA

parameters inside the building, implying that the air retention period is shortened. When the opening ratio reaches 1:4, the AOA reaches the minimum value, and the air retention time reaches the best state.

In the cases of nine buildings with openings for the around buildings, because there are obstacles with openings around the target building, compared with the case of one building, the air in the building stays longer. The air flow speed within and outside the building is improved with the steady increase of the outlet opening area, residence time of air in the building is shortened, which is intuitively shown by the reduction of air AOA parameters inside the building, implying that the air retention period is shortened. When the opening ratio reaches 1:4, the AOA reaches the minimum value, and the air retention time reaches the best state.

In the cases of nine buildings without openings for the around building, because there are obstacles without openings around the target building, compared with the case of case of nine buildings with openings for the around buildings the air in the building stays longer. The air flow speed within and outside the building is improved with the steady increase of the outlet opening area, residence time of air in the building is shortened, which is intuitively shown by the reduction of air AOA parameters inside the building, implying that the air retention period is shortened. When the opening ratio reaches 1:4, the AOA reaches the minimum value, and the air retention time reaches the best state.

All cases have one thing in common. The distribution of AOA is mainly affected by the air flow state, which is consistent with the results of many studies. (Tominaga and Blocken 2016; Kosutova 2015; Park and Rhee 2017). And case of two buildings without openings for the front building AOA distribution mainly shows that the air retention time in the upper part of the building is shorter and that in the lower part of the building is longer. While the other 20 cases are opposite. The air retention time above the building is longer, and the air retention time below the building is shorter. This is influenced by the position of Horseshoe-shaped vortex in the room. The larger the Horseshoe-shaped vortex area of table 4.1, the larger the AOA area of the corresponding position. Therefore, the change of air velocity and AOA is in direct proportion.

Table 4.3: Age of air contours for one building, two buildings with/without opening for the front building, and nine buildings with/without opening around buildings with opening ratio of 4:1. 2:1, 1:1, 1:2, and 1:4.

opening ratio	Legend	One building	Two buildings with openings for the front building	Two buildings without openings for the front building	Nine buildings with openings around buildings	Nine buildings without openings around buildings
4 : 1	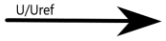	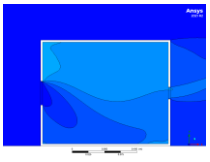	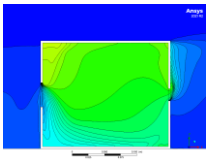	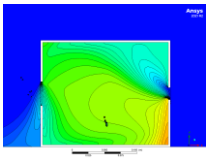	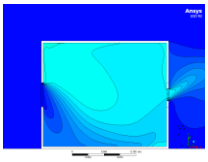	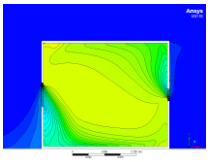
2 : 1	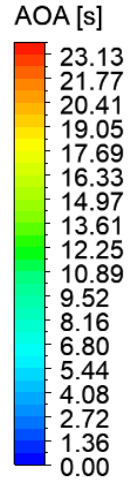	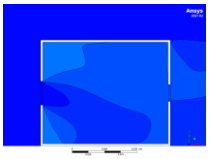	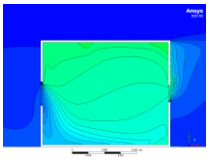	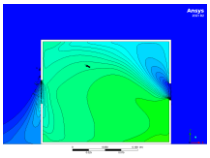	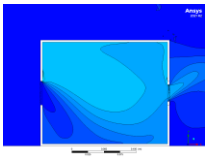	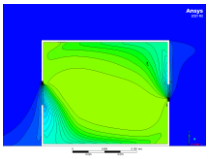
1 : 1		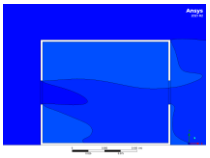	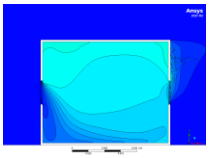	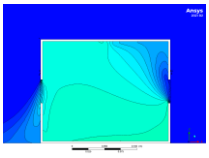	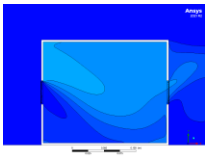	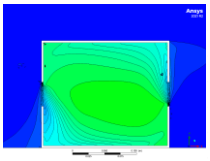
1 : 2		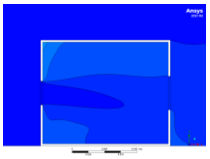	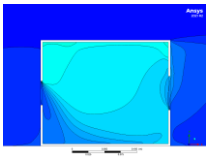	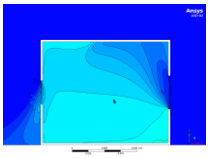	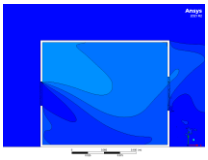	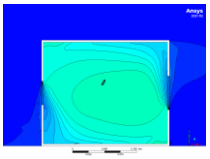
1 : 4		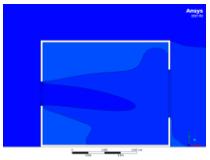	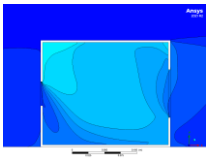	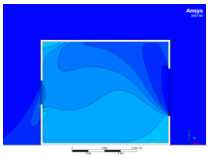	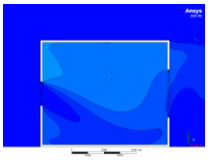	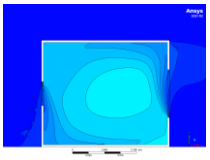

4.5 Ventilation Rate

Figure 4.1 shows the ventilation of different opening rates in each case in this simulation study. In case of one building, there is no obstacle to prevent ventilation, and the overall ventilation is the best, with the highest ventilation rate of 0.00453 m^3/s at 1:4 opening rate and the lowest ventilation rate of 0.0032 m^3/s at 4:1 opening ratio. Table 4.4 shows the ventilation rate values of different opening rates in one building, two buildings with/without opening for the front building, nine buildings with/without opening around buildings, with opening ratio of 4:1. 2:1, 1:1, 1:2, and 1:4.

In the cases of the case of two buildings with openings for the front building, because there is a building with openings in the entrance opening direction to block the air flow, the overall ventilation rate in general, with the highest ventilation rate of 0.00163 m^3/s at the opening ratio of 1:4 and the lowest ventilation rate of 0.00012 m^3/s at the opening ratio of 4:1.

n the case of two buildings without openings for the front building, there is a building without openings in the inlet opening direction to block the air flow, so the overall ventilation is general. But it is worse than in the case of two buildings with openings for the front building, with the highest ventilation rate of 0.00134 m^3/s at the opening ratio of 1:4 and the lowest ventilation rate of 0.00011 m^3/s at the opening ratio of 4:1.

In the cases of nine buildings with openings for the around buildings, because there are buildings with openings around the target building that affect the air flow, the overall ventilation rate is better than that of two buildings cases, with the highest ventilation rate of 0.00261 m^3/s at the opening ratio of 1:4 and the lowest ventilation rate of 0.00087 m^3/s at the opening ratio of 4:1.

In the cases of nine buildings without openings for the around building, because there are buildings without openings around the target building that affect the air flow, the overall ventilation rate is better than that of two buildings cases, however, it is lower than that of Nine Buildings with Openings for the around building, with the highest ventilation rate of 0.00221 m^3/s at the opening ratio of 1:4 and the lowest ventilation rate of 0.00041 m^3/s at the opening ratio of 4:1.

Overall, one building has the best ventilation rate, followed by nine buildings with openings for the around building, and two buildings without openings for the front building has the worst ventilation rate.

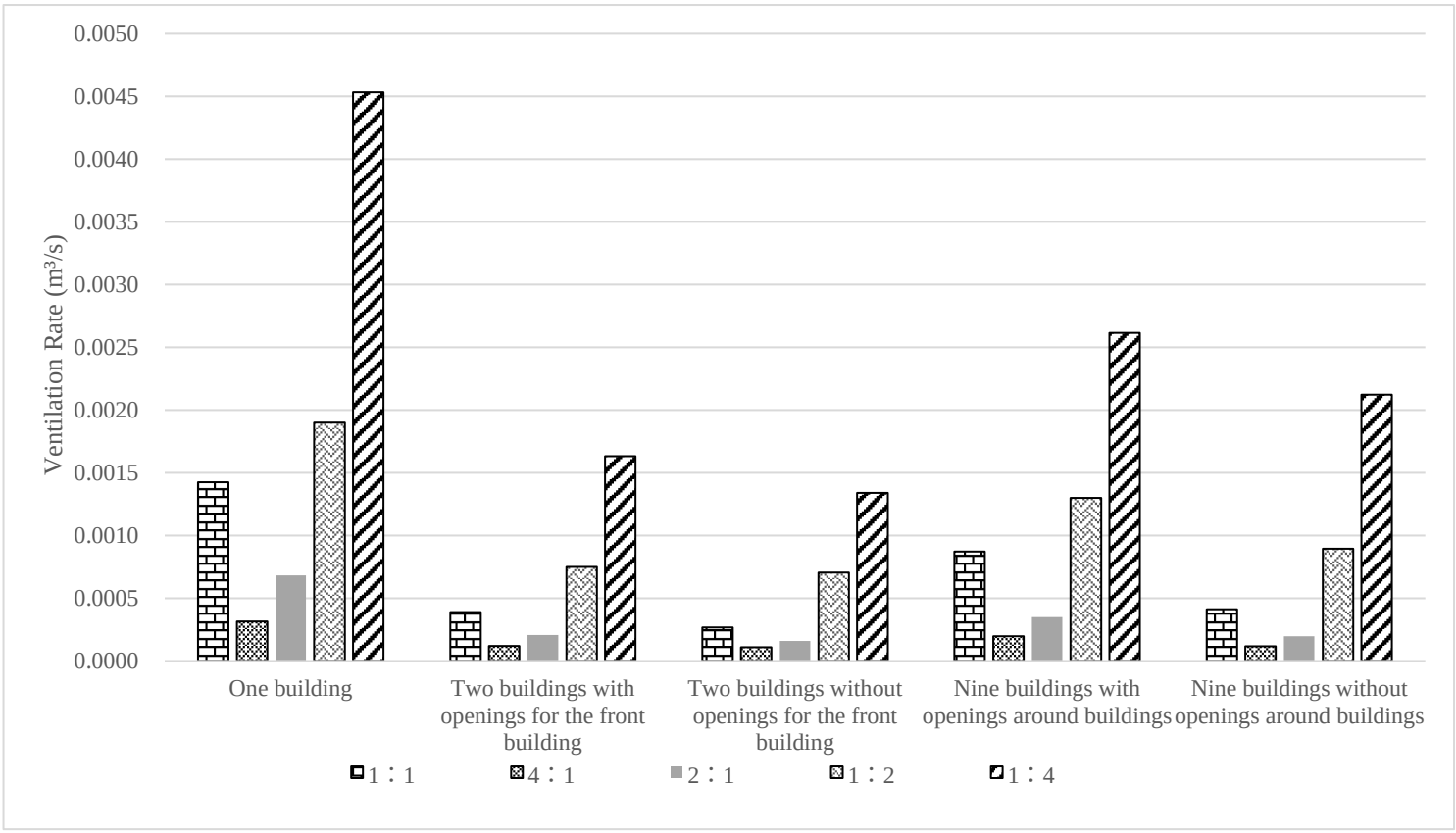

Figure 4.1: Ventilation rate under different opening ratio in each building layout.

Table 4.4: Ventilation rate for different opening ratio.

Opening rate	One building	Two buildings with openings for the front building	Two buildings without openings for the front building	Nine buildings with openings around buildings	Nine buildings without openings around buildings
1：1	0.00143	0.00039	0.00027	0.00087	0.00041
4：1	0.00032	0.00012	0.00011	0.00020	0.00012
2：1	0.00068	0.00021	0.00016	0.00035	0.00020
1：2	0.00190	0.00075	0.00070	0.00130	0.00089
1：4	0.00453	0.00163	0.00134	0.00261	0.00212

Figure 4.2 shows the comparison of twenty-five different cases and one building case with 1:1 opening size, which helps to better understand the ventilation performance of each case. From figure 4.2, it can be seen that the percentage for the one building case with an opening ratio of 1:4 is the highest at 318.0%, and the percentage for the case of two buildings without openings for the front building with the opening ratio of 4:1 is the lowest at 7.7%. When the opening ratio is greater than 1, the inlet opening area is larger than the outlet opening, and the ventilation rate will be less than 1:1 for the case of the same arrangement structure, and vice versa. The result is consistent with the literature (Moey et al. 2022). This phenomenon is the same in every building arrangement

In the two building cases, the ventilation rate performance for the case of with opening for the front building is better than that of the case without opening for the front building, and the highest ventilation efficiency reaches 114.5%. In the nine buildings cases, the ventilation rate performance of the case with opening around building is better than that of the case without opening around building, and the highest ventilation efficiency reaches 183.4%. This result shows that the ventilation performance of the target building with openings in the surrounding buildings is better than that of the surrounding buildings without openings in urban ventilation.

When the opening ratio is 1:1, the case ventilation rate of two building with opening for the front building is 27.4% of that of one building, and the case ventilation rate of two building without opening for the front building is 18.8% of that of one building,nine The case ventilation rate of buildings with opening around buildings is 61.2% of that one building, and the case ventilation rate of nine buildings without opening around buildings is 28.9% of that of one building. Nine buildings with opening around buildings and a case with an opening ratio of 1:1 is better ventilated. By comparing the cases of two buildings and nine buildings with the same opening ratio, the same case comparison of nine buildings with opening around buildings is better.

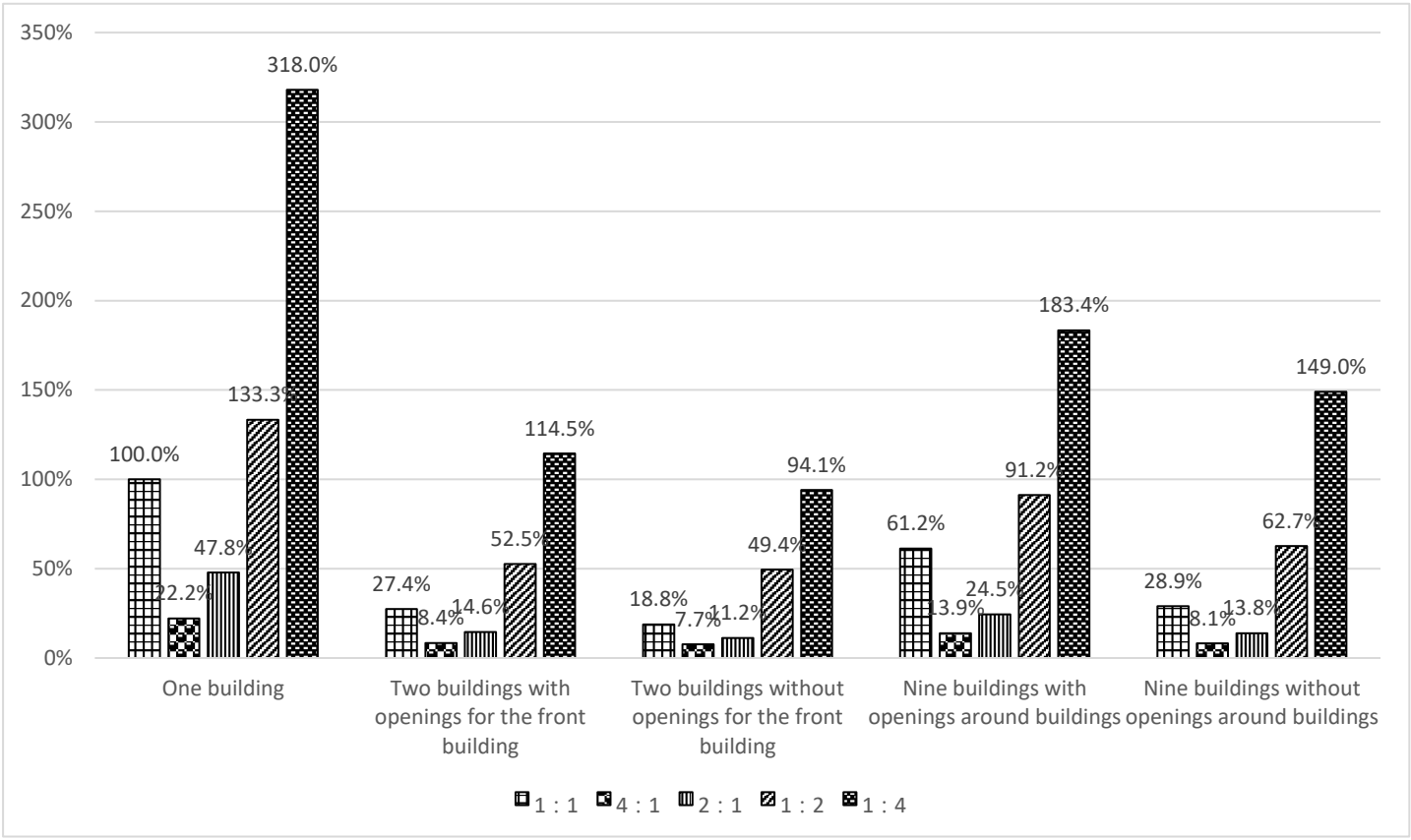

Figure 4.2: Comparison of ventilation rate between one building (opening ratio of 1:1) and two buildings with/without opening for the front building, and nine buildings with/without opening around buildings with opening ratio of 4:1. 2:1, 1:1, 1:2, and 1:4.

The percentage difference of ventilation rate of five arranged cases and one building case is shown in figure 4.3. The higher the percentage, the smaller the loss of ventilation rate in this case is when the ventilation rate and one building have the corresponding opening ratio. The percentage does not indicate a comparison of each instance to the best ventilation case of a single building, but rather a comparison of two distinct display specifications within the same opening. Follow figure 4.3 can be seen that nine buildings with openings for the around building with an opening ratio of 1：2 has reached the maximum percentage of 68.44%. Two buildings without openings for the front building with an opening ratio of 1：1 achieved a minimum percentage of 18.79%.

Compared with the ventilation rate of one building, the percentage of all kinds of arrangement modes with 1:2 opening is the highest, and the loss caused by the arrangement modes of buildings is the lowest. Compared with the ventilation rate of one building, the percentage of all kinds of arrangement modes with 2:1 opening is the lowest, and the loss caused by the arrangement modes of buildings is the highest. These different percentage changes show that simply increasing the outlet area will not keep the ventilation rate up. Changing the arrangement of buildings and matching the appropriate opening ratio is the key to decrease the loss of ventilation rate.

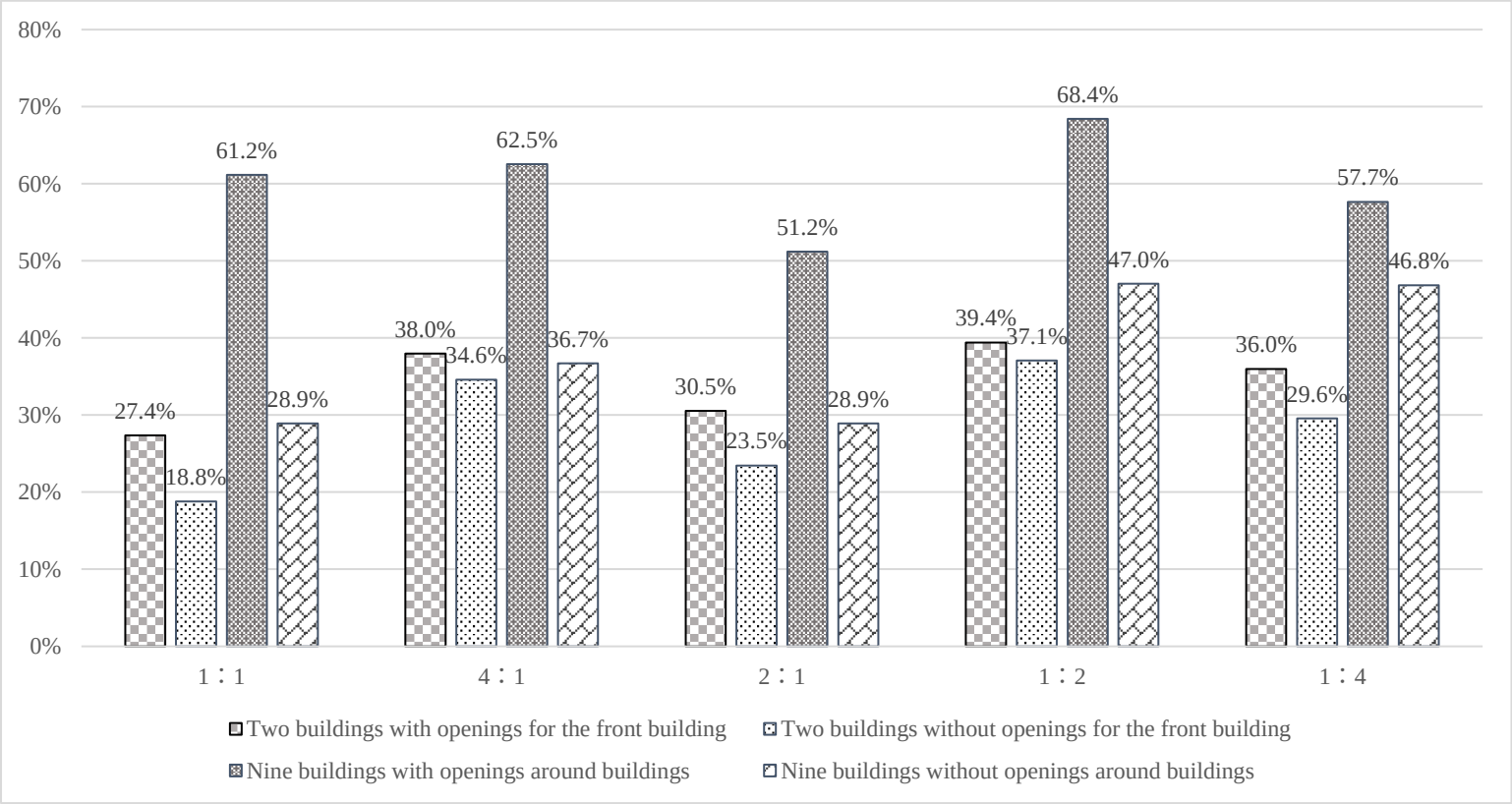

Figure 4.3: Ventilation rate values are compared between different display structures and one building in each case.

4.6 Ventilation Contours in Different Building Layout.

Figure 4.4 shows the contour of the velocity at the building height of 0.5H, which helps to observe the influence of opening size on the surrounding wind field. and the contours are cut from the plane of symmetry, It can be seen that after the air touches the building, it forms a surface jet on the surface of the building due to the Coanda effect. The two building cases show wakes of similar length but shorter than one building case. In the case with opening for the front building, part of the air passes to the front of the target building, but not in the case without opening for the front building. This makes the ventilation efficiency of with opening for the front building case better than that of with out opening

In the cases of nine buildings, both of them show wakes of similar length but longer than those of one building. In the case of with opening around buildings, a higher low-pressure area is generated between the two buildings and spreads rapidly backwards. This is The ventilation efficiency of nine cases is generally better than that of two building cases; the low-pressure area in the middle of the two rows of buildings will effectively accelerate the flow of air between each row, thus achieving the purpose of improving the air flow inside the target buildings. At the same time with opening around buildings, Air can flow to the rear through the openings in the front building, which effectively improves air circulation and makes the ventilation rate higher than without opening around buildings. Also in the case of nine building without opening around buildings the result is consistent with the literature(Shirzadi et al. 2020).

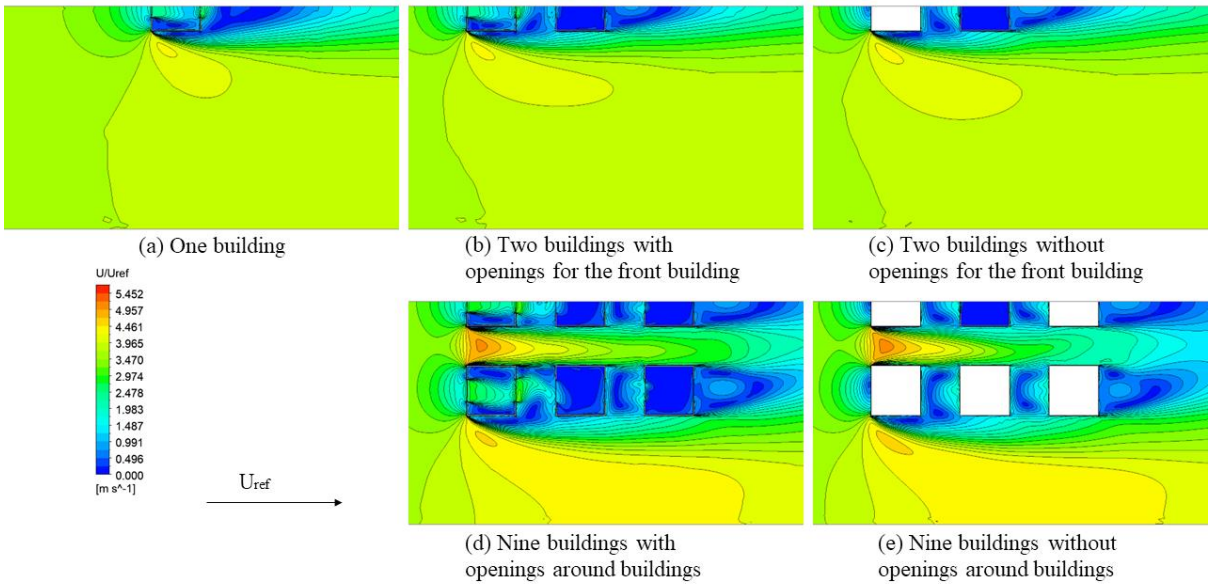

Figure 4.4: Contours of the velocity and over a horizontal plane at z/H= 0.5 for different building layout.

As the building layout changes, the airflow inside the target building also changes. For the cases of two buildings, a building is added to the inlet opening side of the target building, the air flow into the target building decreases, the pressure inside the building becomes lower, the air flow rate inside becomes slower, and the age of air (AOA) becomes longer. In the case of the same opening ratio, the overall ventilation performance of nine building cases is worse than that of one building, but better than that of two buildings. There are other buildings around the target building arranged in 3 × 3, although the air velocity flow into the target building is affected to a certain extent, but under the same opening ratio, the air velocity inside the target building of nine buildings cases is still higher than that of the two building faster phenomena, this directly reduces the time of AOA and increases the ventilation rate.The reason for this phenomenon is that due to the characteristics of the nine buildings arrangement, a relatively fast air velocity is formed around the target building. In the fluid, according to Bernoulli's law, the faster the area in the fluid, the lower the pressure, so it can be understood that the lower pressure sucks out the air inside the building to a certain extent. In the arrangement of Two buildings, when the target building is blocked by the building in front of the airflow, there is no high-speed airflow in the surrounding environment. This makes the ventilation performance of the two building cases not as good as the nine building cases under the same opening ratio.

Figure 4.5 shows the nine building with opening around buildings cases. Changing the opening ratio of the target building has little effect on the overall wind field, and some obvious changes exist in the area near the inlet and outlet opening of the target building. This feature shows that The opening change of a single house cannot change the air flow field in a larger area. With the gradual increase of the outlet opening area, the pressure around the inlet opening of the target building gradually decreases, and the air flow speed gradually becomes faster.

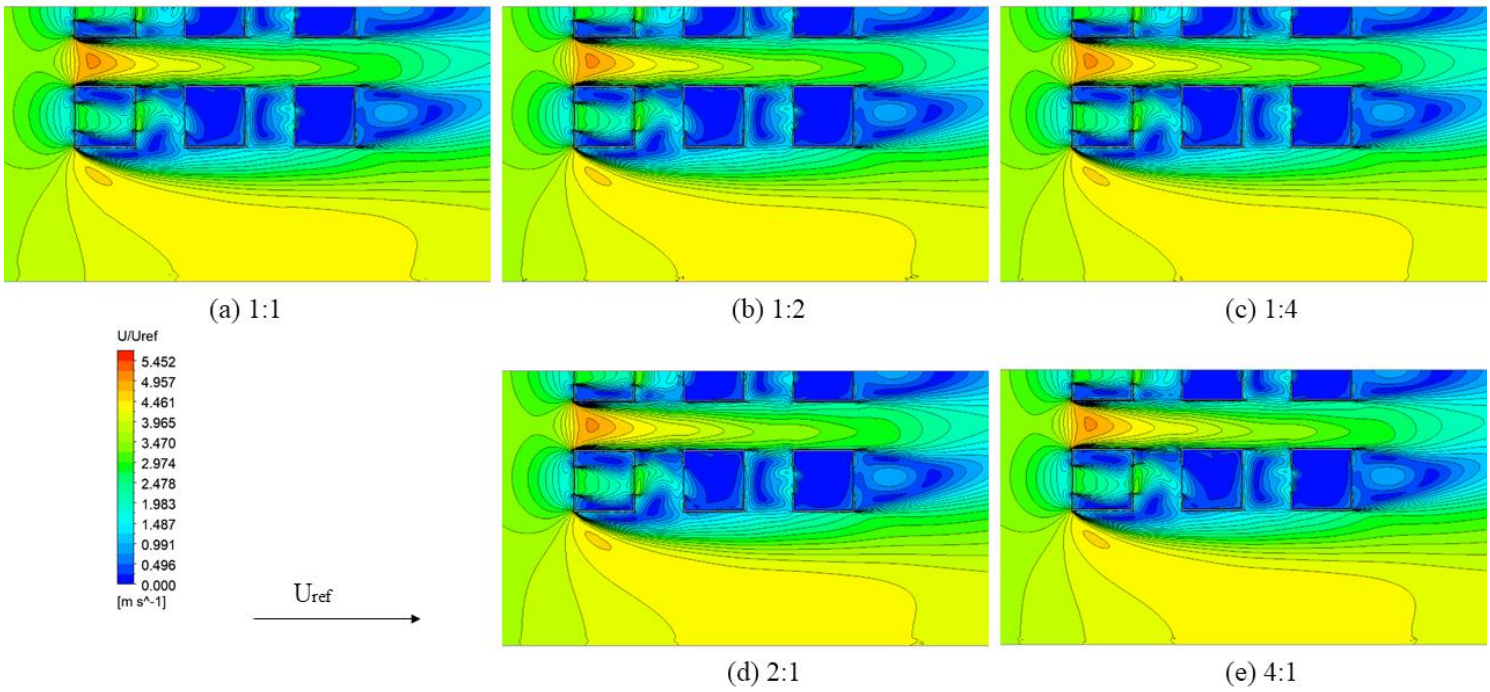

Figure 4.5: Contours of the velocity and over a horizontal plane at z/H= 0.5 for nine buildings with opening around buildings.

CHAPTER 5

CONCLUSION AND FUTURE WORK RECOMMENDATION

5.1 Conclusions

The effects of varying opening ratio and building arrangement have been studied. The building arrangement (i) one building, (ii) two buildings with opening for the infront building, (iii) two buildings without opening for the infront building, (iv) nine buildings with opening around buildings, (v) nine buildings without opening around buildings. have been performed with opening configurations,4:1,2:1,1:1,1:2,1:4. When the configurations are described as "inlet" and "outlet." Best practises from the literature are used to build the computational domain, and numerical simulations are carried out by interpreting an atmospheric boundary layer (ABL). Through study of the grid convergence index (GCI), the reference grid is chosen. The factor of two of observation (FAC2) study of the numerical simulation utilising the 3D-RANS equation standard k-ε (SKE) with enhanced wall treatment (EWT) demonstrates excellent accuracy. This study concludes the research of the internal air profiles, internal velocities, pressure coefficient, age of air, ventilation rate, and ventilation contours in various building layouts. This report has contributed the following advances:

i. The pressure of the windward port and the pressure of the leeward port are affected by the ratio of the two areas; when the air outlet opening size is larger than the inlet opening size, smaller openings create higher pressures, which also create faster air flows through smaller openings, and this feature holds true in all cases in the study.

ii. As the opening ratio is adjusted from 4:1 to 1:4, the inlet openin area remains unchanged, the outlet opening area gradually increases, and ΔCp decreases gradually.

iii. As the opening ratio is adjusted from 4:1 to 1:4, the inlet openin area remains unchanged, the outlet opening area gradually increases, and the value of age of air (AOA) decreases gradually, which means that the time for air to stay in the room is reduced. And the position where the air flow is fast has a lower AOA than the position where the air flow is slow. This feature is reflected in each case

iv. The case ventilation performance of the nine building is better than that of the two building, which is due to case of nine building, the dense city produces a higher negative pressure zone between each row of buildings, but in the case of two building, there is no, so the air circulation performance is higher in the target building of nine building.

v. There is a difference between the flow state of the wind field passing through the urban environment and the individual buildings. The air flow in the urban environment will flow into the target building after passing through buildings. However, air enters directly into buildings when they stand alone, which is less the case in urban environments.

vi. The results of Ventilation Contours In Different Building Layout Schemes show that the airflow passing through the building openings has an impact on the wake behind the building, changing the flow state of the wake behind the building.

vii. The urban environment determines the state of the urban airflow, and the urban airflow determines the air flow performance of the cross ventilation inside the building.

5.2 Recommendation for Future Work

The following recommendation include but are not limited to:

- Future work should compare the results of various CFD turbulence models..
- Future work should manipulate the wind direction.
- Future simulations can further study different opening configurations, such as circles and trapezoids, etc.
- Future simulation research should consider to include more buildings.

References

Addis, B. （2020）. The historical use of physical model testing in wind engineering. PHYSICAL MODELS: Their historical and current use in civil and building engineering design, 711-751. https://doi.org/10.1002/9783433609613.ch25**.**

Bangalee, M. Z. I., Miau, J. J., Lin, S. Y., & Ferdows, M. (2014). Effects of lateral window position and wind direction on wind-driven natural cross ventilation of a building: a computational approach. *Journal of Computational Engineering*, *2014*. http://dx.doi.org/10.1155/2014/310358.

Blocken, B. (2015). Computational Fluid Dynamics for urban physics: Importance, scales, possibilities, limitations and ten tips and tricks towards accurate and reliable simulations. *Building and Environment*, *91*, 219-245. https://doi.org/10.1016/j.buildenv.2015.02.015

Brown, M. J., Lawson, R. E., DeCroix, D. S., & Lee, R. L. (2001). Comparison of centerline velocity measurements obtained around 2D and 3D building arrays in a wind tunnel. Int. Soc. Environ. Hydraulics, Tempe, AZ, 5, 495.

Chang, C. H., & Meroney, R. N. (2003). Concentration and flow distributions in *engineering and industrial aerodynamics*, *91*(9), 1141-1154. https://doi.org/10.1016/S0167-6105(03)00056-4.

Cho, J., Yoo, C., & Kim, Y. (2012). Effective opening area and installation location of windows for single sided natural ventilation in high-rise residences. *Journal of Asian Architecture and Building Engineering*, *11*(2), 391-398. https://doi.org/10.3130/jaabe.11.391.

Cionco, R. M., & Ellefsen, R. (1998). High resolution urban morphology data for urban wind flow modeling. *Atmospheric Environment*, *32*(1), 7-17. https://doi.org/10.1016/S1352-2310（97）00274-4.

Dascalaki, E., Santamouris, M., Argiriou, A., Helmis, C., Asimakopoulos, D. N., Papadopoul os, K., & Soilemes, A. (1995). Predicting single sided natural ventilation rates in buildings. S olar Energy, 55(5), 327–341. doi:10.1016/0038-092x(95)00057-x.

DEPARTMENT OF STANDARDS MALAYSIA. (2014). Energy efficiency and use of renewable energy for non -residential buildings - Code of practice (Second revision).

Endo, T., Kurabuchi, T., Nonaka, T., Ishii, M., Ohba, M., Goto, T., & Akamine, Y. (2006). Development of a simulator for indoor airflow distribution in a cross-ventilated building using the local dynamic similarity model. *International Journal of Ventilation*, *5*(1), 31-42. h ttps://doi.org/10.1080/14733315.2006.11683725

Fan, M., Fu, Z., Wang, J., Wang, Z., Suo, H., Kong, X., & Li, H. (2022). A review of different ventilation modes on thermal comfort, air quality and virus spread control. Building and Environment, 108831. https://doi.org/10.1016/j.buildenv.2022.108831.

Fan, S., Wykes, M. D., Lin, W. E., Jones, R. L., Robins, A. G., & Linden, P. F. (2021). A full-scale field study for evaluation of simple analytical models of cross ventilation and single-sided ventilation. Building and Environment, 187, 107386. https://doi.org/10.1016/j.buildenv.2020.107386.

Franke, J., Hellsten, A., Schlünzen, K. H., & Carissimo, B. (2007). Best practice guideline for the CFD simulation of flows in the urban environment-a summary. In *11th Conference on Harmonisation within Atmospheric Dispersion Modelling for Regulatory Purposes, Cambridge, UK, July 2007*. Cambridge Environmental Research Consultants.

Gousseau, P., Blocken, B., Stathopoulos, T., & Van Heijst, G. J. F. (2011). CFD simulation of near-field pollutant dispersion on a high-resolution grid: a case study by LES and RANS for a building group in downtown Montreal. Atmospheric Environment, 45(2), 428-438. https://doi.org/10.1016/j.atmosenv.2010.09.065.

Hachem M, Saleh N, Paunescu AC, Momas I, Bensefa-Colas L.(2019). Exposure to traffic air pollutants in taxicabs and acute adverse respiratory effects: a systematic review. Sci Total Environ. 2019;693:133439. https://doi.org/10.1016/j.scitotenv.2019.07.245.

Hadavi, M., & Pasdarshahri, H. (2020). Quantifying impacts of wind speed and urban neighborhood layout on the infiltration rate of residential buildings. *Sustainable Cities and Society*, *53*, 101887. https://doi.org/10.1016/j.scs.2019.101887.

Hadavi, M., & Pasdarshahri, H. (2020). Quantifying impacts of wind speed and urban neighborhood layout on the infiltration rate of residential buildings. *Sustainable Cities and Society*, *53*, 101887. https://doi.org/10.1016/j.scs.2019.101887.

Hang, J., Luo, Z., Sandberg, M., & Gong, J. (2013). Natural ventilation assessment in typical open and semi-open urban environments under various wind directions. Building and environment, 70, 318-333. https://doi.org/10.1016/j.buildenv.2013.09.002

Hawendi, S., & Gao, S. (2016). Investigation of opening positions on the natural ventilation in a low-rise building by CFD analysis. In *Proceedings of the 3rd International Conference on Fluid Flow, Heat and Mass Transfer (FFHMT'16, Paper No151). Ottawa, Canada*.

Hayden, J., Capece, V., Lepicovsky, J., & McFarland, E. (2002). The Influence Coefficient Method for Airfoils Oscillating in Pitch at Large Incidence. In *38th AIAA/ASME/SAE/ASEE Joint Propulsion Conference & Exhibit* (p. 4087). https://doi.org/10.2514/6.2002-4087.

He, B. J., Ding, L., & Prasad, D. (2020). Wind-sensitive urban planning and design: Precinct ventilation performance and its potential for local warming mitigation in an open midrise gridiron precinct. *Journal of Building Engineering*, *29*, 101145. https://doi.org/10.1016/j.jobe.2019.101145.

Heist, D. K., Perry, S. G., & Brixey, L. A. (2009). A wind tunnel study of the effect of roadway configurations on the dispersion of traffic-related pollution. *Atmospheric Environment*, *43*(32), 5101-5111. https://doi.org/10.1016/j.atmosenv.2009.06.034.

Hongshan, L., Yubin, L., Xinyu, X., Zhiyan, Z., & Xiwen, L. (2015). Development of wind tunnel test technologies in agricultural aviation engineering, 31. doi：10.11975/j.issn.1002-6819.2015.z2.001.

Hu, C. H., Kurabuchi, T., & Ohba, M. (2005). Numerical study of cross-ventilation using two-equation RANS turbulence models. *International Journal of Ventilation*, *4*(2), 123-132.

Hu, C. H., Ohba, M., & Yoshie, R. (2008). CFD modelling of unsteady cross ventilation flows using LES. Journal of Wind Engineering and Industrial Aerodynamics, 96(10-11), 1692-1706. https://doi.org/10.1016/j.jweia.2008.02.031.

Hu, S., Yan, D., Cui, Y., & Guo, S. (2016). Urban residential heating in hot summer and cold winter zones of China—Status, modeling, and scenarios to 2030. *Energy Policy*, *92*, 158-170. https://doi.org/10.1016/j.enpol.2016.01.032.

Huang, Y., Hu, X., & Zeng, N. (2009). Impact of wedge-shaped roofs on airflow and pollutant dispersion inside urban street canyons. Building and Environment, 44(12), 2335-2347. https://doi.org/10.1016/j.buildenv.2009.03.024.

Bady, M., Kato, S., Takahashi, T., & Huang, H. (2011). An experimental investigation of the wind environment and air quality within a densely populated urban street canyon. *Journal of Wind Engineering and Industrial Aerodynamics*, *99*(8), 857-867. https://doi.org/10.1016/j.jweia.2011.06.005

Jiang, Y., & Chen, Q. (2002). Effect of fluctuating wind direction on cross natural ventilation in buildings from large eddy simulation. *Building and environment*, *37*(4), 379-386. https://doi.org/10.1016/S0360-1323（01）00036-1.

Jiang, Y., & Chen, Q. (2002). Effect of fluctuating wind direction on cross natural ventilation in buildings from large eddy simulation. *Building and environment*, *37*(4), 379-386. https://doi.org/10.1016/S0360-1323（01）00036-1

Jiang, Y., & Chen, Q. (2003). Buoyancy-driven single-sided natural ventilation in buildings with large openings. International Journal of heat and mass transfer, 46(6), 973-988. https://doi.org/10.1016/S0017-9310(02)00373-3

Jiang, Y., & Chen, Q. (2003). Buoyancy-driven single-sided natural ventilation in buildings with large openings. International Journal of heat and mass transfer, 46(6), 973-988. https://doi.org/10.1016/S0017-9310(02)00373-3.

Jomehzadeh, F., Nejat, P., Calautit, J. K., Yusof, M. B. M., Zaki, S. A., Hughes, B. R., & Yazid, M. N. A. W. M. (2017). A review on windcatcher for passive cooling and natural ventilation in buildings, Part 1: Indoor air quality and thermal comfort assessment. Renewable and Sustainable Energy Reviews, 70, 736-756. https://doi.org/10.1016/j.rser.2016.11.254

Karava, P., & Stathopoulos, T. (2012). Wind-induced internal pressures in buildings with large façade openings. Journal of engineering mechanics, 138(4), 358-370. https://doi.org/10.1061/（ASCE）EM.1943-7889.0000296.

Karava, P., Stathopoulos, T., & Athienitis, A. K. (2011). Airflow assessment in cross-ventilated buildings with operable façade elements. *Building and environment*, *46*(1), 266-279. https://doi.org/10.1016/j.buildenv.2010.07.022.

Kastner-Klein, P., & Plate, E. J. (1999). Wind-tunnel study of concentration fields in street canyons. *Atmospheric Environment*, *33*(24-25), 3973-3979. https://doi.org/10.1016/S1352-2310(99)00139-9.

King, M. F., Khan, A., Delbosc, N., Gough, H. L., Halios, C., Barlow, J. F., & Noakes, C. J. (2017). Modelling urban airflow and natural ventilation using a GPU-based lattice-Boltzmann method. *Building and Environment*, *125*, 273-284. https://doi.org/10.1016/j.buildenv.2017.08.048

Kosutova, K. A. T. A. R. I. N. A., van Hooff, T., Blocken, B., & Hensen, J. L. M. (2015). CFD analysis of ventilative cooling in a generic isolated building equipped with ventilation louvers. *Healthy Buildings Europe*, *2015*. https://doi.org/10.1016/j.scs.2020.102196

Larsen, T. S., & Heiselberg, P. (2008). Single-sided natural ventilation driven by wind pressure and temperature difference. *Energy and buildings*, *40*(6), 1031-1040. https://doi.org/10.1016/j.enbuild.2006.07.012.

Li, C., Li, X., Su, Y., & Zhu, Y. (2012). A new zero-equation turbulence model for micro-scale climate simulation. *Building and environment*, *47*, 243-255. https://doi.org/10.1016/j.buildenv.2011.07.015.

Liu, X. P., Niu, J. L., Kwok, K. C., Wang, J. H., & Li, B. Z. (2010). Investigation of indoor air pollutant dispersion and cross-contamination around a typical high-rise residential building: wind tunnel tests. *Building and Environment*, *45*(8), 1769-1778. https://doi.org/10.1016/j.buildenv.2010.02.003.

Liu, X. P., Niu, J. L., Kwok, K. C., Wang, J. H., & Li, B. Z. (2010). Investigation of indoor air pollutant dispersion and cross-contamination around a typical high-rise residential building: wind tunnel tests. *Building and Environment*, *45*(8), 1769-1778. https://doi.org/10.1016/j.buildenv.2010.02.003.

Mahadi, N. F., Zain, N. R. M., & Othman, A. H. A. (2021). The Role of Zakat in Achieving Economic Empowerment, Environmental Sustainability, and Social Re-Engineering as Promoted in the 12th Malaysia Plan. In Handbook of Research on Islamic Social Finance and Economic Recovery After a Global Health Crisis (pp. 30-46). IGI Global. DOI: 10.4018/978-1-7998-6811-8.ch003

Meroney, R. N. (2009, June). CFD prediction of airflow in buildings for natural ventilation. In *11th Americas Conference on Wind Engineering*.

Miao, S., & Chen, F. (2008). Formation of horizontal convective rolls in urban areas. *Atmospheric Research*, *89*(3), 298-304. https://doi.org/10.1016/j.atmosres.2008.02.013.

Moey, L. K., Sing, Y. H., Tai, V. C., Go, T. F., & Ng, J. Y. (2022). Numerical investigation of inlet opening size on wind-driven cross ventilation. Journal of Mechanical Engineering and Sciences, 16(1), 8662-8672. https://doi.org/10.15282/jmes.16.1.2022.02.0685.

Moey, L. K., Sing, Y. H., Tai, V. C., Go, T. F., & Sia, Y. Y. (2021). Effect of Opening Size on Wind-Driven Cross Ventilation. International Journal of Integrated Engineering, 13(6), 99-108. https://doi.org/10.30880/ijie.2020.13.06.009.

Moonen, P., Blocken, B., & Carmeliet, J. （2007）. Indicators for the evaluation of wind tunnel test section flow quality and application to a numerical closed-circuit wind tunnel. Journal of wind engineering and industrial aerodynamics, 95（9-11）, 1289-1314. https://doi.org/10.1016/j.jweia.2007.02.027.

Niachou, K., Hassid, S., Santamouris, M., & Livada, I. (2005). Comparative monitoring of natural, hybrid and mechanical ventilation systems in urban canyons. Energy and Buildings, 37(5), 503-513. https://doi.org/10.1016/j.enbuild.2004.09.016

Nikas, K. S., Nikolopoulos, N., & Nikolopoulos, A. (2010). Numerical study of a naturally cross-ventilated building. *Energy and Buildings*, *42*(4), 422-434. https://doi.org/10.1016/j.enbuild.2009.10.010.

Ohba, M., Irie, K., & Kurabuchi, T. (2001). Study on airflow characteristics inside and outside a cross-ventilation model, and ventilation flow rates using wind tunnel experiments. *Journal of Wind Engineering and Industrial Aerodynamics*, *89*(14-15), 1513-1524. https://doi.org/10.1016/S0167-6105(01)00130-1.

Ramponi, R., & Blocken, B. (2012). CFD simulation of cross-ventilation flow for different isolated building configurations: validation with wind tunnel measurements and analysis of physical and numerical diffusion effects. Journal of Wind Engineering and Industrial Aerodynamics, 104, 408-418. https://doi.org/10.1016/j.jweia.2012.02.005.

Ramponi, R., & Blocken, B. (2012). CFD simulation of cross-ventilation for a generic isolated building: impact of computational parameters. *Building and environment*, *53*, 34-48. https://doi.org/10.1016/j.buildenv.2012.01.004.

Remion, G., Moujalled, B., & El Mankibi, M. (2019). Review of tracer gas-based methods for the characterization of natural ventilation performance: Comparative analysis of their accuracy. *Building and Environment*, *160*, 106180. https://doi.org/10.1016/j.buildenv.2019.106180.

Sacht, H., & Lukiantchuki, M. A. (2017). Windows size and the performance of natural ventilation. *Procedia engineering*, *196*, 972-979. https://doi.org/10.1016/j.proeng.2017.08.038.

Sandberg,M. (1981).What is ventilation efficiency?.Building and Environment,16(2) https://doi.org/10.1016/0360-1323(81)90028-7.

Sharma, R. N. (2007). Fluid dynamics-based analytical model for synthetic jet actuation. *AIAA journal*, *45*(8), 1841-1847. https://doi.org/10.2514/1.25427.

Sharma, R. N., & Richards, P. J. (2005). Net pressures on the roof of a low-rise building with wall openings. *Journal of wind engineering and industrial aerodynamics*, *93*(4), 267-291. https://doi.org/10.1016/j.jweia.2005.01.001.

Shetabivash, H. (2015). Investigation of opening position and shape on the natural cross ventilation. *Energy and Buildings*, *93*, 1-15. https://doi.org/10.1016/j.proeng.2016.10.031.

Tominaga, Y., Mochida, A., Murakami, S., & Sawaki, S. (2008). Comparison of various revised k–ε models and LES applied to flow around a high-rise building model with 1: 1: 2 shape placed within the surface boundary layer. *Journal of Wind Engineering and Industrial Aerodynamics*, *96*(4), 389-411.

Shirzadi, M., & Tominaga, Y. (2022). CFD evaluation of mean and turbulent wind characteristics around a high-rise building affected by its surroundings. *Building and Environment*, *225*, 109637. https://doi.org/10.1016/j.buildenv.2022.109637

Shirzadi, M., Mirzaei, P. A., & Naghashzadegan, M. (2017). Improvement of k-epsilon turbulence model for CFD simulation of atmospheric boundary layer around a high-rise building using stochastic optimization and Monte Carlo Sampling technique. *Journal of Wind Engineering and Industrial Aerodynamics*, *171*, 366-379. https://doi.org/10.1016/j.jweia.2017.10.005

Shirzadi, M., Mirzaei, P. A., & Tominaga, Y. (2021). LES analysis of turbulent fluctuation in cross-ventilation flow in highly-dense urban areas. *Journal of Wind Engineering and Industrial Aerodynamics*, *209*, 104494. https://doi.org/10.1016/j.jweia.2020.104494.

Shirzadi, M., Mirzaei, P. A., Naghashzadegan, M., & Tominaga, Y. (2018). Modelling enhancement of cross-ventilation in sheltered buildings using stochastic optimization. *International Journal of Heat and Mass Transfer*, *118*, 758-772. https://doi.org/10.1016/j.ijheatmasstransfer.2017.10.107

Shirzadi, M., Naghashzadegan, M., & Mirzaei, P. A. (2018). Improving the CFD modelling of cross-ventilation in highly-packed urban areas. *Sustainable cities and society*, *37*, 451-465. https://doi.org/10.1016/j.scs.2017.11.020

Shirzadi, M., Tominaga, Y., & Mirzaei, P. A. (2019). Wind tunnel experiments on cross-ventilation flow of a generic sheltered building in urban areas. *Building and Environment*, *158*, 60-72. https://doi.org/10.1016/j.buildenv.2019.04.057

Shirzadi, M., Tominaga, Y., & Mirzaei, P. A. (2020). Experimental study on cross-ventilation of a generic building in highly-dense urban areas: Impact of planar area density and wind direction. *Journal of Wind Engineering and Industrial Aerodynamics*, *196*, 104030. https://doi.org/10.1016/j.jweia.2019.104030.

Song, J., Fan, S., Lin, W., Mottet, L., Woodward, H., Davies Wykes, M., ... & Linden, P. F. (2018). Natural ventilation in cities: the implications of fluid mechanics. *Building Research & Information*, *46*(8), 809-828. https://doi.org/10.1080/09613218.2018.1468158.

Tecle, A., Bitsuamlak, G. T., & Jiru, T. E. (2013). Wind-driven natural ventilation in a low-rise building: A Boundary Layer Wind Tunnel study. *Building and Environment*, *59*, 275-289. https://doi.org/10.1016/j.buildenv.2012.08.026.

Tominaga, Y. (2015). Flow around a high-rise building using steady and unsteady RANS CFD: Effect of large-scale fluctuations on the velocity statistics. *Journal of Wind Engineering and Industrial Aerodynamics*, *142*, 93-103. https://doi.org/10.1016/j.jweia.2015.03.013

Tominaga, Y., & Blocken, B. (2015). Wind tunnel experiments on cross-ventilation flow of a generic building with contaminant dispersion in unsheltered and sheltered conditions. *Building and Environment*, *92*, 452-461. https://doi.org/10.1016/j.buildenv.2015.05.026.

Tominaga, Y., & Blocken, B. (2016). Wind tunnel analysis of flow and dispersion in cross-ventilated isolated buildings: Impact of opening positions. Journal of Wind Engineering and Industrial Aerodynamics, 155, 74-88. https://doi.org/10.1016/j.jweia.2016.05.007.

Tominaga, Y., & Stathopoulos, T. (2018). CFD simulations of near-field pollutant dispersion with different plume buoyancies. *Building and Environment*, *131*, 128-139. https://doi.org/10.1016/j.buildenv.2018.01.008

Tominaga, Y., Akabayashi, S. I., Kitahara, T., & Arinami, Y. (2015). Air flow around isolated gable-roof buildings with different roof pitches: Wind tunnel experiments and CFD simulations. *Building and Environment*, *84*, 204-213. https://doi.org/10.1016/j.buildenv.2014.11.012.

van Hooff, T., Blocken, B., & Tominaga, Y. (2017). On the accuracy of CFD simulations of cross-ventilation flows for a generic isolated building: comparison of RANS, LES and experiments. *Building and Environment*, *114*, 148-165. https://doi.org/10.1016/j.buildenv.2016.12.019.

Varela-Boydo, C. A., Moya, S. L., & Watkins, R. (2021). Analysis of traditional windcatchers and the effects produced by changing the size, shape, and position of the outlet opening. Journal of Building Engineering, 33, 101828. https://doi.org/10.1016/j.jobe.2020.101828.

Wang, H., & Chen, Q. (2012). A new empirical model for predicting single-sided, wind-driven natural ventilation in buildings. Energy and Buildings, 54, 386-394. https://doi.org/10.1016/j.enbuild.2012.07.028.

Wang, Q., Xue, M., Lin, B. L., Lei, Z., & Zhang, Z. (2020). Well-to-wheel analysis of energy consumption, greenhouse gas and air pollutants emissions of hydrogen fuel cell vehicle in China. *Journal of Cleaner Production*, *275*, 123061. https://doi.org/10.1016/j.jclepro.2020.123061

Wen, C. Y., Juan, Y. H., & Yang, A. S. (2017). Enhancement of city breathability with half open spaces in ideal urban street canyons. *Building and Environment*, *112*, 322-336. https://doi.org/10.1016/j.buildenv.2016.11.048

Willmott, C. J., & Matsuura, K. (2005). Advantages of the mean absolute error (MAE) over the root mean square error (RMSE) in assessing average model performance. *Climate research*, *30*(1), 79-82.

Wong, N. H., & Loke, A. (2001). A study of natural ventilation of public housing in Singapore using Computational Fluid Dynamics (CFD) simulations. International Journal on Architectural Science, 2(2), 35-45.

Yang, X., Zhang, Y., Hang, J., Lin, Y., Mattsson, M., Sandberg, M., ... & Wang, K. (2020). Integrated assessment of indoor and outdoor ventilation in street canyons with naturally-ventilated buildings by various ventilation indexes. Building and Environment, 169, 106528. https://doi.org/10.1016/j.buildenv.2019.106528

Z. Krishna, P. Gandhar, Balasubramanyam, A. Varghese, ANSYS Inc, K. Zore, B. Sasanapuri, G. Parkhi, and A. Varghese, "Ansys mosaic poly-hexcore mesh for high-lift aircraft configuration", 21 st Annu. CFD Symp., no. September, pp. 1–11, 2019.

Zhang, X., Weerasuriya, A. U., Wang, J., Li, C. Y., Chen, Z., Tse, K. T., & Hang, J. (2022). Cross-ventilation of a generic building with various configurations of external and internal openings. Building and Environment, 207, 108447. https://doi.org/10.1016/j.buildenv.2021.108447.

Zhao, L., Zeng, W., & Yuan, Z. (2015). Reduction of potential greenhouse gas emissions of room air-conditioner refrigerants: a life cycle carbon footprint analysis. *Journal of Cleaner Production*, *100*, 262-268. https://doi.org/10.1016/j.jclepro.2015.03.063.

Zhu, Y., Hinds, W. C., Kim, S., Shen, S., & Sioutas, C. (2002). Study of ultrafine particles near a major highway with heavy-duty diesel traffic. *Atmospheric environment*, *36*(27), 4323-4335. https://doi.org/10.1016/S1352-2310（02）00354-0)

Allocca, C., Chen, Q., & Glicksman, L. R. (2003). Design analysis of single-sided natural ventilation. *Energy and buildings*, *35*(8), 785-795.

Stavrakakis, G. M., Koukou, M. K., Vrachopoulos, M. G., & Markatos, N. C. (2008). Natural cross-ventilation in buildings: Building-scale experiments, numerical simulation and thermal comfort evaluation. *Energy and buildings*, *40*(9), 1666-1681.

Gilani, S., Montazeri, H., & Blocken, B. (2013, August). CFD simulation of temperature stratification for a building space: validation and sensitivity analysis. In *13th conference of international building performance simulation association, Chambery, France*.

Kosutova, K., van Hooff, T., Vanderwel, C., Blocken, B., & Hensen, J. (2019). Cross-ventilation in a generic isolated building equipped with louvers: Wind-tunnel experiments and CFD simulations. Building and Environment, 154, 263-280.

Swami, M. V., & Chandra, S. (1988). Correlations for pressure distribution on buildings and calculation of natural-ventilation airflow. ASHRAE transactions, 94(1), 243-266.

Park, J., & Rhee, G. H. (2017). Comparison of volume flow rate and volume-averaged local mean age of air for evaluating ventilation performance in natural ventilation. Journal of Mechanical Science and Technology, 31(12), 5801-5812.

Appendix A: GANTT CHART

Final Year Project 1														
Activities		Week												
		1	2	3	4	5	6	7	8	9	10	11	12	13	14
1	Project Briefing														
2	Gathering and understanding information														
3	Generate and discuss ideas														
4	Project title writing and submission														
5	Practising software														
6	Presentation														
7	Complete interim report														

GANTT CHART 1: FYP 1

Final Year Project 2														
Activities		Week												
		1	2	3	4	5	6	7	8	9	10	11	12	13	14
9	Model design and Mesh														
10	Identify and set boundary condition														
11	Grid sensitivity analysis and Model validation														
12	Run simulation														
13	Troubleshoot on software setting														
14	Collect and analyse simulation data														
15	Presentation														
16	Complete project report														
17	Complete logbook														

GANTT CHART 2: FYP 2

Appendix B: LOG SHEET: FYP

FINAL YEAR PROJECT 1
WEEK1

Date	2/14/2022	**Venue**	
Description of Activities			**Remarks by Supervisor**
Proposal			
Task for next week: Content plan and start the chapter 1			
Student's Signature : Feng YunXuan **Date :** 2/14/2022		**Supervisor's Signature:** _____ **Date :** _____	

FINAL YEAR PROJECT 1
WEEK 2

Date	2/21/2022	**Venue**	
Description of Activities			**Remarks by Supervisor**
Write the first chapter to improve the content.			
Task for next week: Continue to work			
Student's Signature : Feng YunXuan **Date :** 2/21/2022		**Supervisor's Signature:** _____ **Date :** _____	

FINAL YEAR PROJECT 1

WEEK 3

Date	2/28/2022	**Venue**	
Description of Activities			**Remarks by Supervisor**
Reading in large quantities of articles ,write the first chapter and improve the content.			
Task for next week: Continue to work			
Student's Signature : Feng YunXuan **Date :** 2/28/2022		**Supervisor's Signature:** _____ **Date :** _____	

FINAL YEAR PROJECT 1

WEEK 4

Date	3/7/2022	**Venue**	
Description of Activities			**Remarks by Supervisor**
Reading in large quantities of articles ,write the first chapter and improve the content.			
Task for next week: Discussion and start the second chapter.			
Student's Signature : Feng YunXuan **Date :** 3/7/2022		**Supervisor's Signature:** _____ **Date :** _____	

FINAL YEAR PROJECT 1

WEEK 5

Date	3/14/2022	**Venue**	
Description of Activities			**Remarks by Supervisor**
Discussion and start the second chapter.			
Task for next week: Reading in large quantities of articles and writing chapter 2			
Student's Signature : Feng YunXuan **Date :** 3/14/2022		**Supervisor's Signature:** _____ **Date :** _____	

FINAL YEAR PROJECT 1

WEEK 6

Date	3/21/2022	**Venue**	
Description of Activities			**Remarks by Supervisor**
Reading in large quantities of articles and writing chapter 2			
Task for next week: Reading in large quantities of articles and writing chapter 2.			
Student's Signature : Feng YunXuan **Date :** 3/21/2022		**Supervisor's Signature:** _____ **Date :** _____	

FINAL YEAR PROJECT 1

WEEK 7

Date	3/28/2022	**Venue**	
Description of Activities			**Remarks by Supervisor**
Reading in large quantities of articles and writing chapter 2.			
Task for next week: Reading in large quantities of articles and writing chapter 2.			
Student's Signature : Feng YunXuan **Date :** 3/28/2022		**Supervisor's Signature:** _____ **Date :** _____	

FINAL YEAR PROJECT 1

WEEK 8

Date	4/4/2022	**Venue**	
Description of Activities			**Remarks by Supervisor**
Reading in large quantities of articles and writing chapter 2.			
Task for next week: CFD simulation and discuss the experimental methods.			
Student's Signature : Feng YunXuan **Date :** 4/4/2022		**Supervisor's Signature:** _____ **Date :** _____	

FINAL YEAR PROJECT 1

WEEK 9

Date	4/11/2022	**Venue**	
Description of Activities			**Remarks by Supervisor**
CFD simulation and discuss the experimental methods.			
Task for next week: CFD simulation and discuss the experimental methods.			
Student's Signature : Feng YunXuan **Date :** 4/11/2022		**Supervisor's Signature:** _____ **Date :** _____	

FINAL YEAR PROJECT 1
WEEK 10

Date	4/18/2022	**Venue**	
Description of Activities			**Remarks by Supervisor**
CFD simulation and discuss the experimental methods.			
Task for next week: Optimized geometric modeling			
Student's Signature : Feng YunXuan **Date :** 4/18/2022		**Supervisor's Signature:** _____ **Date :** _____	

FINAL YEAR PROJECT 1

WEEK 11

Date	4/25/2022	**Venue**	
Description of Activities			**Remarks by Supervisor**
Optimized geometric modeling			
Task for next week: Optimized geometric modeling			
Student's Signature : Feng YunXuan **Date :** 4/25/2022		**Supervisor's Signature:** _____ **Date :** _____	

FINAL YEAR PROJECT 1
WEEK 12

Date	5/2/2022	**Venue**	
Description of Activities			**Remarks by Supervisor**
CFD Geometric modeling and discuss the experimental methods.			
Task for next week: Optimized geometric modeling			
Student's Signature : Feng YunXuan **Date :** 5/2/2022		**Supervisor's Signature:** _____ **Date :** _____	

FINAL YEAR PROJECT 2

WEEK 1

Date	9/12/2022	**Venue**	
Description of Activities			**Remarks by Supervisor**
Discuss questions about simulation.			
Task for next week: Run simulation.			
Student's Signature : Feng YunXuan **Date :** 9/12/2022		**Supervisor's Signature:** _____ **Date :** _____	

FINAL YEAR PROJECT 2

WEEK 2

Date	9/19/2022	**Venue**	
Description of Activities			**Remarks by Supervisor**
Discuss questions about simulation.			
Task for next week: Run simulation.			
Student's Signature : Feng YunXuan **Date :** 9/19/2022		**Supervisor's Signature:** _____ **Date :** _____	

FINAL YEAR PROJECT 2

WEEK 3

Date	9/26/2022	**Venue**	
Description of Activities			**Remarks by Supervisor**
Discuss the results of simulation and analyze methods for improvement.			
Task for next week: Run simulation and discuss the results of simulation simulations.			
Student's Signature : Feng YunXuan **Date :** 9/26/2022		**Supervisor's Signature:** _____ **Date :** _____	

FINAL YEAR PROJECT 2

WEEK 4

Date	10/3/2022	**Venue**	
Description of Activities			**Remarks by Supervisor**
Discuss the results of simulation and analyze methods for improvement.			
Task for next week: Run simulation and discuss the results of simulation and write chapter 3.			
Student's Signature : Feng YunXuan **Date :** 10/3/2022		**Supervisor's Signature:** _____ **Date :** _____	

FINAL YEAR PROJECT 2

WEEK 5

Date	10/10/2022	**Venue**	
Description of Activities			**Remarks by Supervisor**
Discuss the results of simulation and analyze methods for improvement.			
Task for next week: Run simulation and discuss the results of simulation and write chapter 3.			
Student's Signature : Feng YunXuan **Date :** 10/10/2022		**Supervisor's Signature:** _____ **Date :** _____	

FINAL YEAR PROJECT 2

WEEK 6

Date	10/17/2022	**Venue**	
Description of Activities			**Remarks by Supervisor**
Discuss the results of simulation and analyze methods for improvement.			
Task for next week: Run simulation and discuss the results of simulation and write chapter 4.			
Student's Signature : Feng YunXuan **Date :** 10/17/2022		**Supervisor's Signature:** _____ **Date :** _____	

FINAL YEAR PROJECT 2

WEEK 7

Date	10/23/2022	**Venue**	
Description of Activities			**Remarks by Supervisor**
Discuss the results of simulation.			
Task for next week: Write chapter 4.			
Student's Signature : Feng YunXuan **Date :** 10/23/2022		**Supervisor's Signature:** _____ **Date :** _____	

FINAL YEAR PROJECT 2

WEEK 8

Date	10/23/2022	**Venue**	
Description of Activities			**Remarks by Supervisor**
Discuss the results of simulation simulations.			
Task for next week: Write chapter 4.			
Student's Signature : Feng YunXuan **Date :** 10/23/2022		**Supervisor's Signature:** _____ **Date :** _____	

FINAL YEAR PROJECT 2

WEEK 9

Date	10/30/2022	**Venue**	
Description of Activities			**Remarks by Supervisor**
Discuss the results of simulation simulations.			
Task for next week: Write chapter 4.			
Student's Signature : Feng YunXuan **Date :** 10/23/2022		**Supervisor's Signature:** _____ **Date :** _____	

FINAL YEAR PROJECT 2
WEEK 10

Date	11/6/2022	**Venue**	
Description of Activities			**Remarks by Supervisor**
Discuss the results of simulation simulations.			
Task for next week: Write chapter 4.			
Student's Signature : Feng YunXuan **Date :** 10/23/2022		**Supervisor's Signature:** _____ **Date :** _____	

FINAL YEAR PROJECT 2

WEEK 11

Date	11/13/2022	**Venue**	
Description of Activities			**Remarks by Supervisor**
Discuss the results of simulation simulations.			
Task for next week: Write chapter 4 and write chapter 5.			
Student's Signature : Feng YunXuan **Date :** 10/23/2022		**Supervisor's Signature:** _____ **Date :** _____	

FINAL YEAR PROJECT 2

WEEK 12

Date	11/20/2022	**Venue**	
Description of Activities			**Remarks by Supervisor**
Submmit FYP			
Task for next week: Continue work.			
Student's Signature : Feng YunXuan **Date :** 10/23/2022		**Supervisor's Signature:** _____ **Date :** _____	

Appendix C: ENGINEERING DRAWING FOR BUILDING MODELS

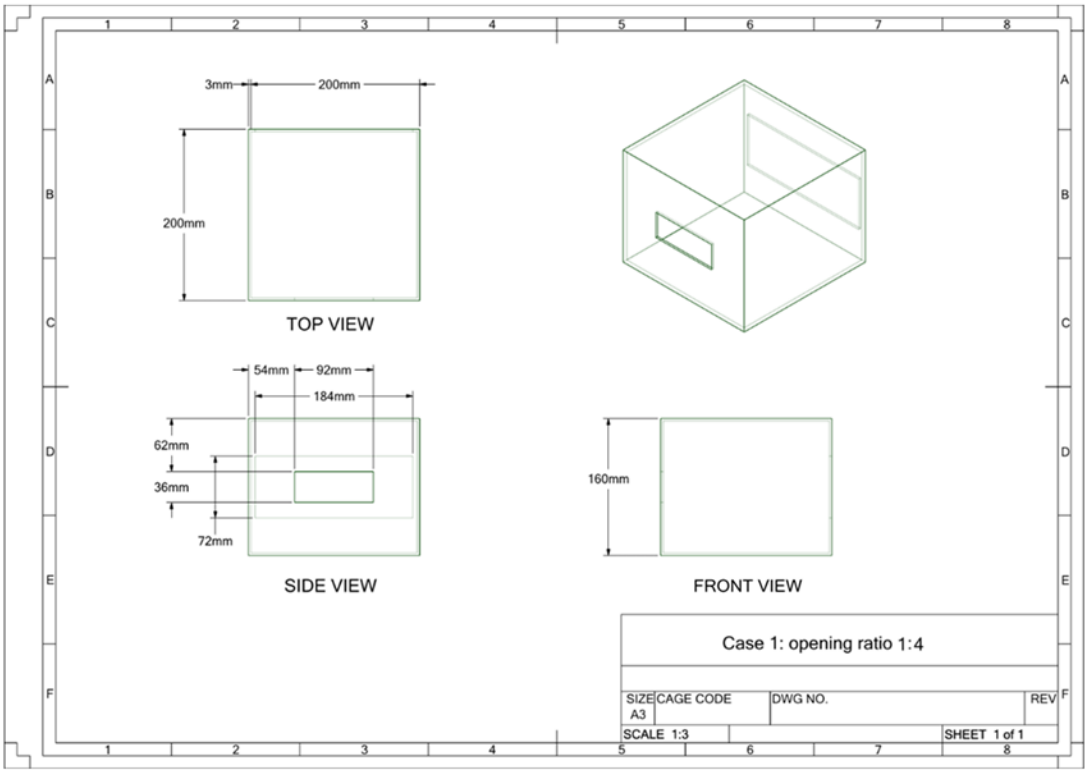

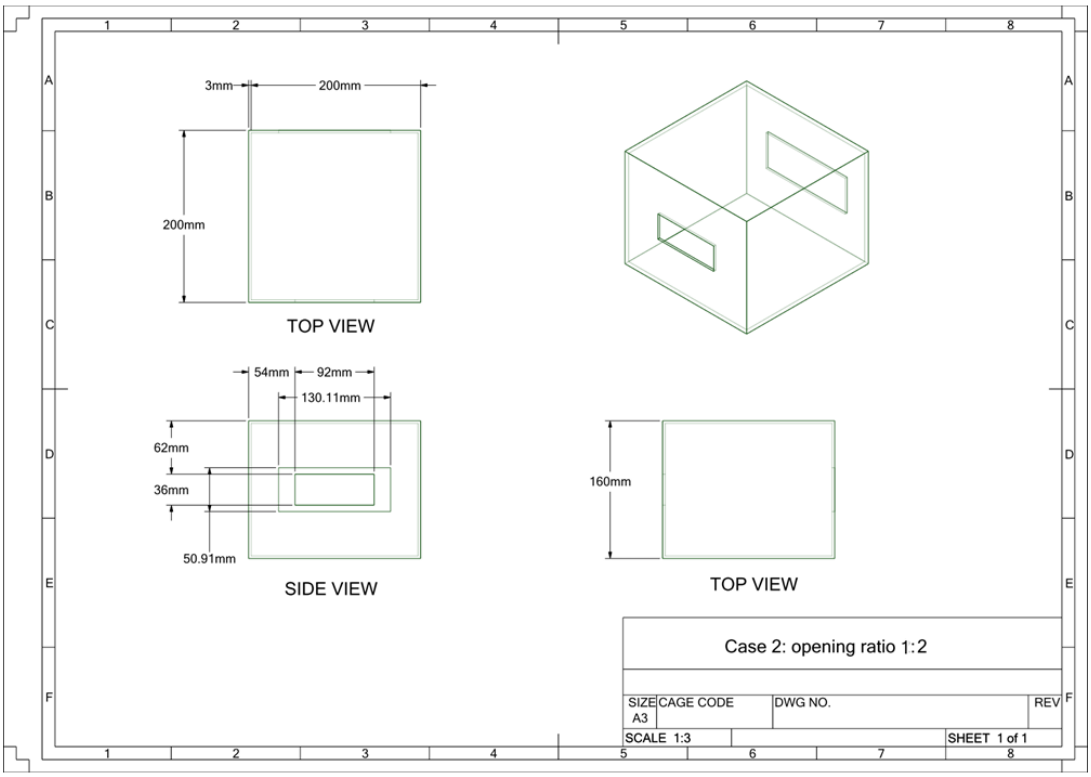

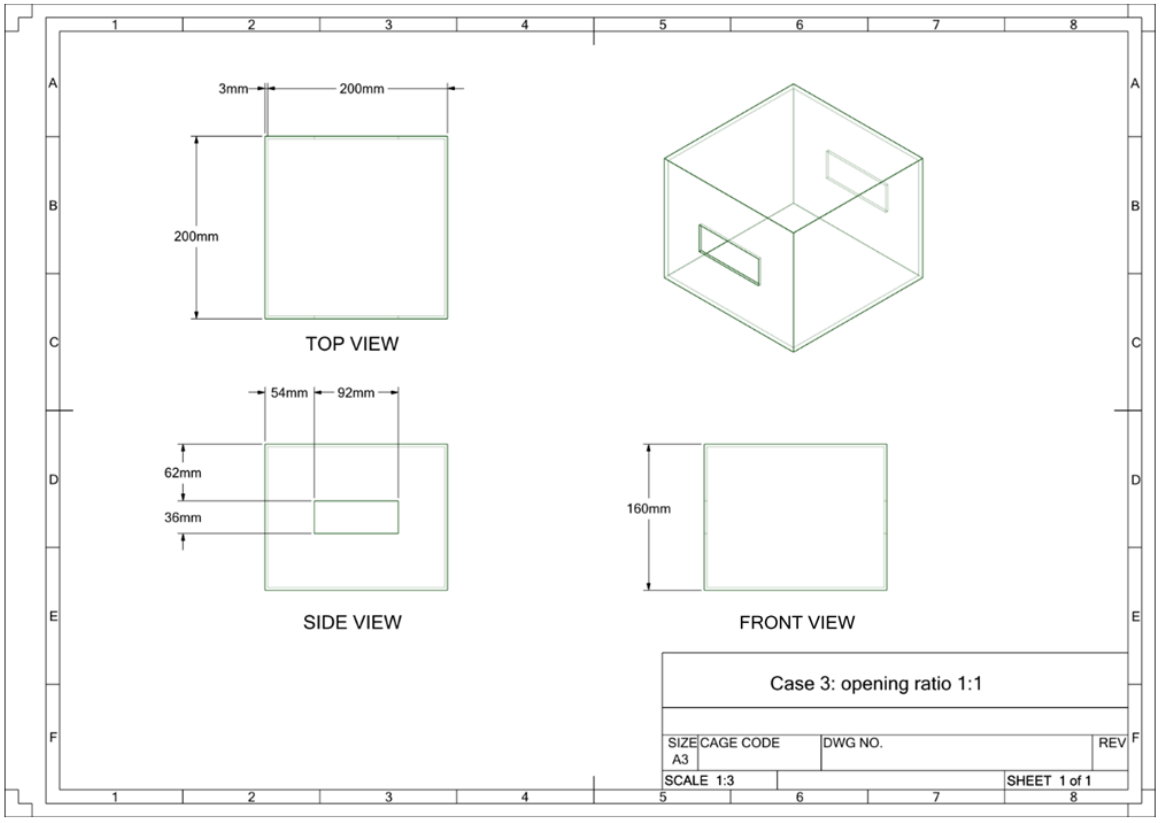
3mm
200mm
200mm
TOP VIEW
54mm
92mm
62mm
36mm
SIDE VIEW
160mm
FRONT VIEW
Case 3: opening ratio 1:1
SIZE A3
CAGE CODE
DWG NO.
REV
SCALE 1:3
SHEET 1 of 1

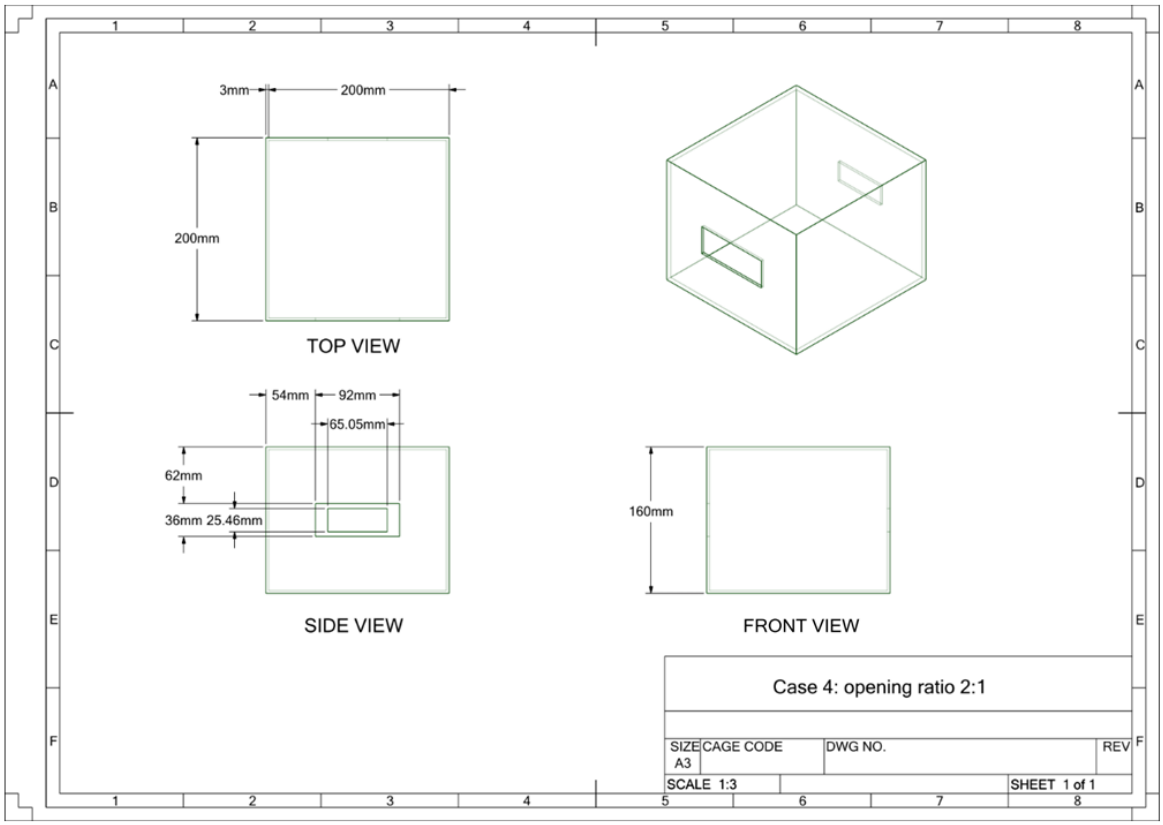
3mm
200mm
200mm
TOP VIEW
54mm
92mm
65.05mm
62mm
36mm
25.46mm
SIDE VIEW
160mm
FRONT VIEW
Case 4: opening ratio 2:1
SIZE A3
CAGE CODE
DWG NO.
REV
SCALE 1:3
SHEET 1 of 1

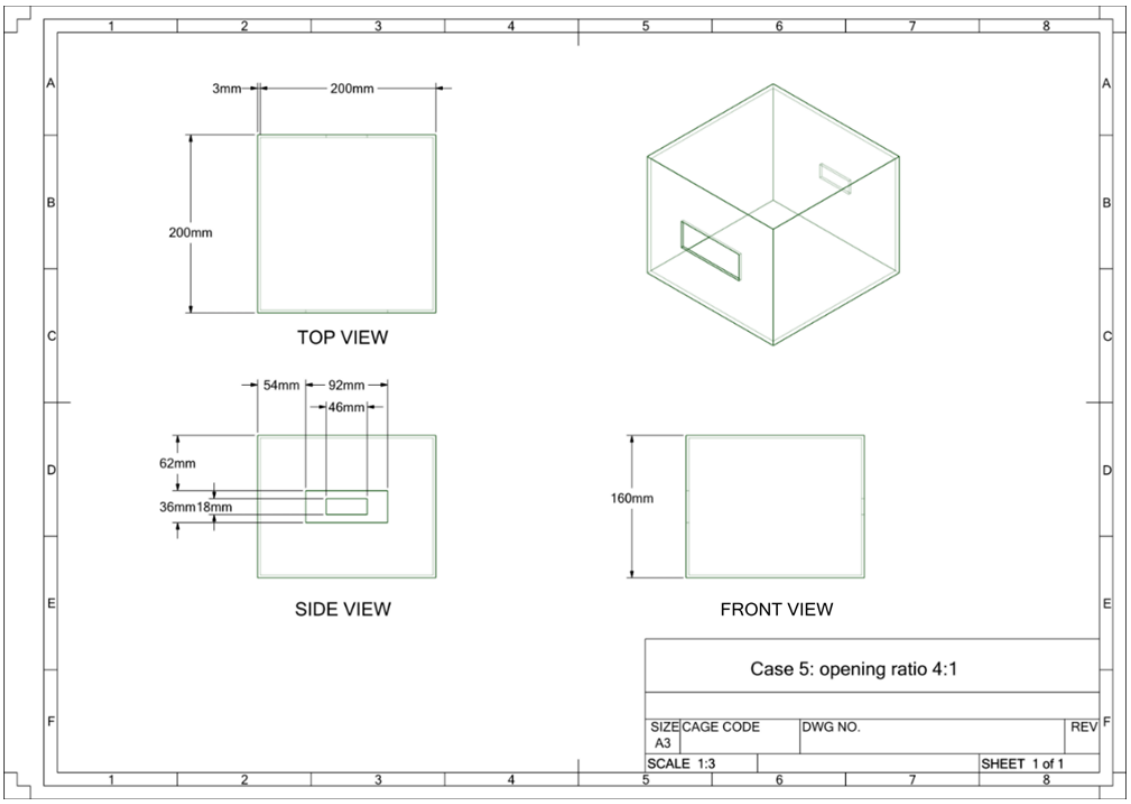
3mm
200mm
200mm
TOP VIEW
54mm
92mm
46mm
62mm
36mm
18mm
SIDE VIEW
160mm
FRONT VIEW
Case 5: opening ratio 4:1
SIZE A3
CAGE CODE
DWG NO.
REV
SCALE 1:3
SHEET 1 of 1

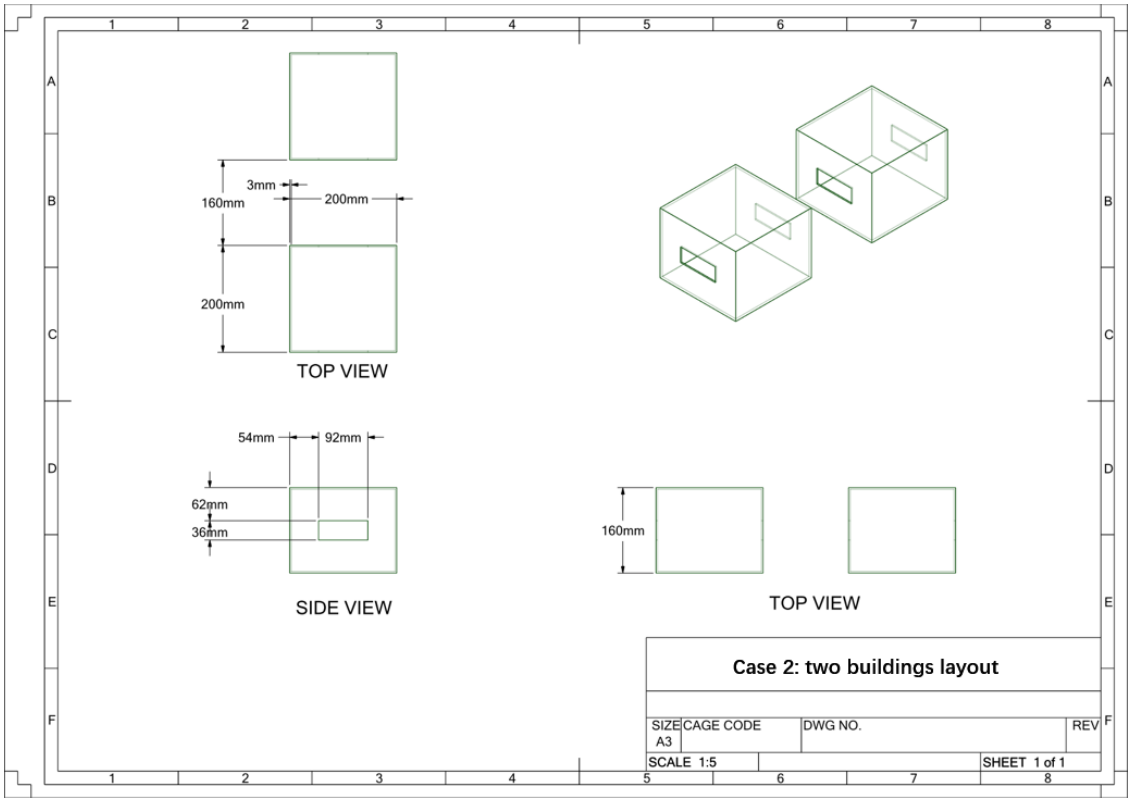
3mm
160mm
200mm
200mm
TOP VIEW
54mm
92mm
62mm
36mm
SIDE VIEW
160mm
TOP VIEW
Case 2: two buildings layout
SIZE A3
CAGE CODE
DWG NO.
REV
SCALE 1:5
SHEET 1 of 1

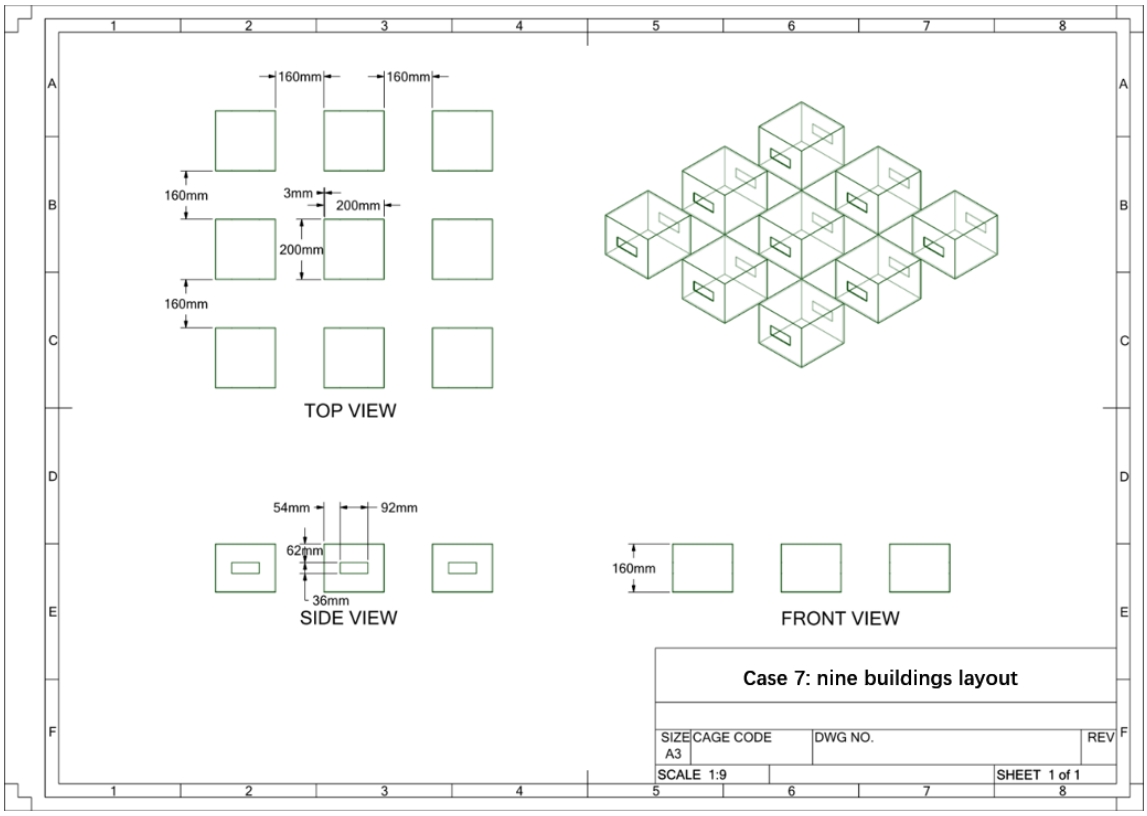
160mm
160mm
160mm
3mm
200mm
200mm
160mm
TOP VIEW
54mm
92mm
62mm
36mm
SIDE VIEW
160mm
FRONT VIEW
Case 7: nine buildings layout
SIZE A3
CAGE CODE
DWG NO.
REV
SCALE 1:9
SHEET 1 of 1

Appendix D: CONVERGED RESIDUAL PLOT

One building and 4:1 opening ratio

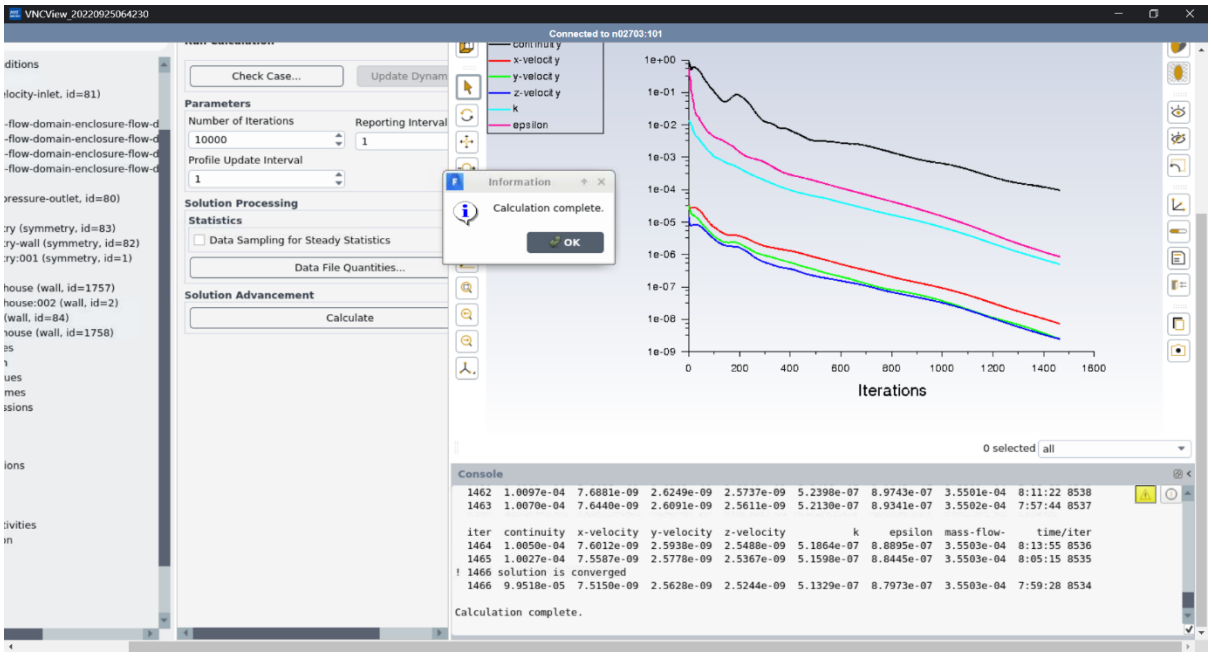

One building and 2:1 opening ratio

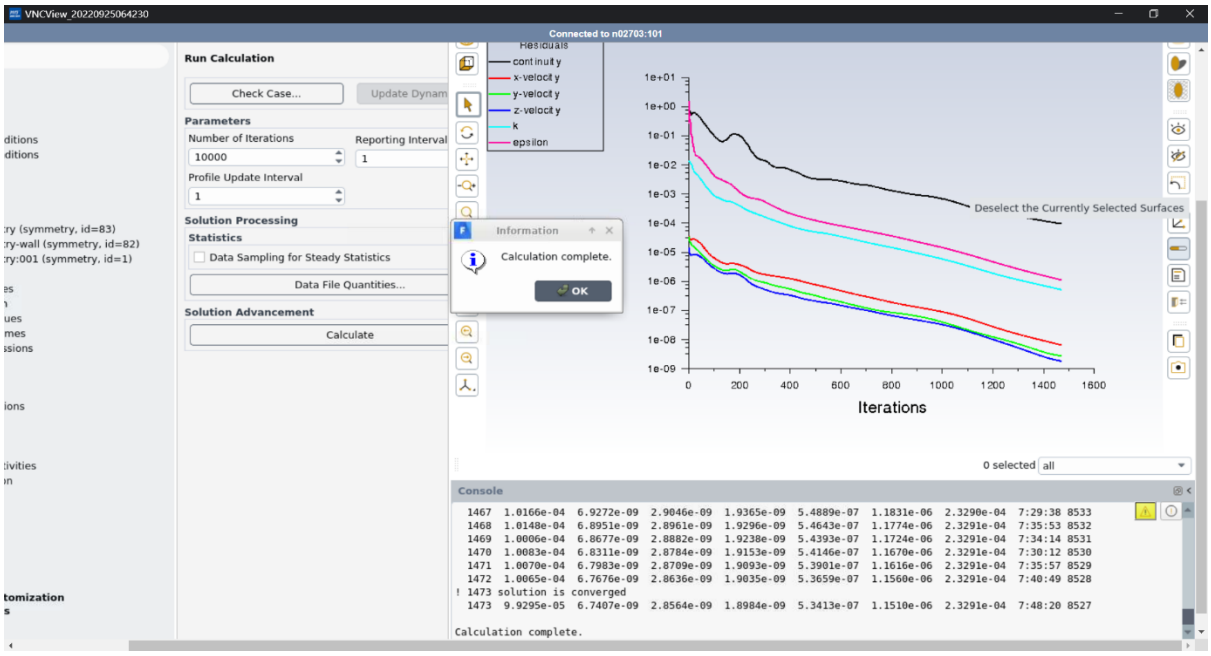

One building and 1:1 opening ratio

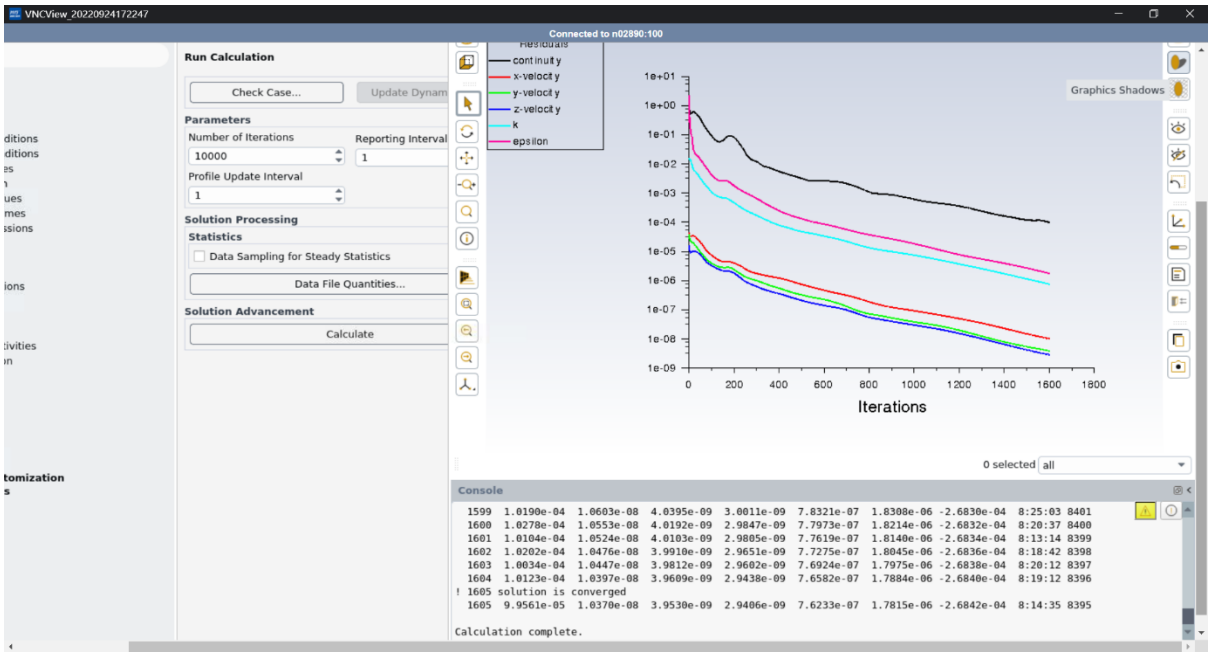

One building and 1:2 opening ratio

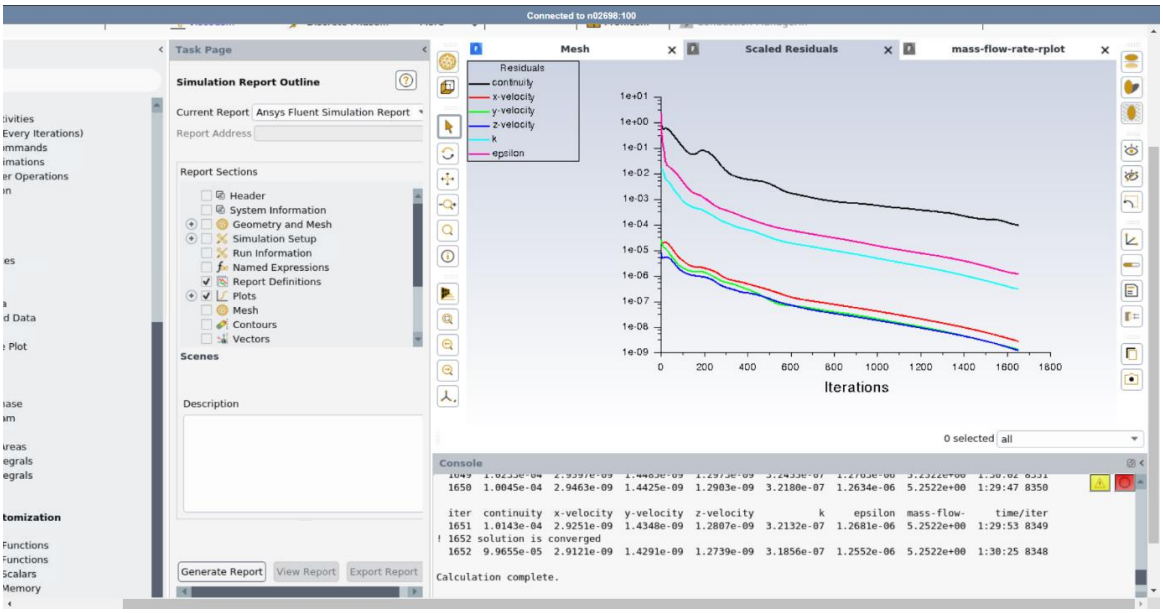

One building and 1:4 opening ratio

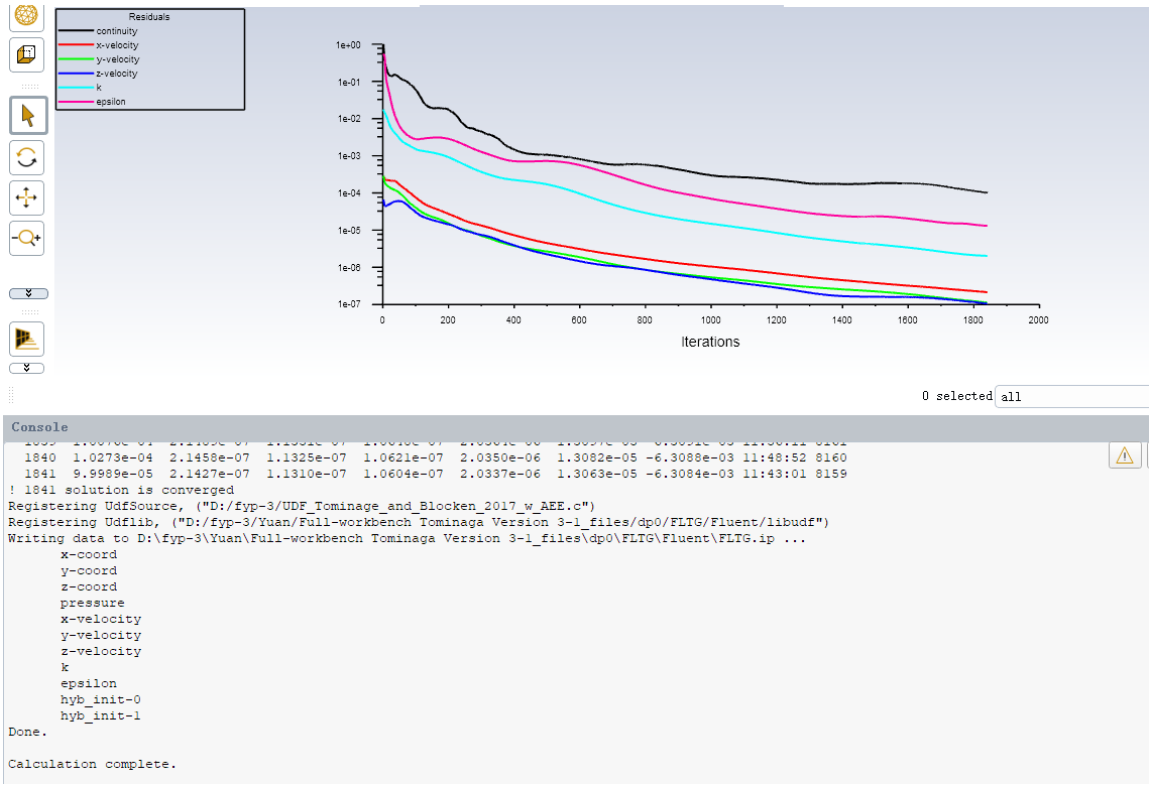

Two building with opening for the front building and 4:1 opening ratio

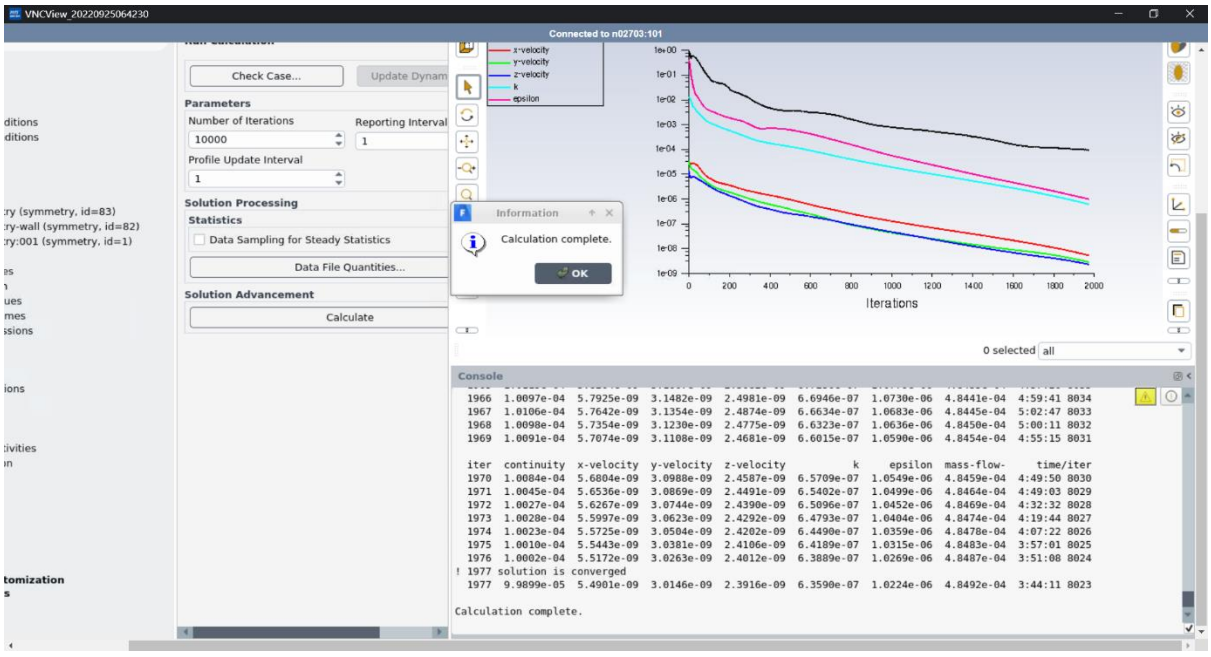

Two building with opening for the front building and 2:1 opening ratio

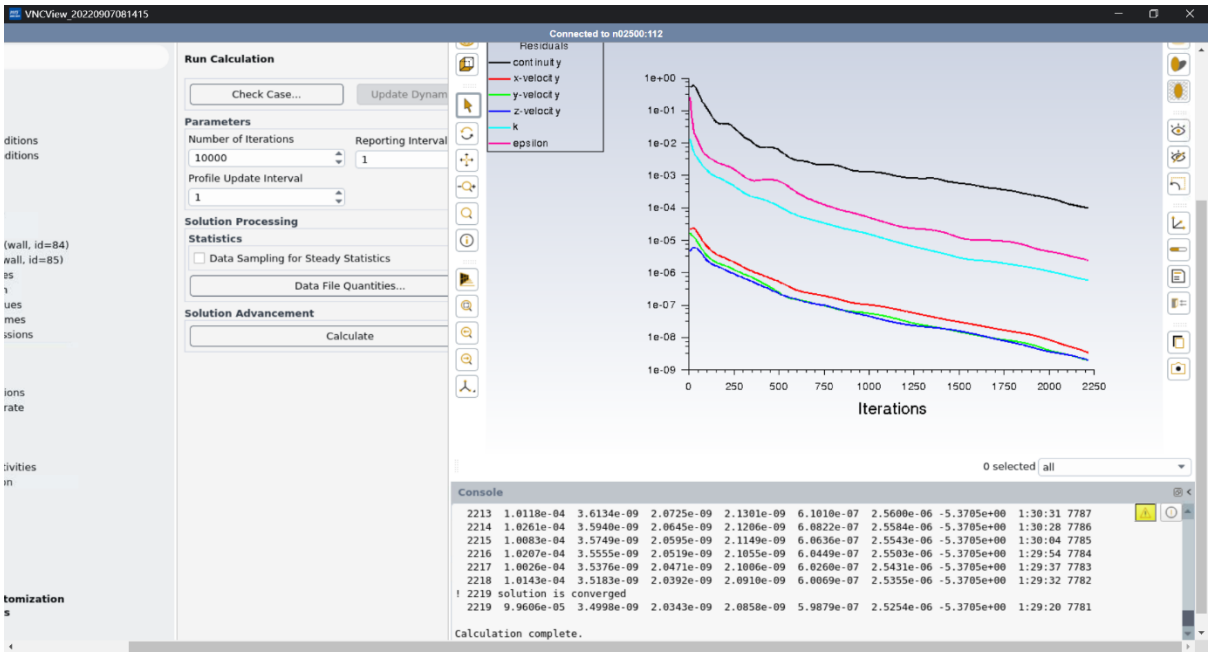

Two building with opening for the front building and 1:1 opening ratio

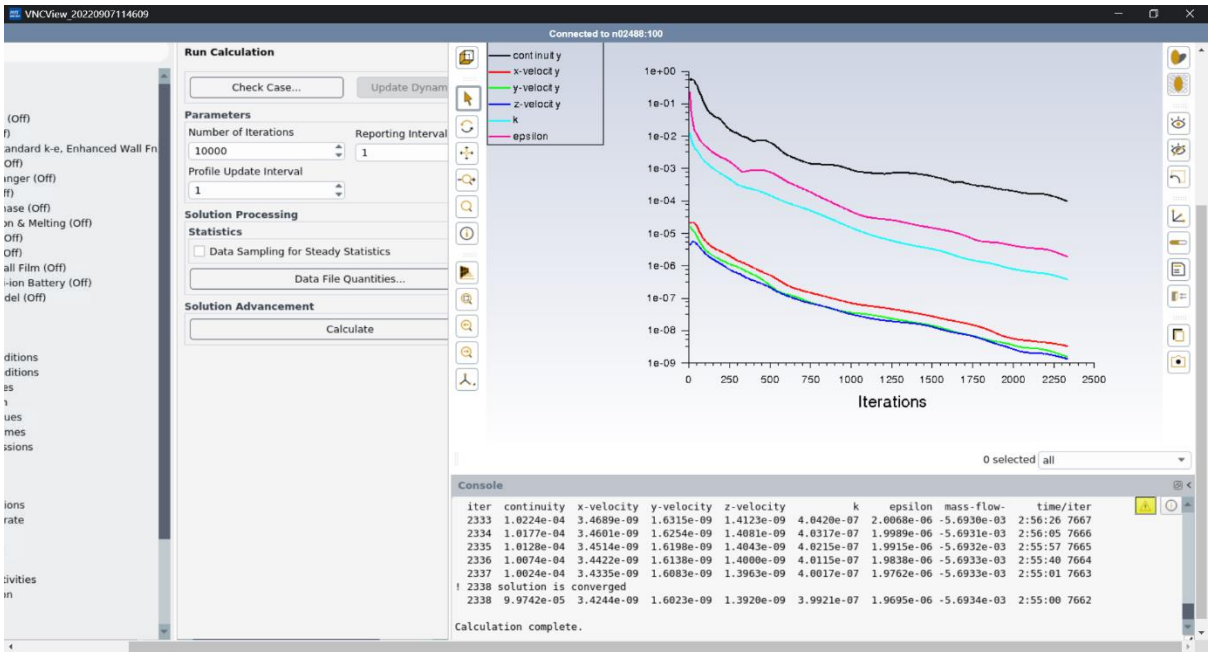

Two building with opening for the front building and 1:2 opening ratio

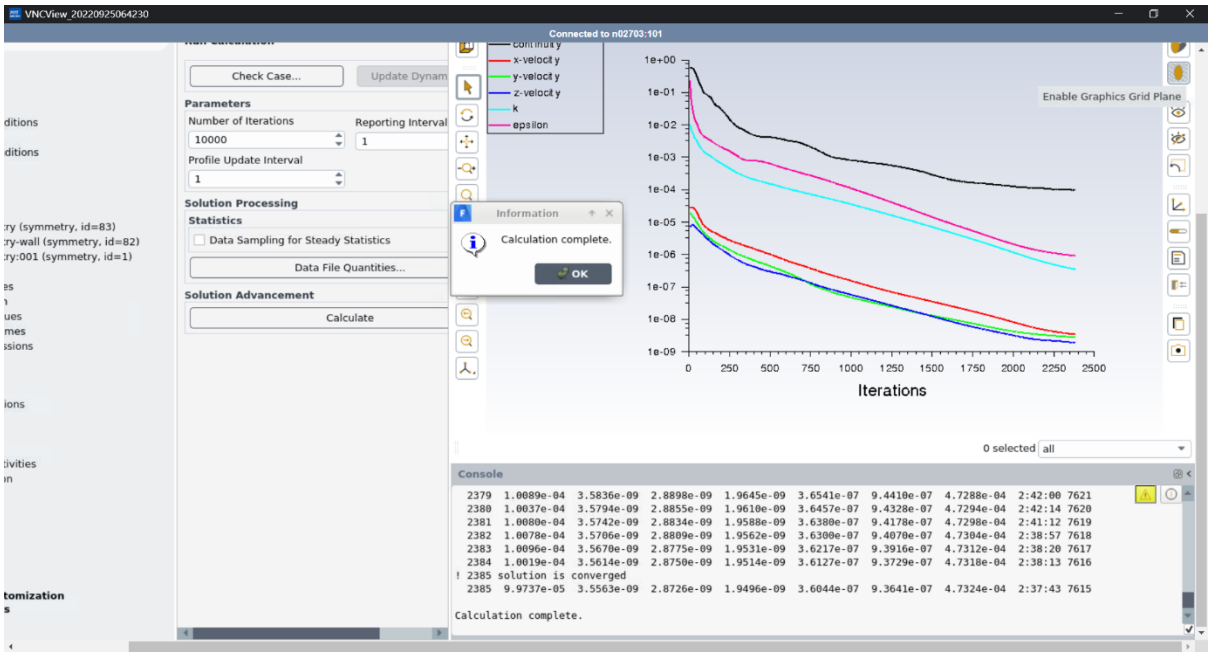

Two building with opening for the front building and 1:4 opening ratio

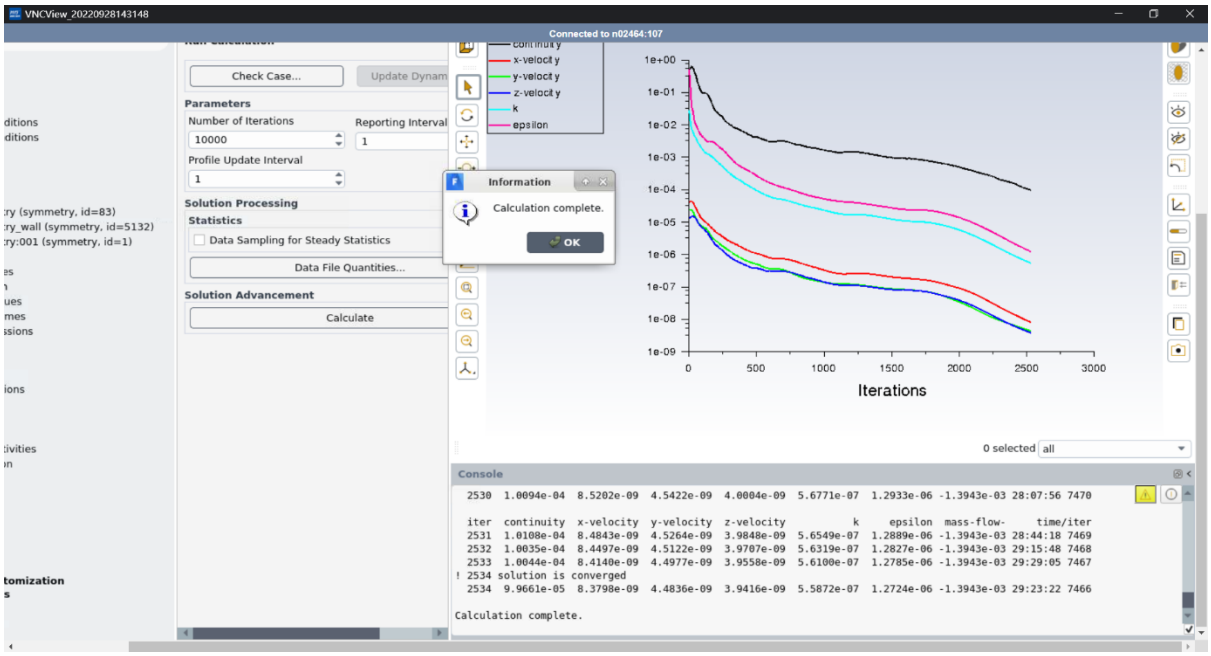

Two building without opening for the front building and 4:1 opening ratio

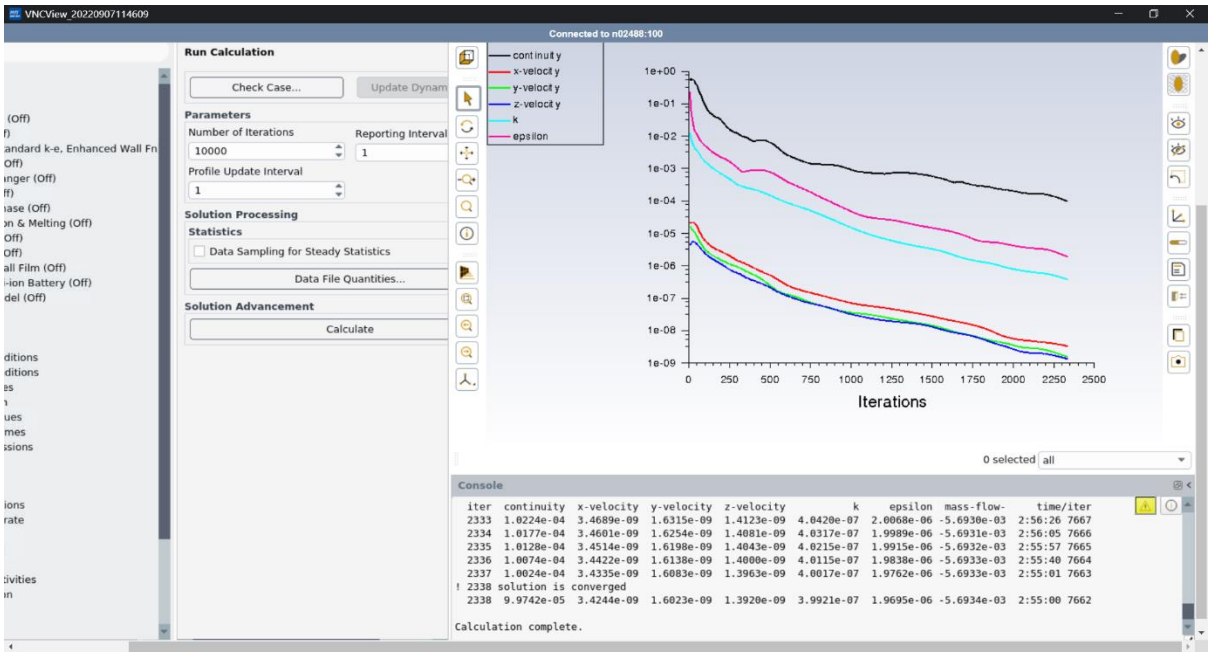

Two building without opening for the front building and 2:1 opening ratio

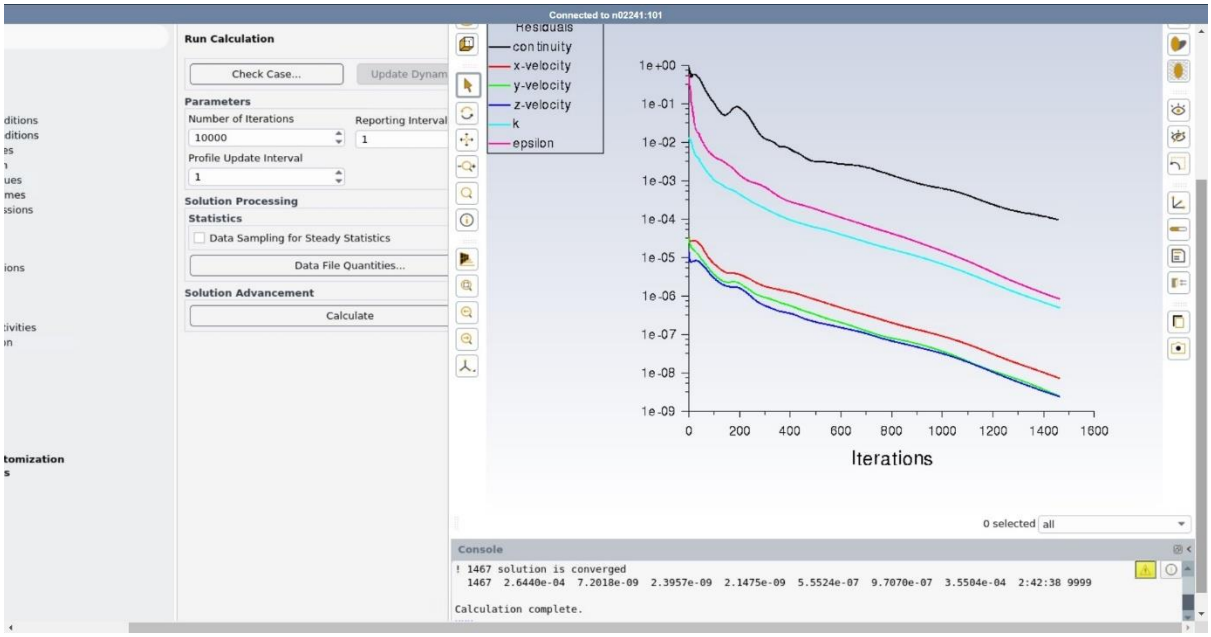

Two building without opening for the front building and 1:1 opening ratio

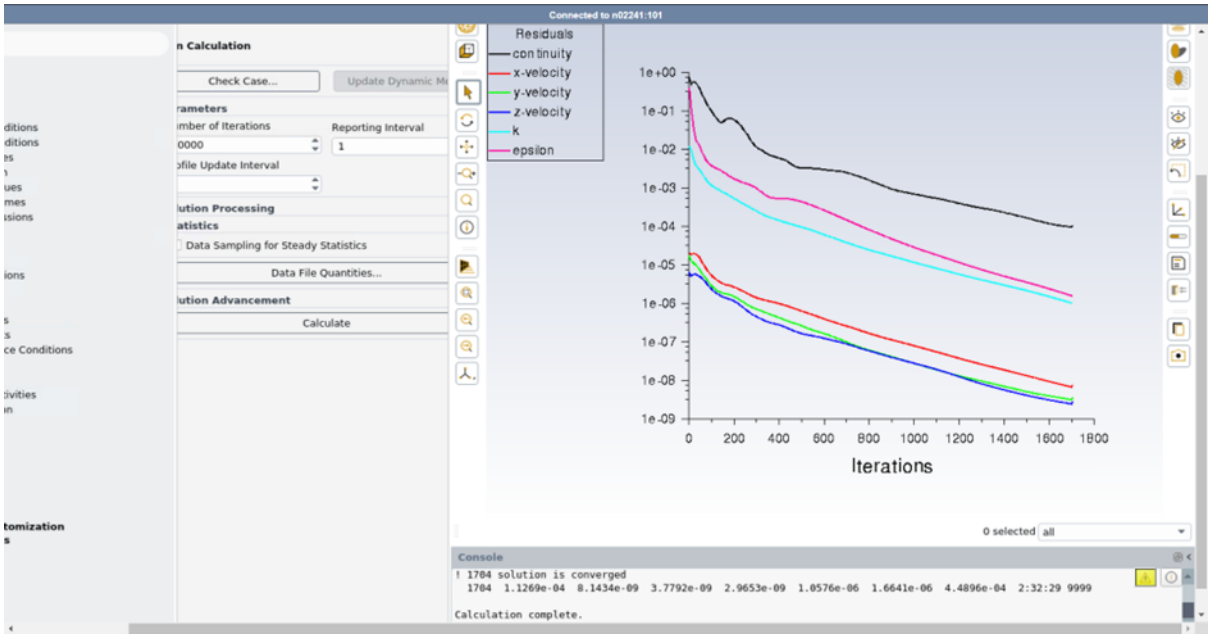

Two building without opening for the front building and 1:2 opening ratio

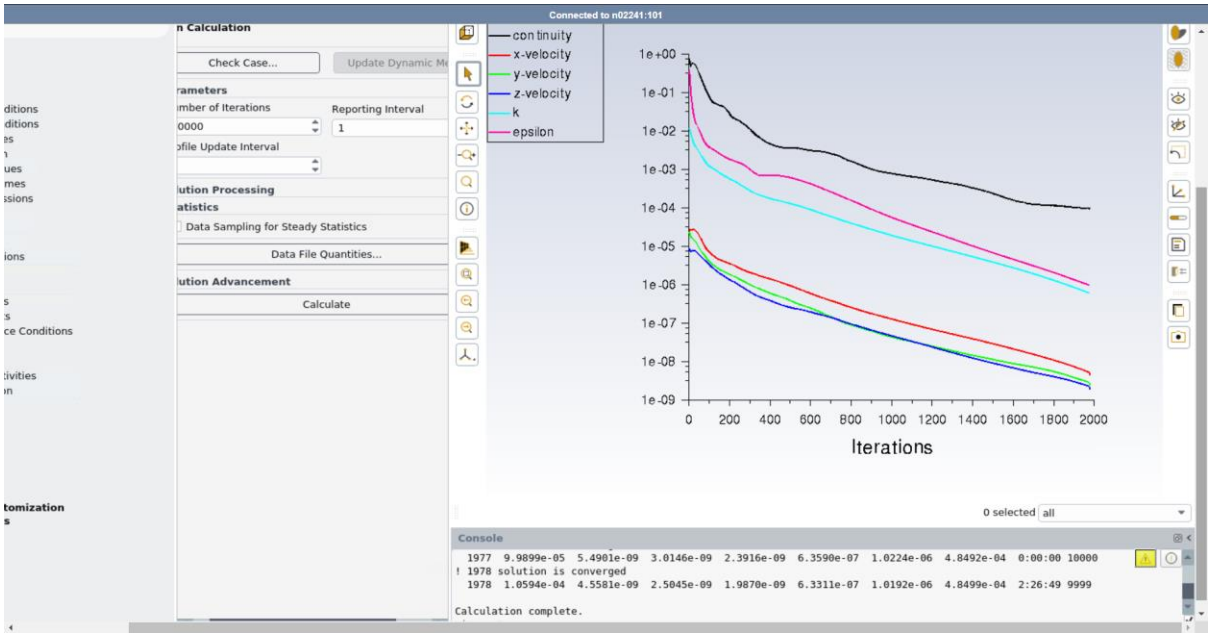

Two building without opening for the front building and 1:4 opening ratio

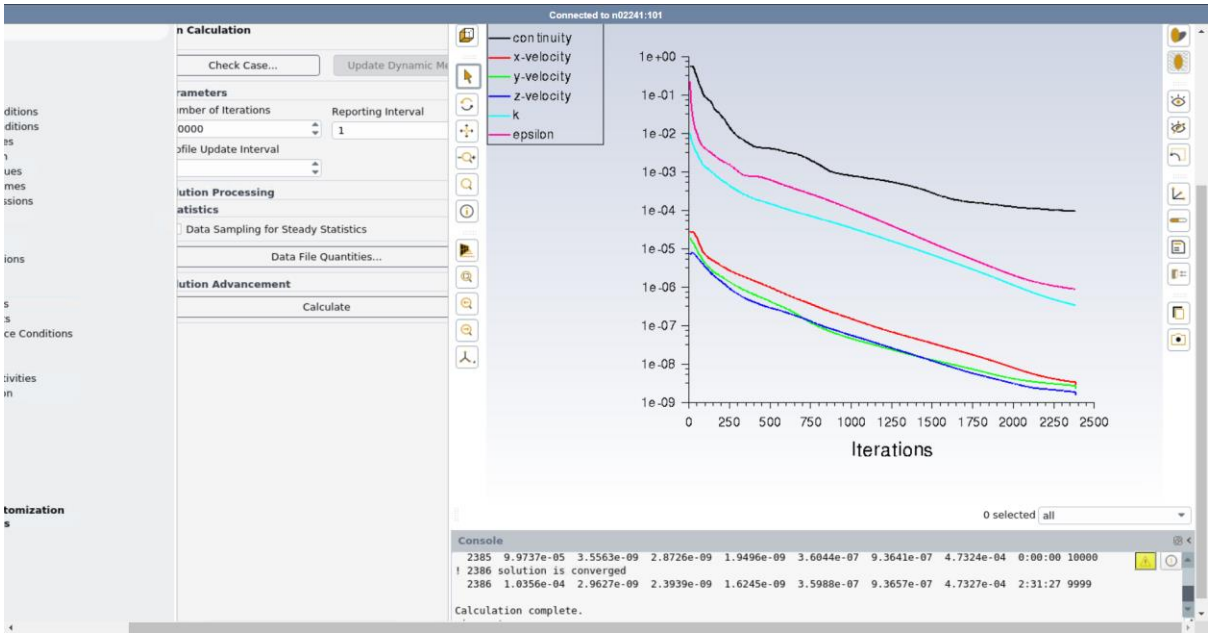

Nine buildings with opening around buildings and 4:1 opening ratio

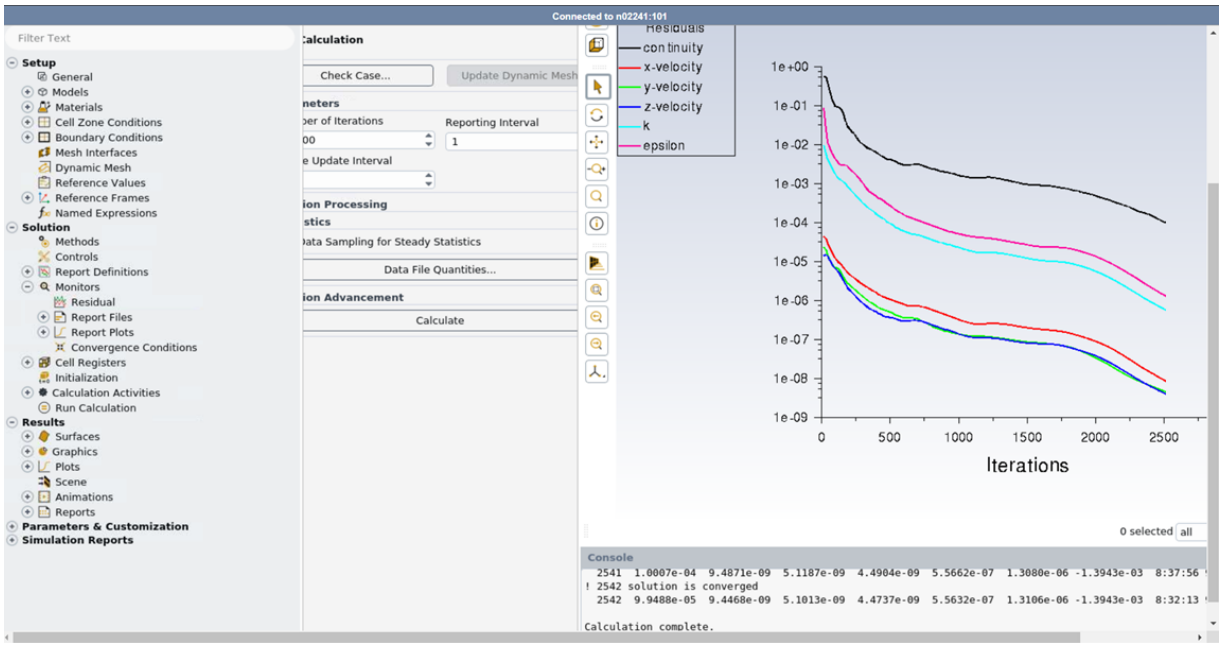

Nine buildings with opening around buildings and 2:1 opening ratio

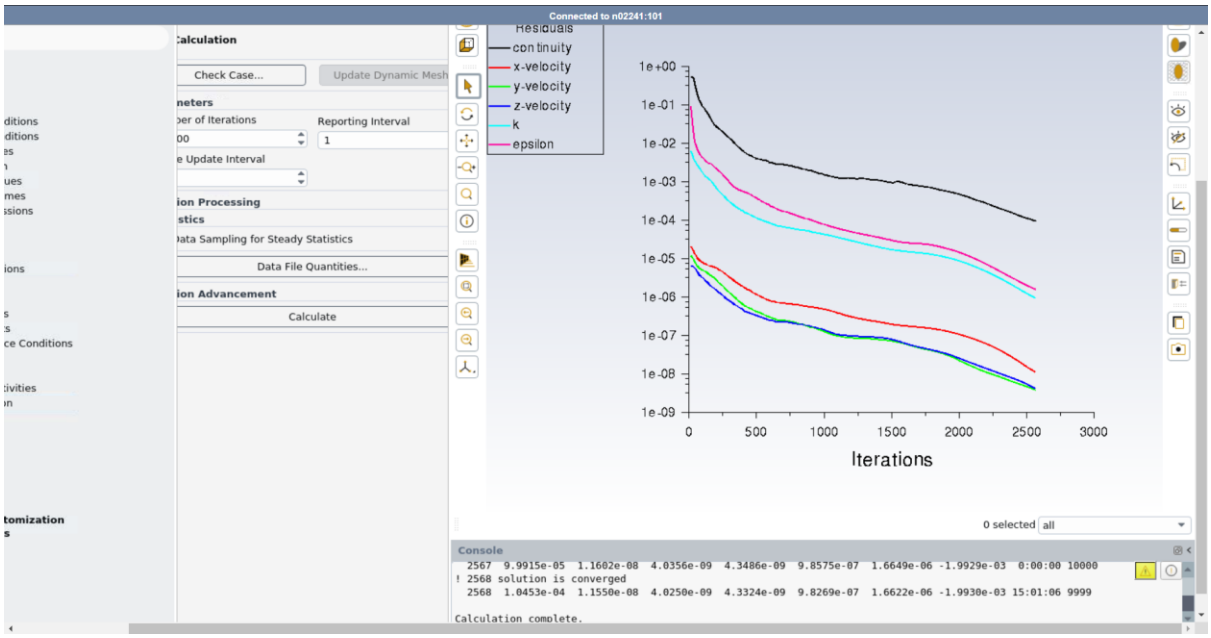

Nine buildings with opening around buildings and 1:1 opening ratio

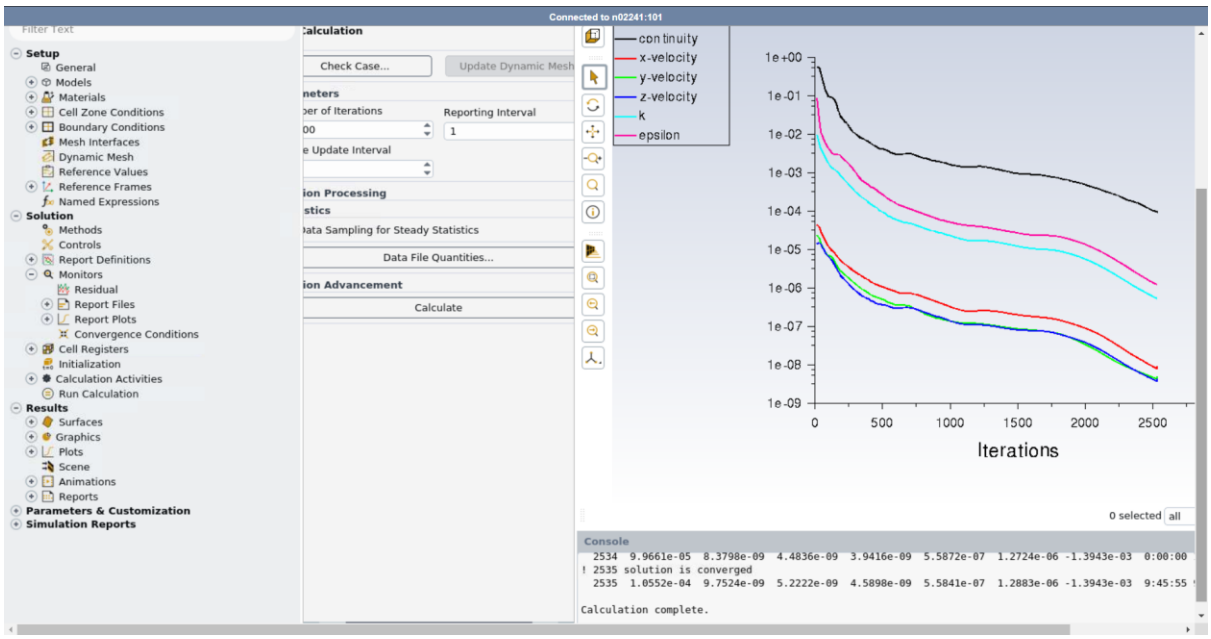

Nine buildings with opening around buildings and 1:2 opening ratio

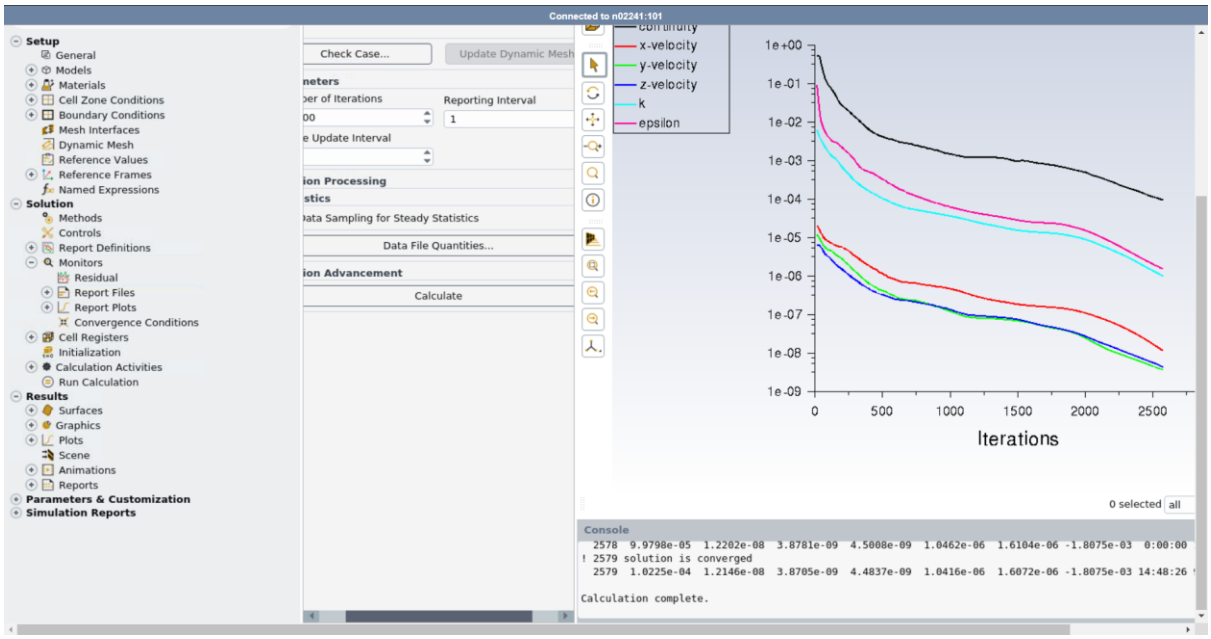

Nine buildings with opening around buildings and 1:4 opening ratio

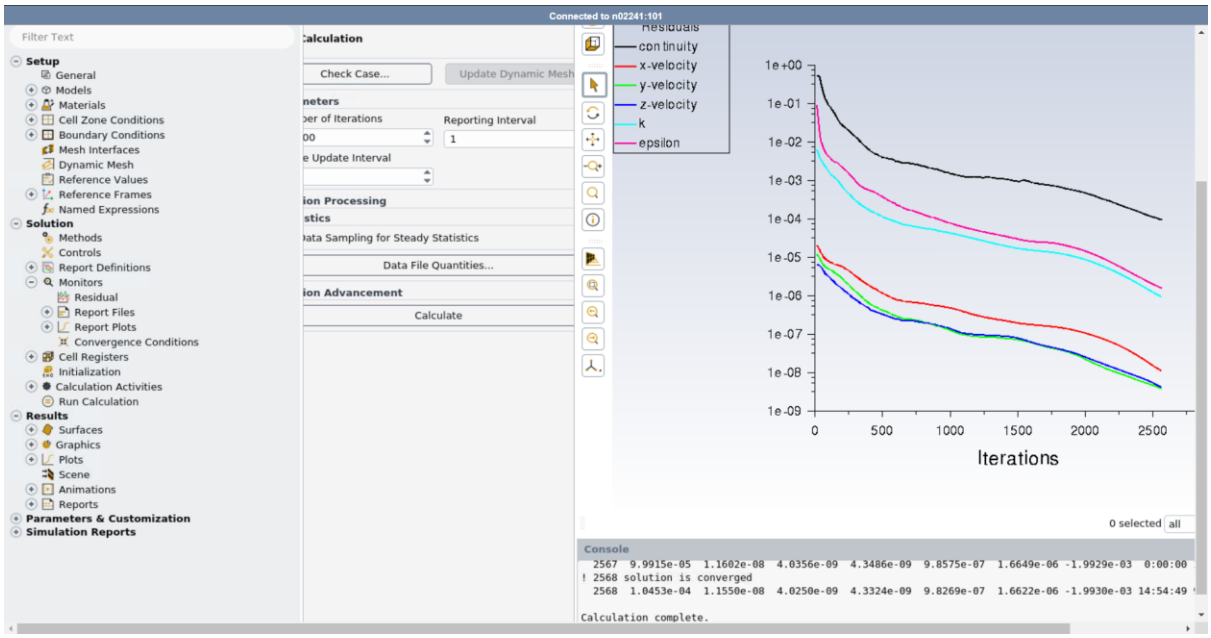

Nine buildings without opening around buildings and 4:1 opening ratio

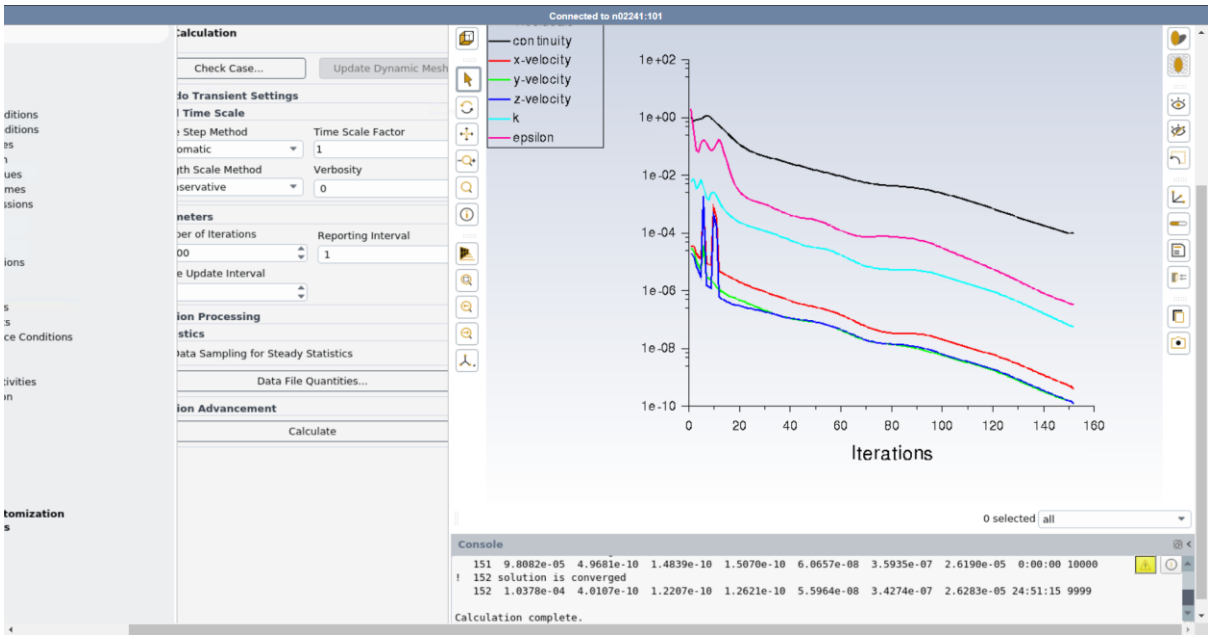

Nine buildings without opening around buildings and 2:1 opening ratio

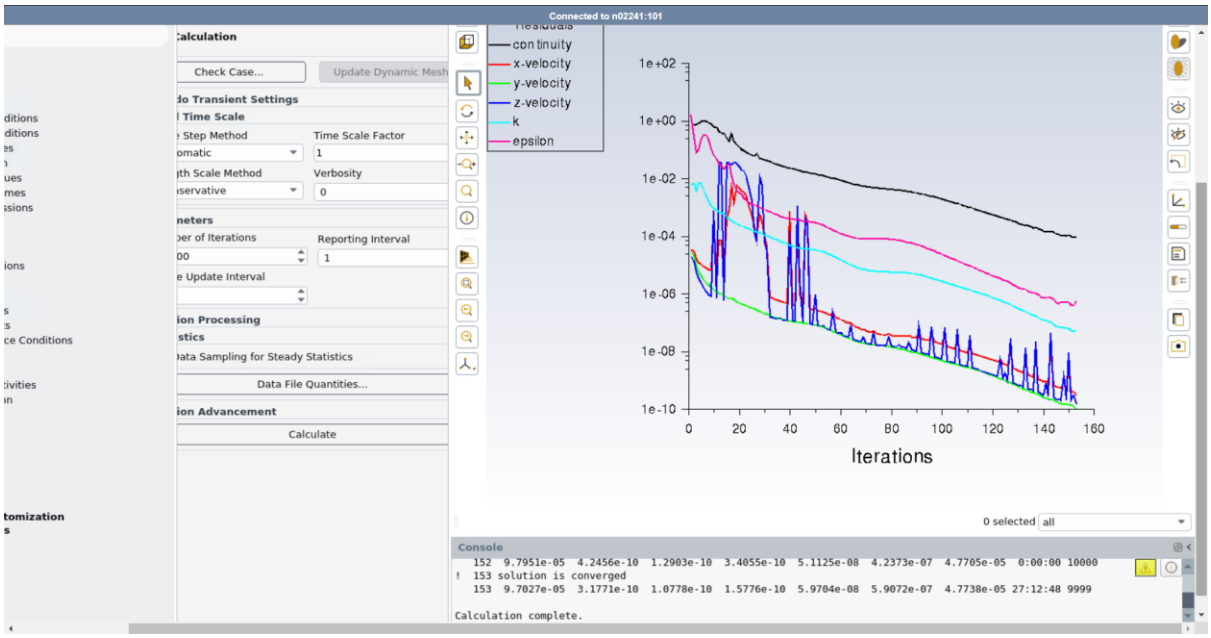

Nine buildings without opening around buildings and 1:1 opening ratio

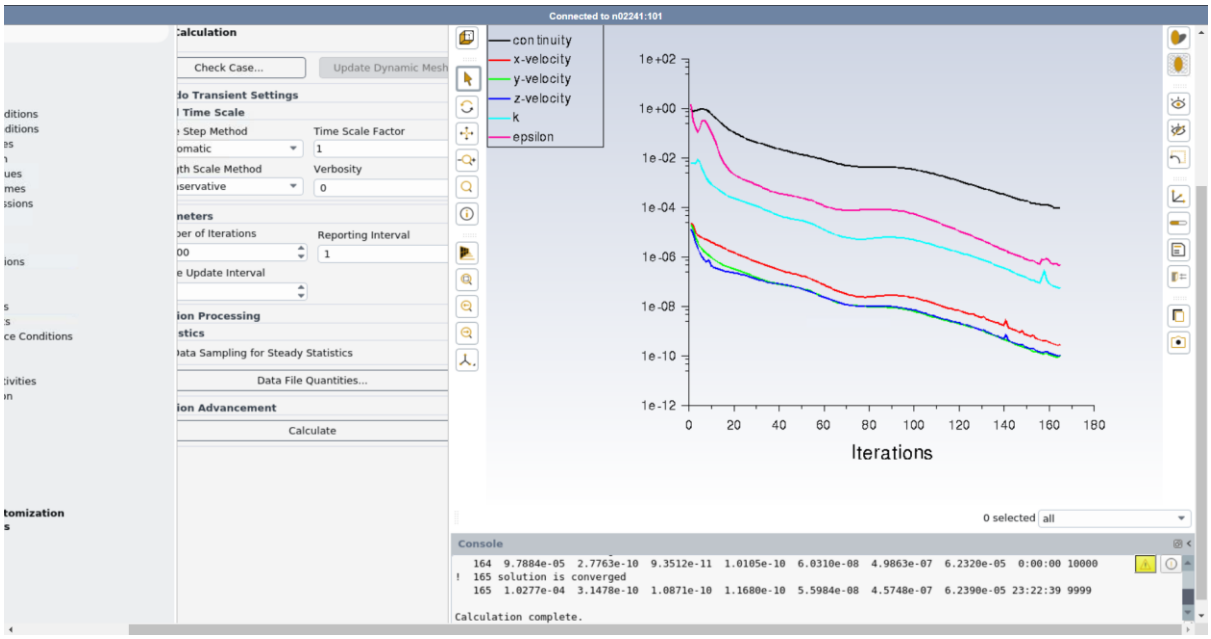

Nine buildings without opening around buildings and 1:2 opening ratio

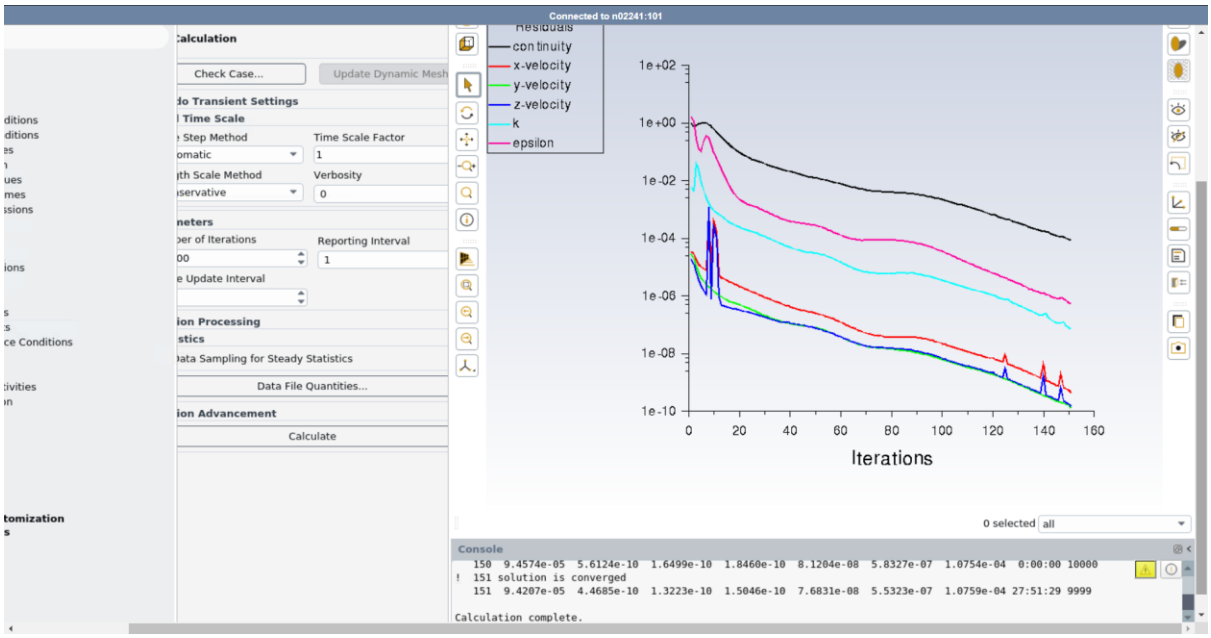

Nine buildings without opening around buildings and 1:4 opening ratio

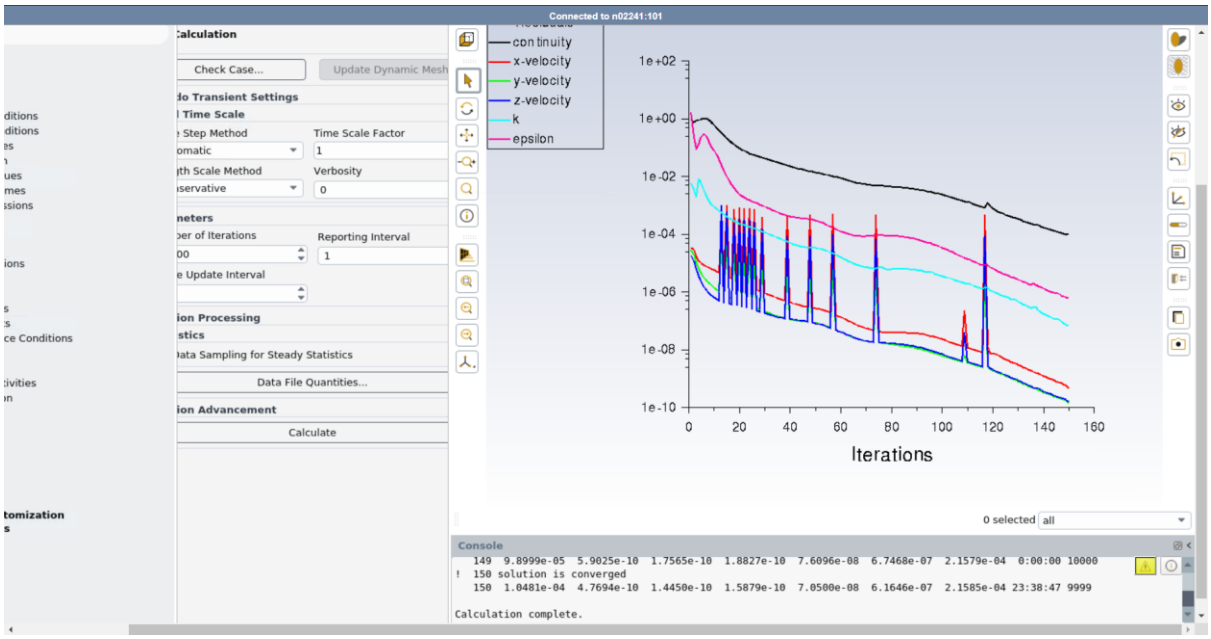

Appendix E: TURNITIN REPORT

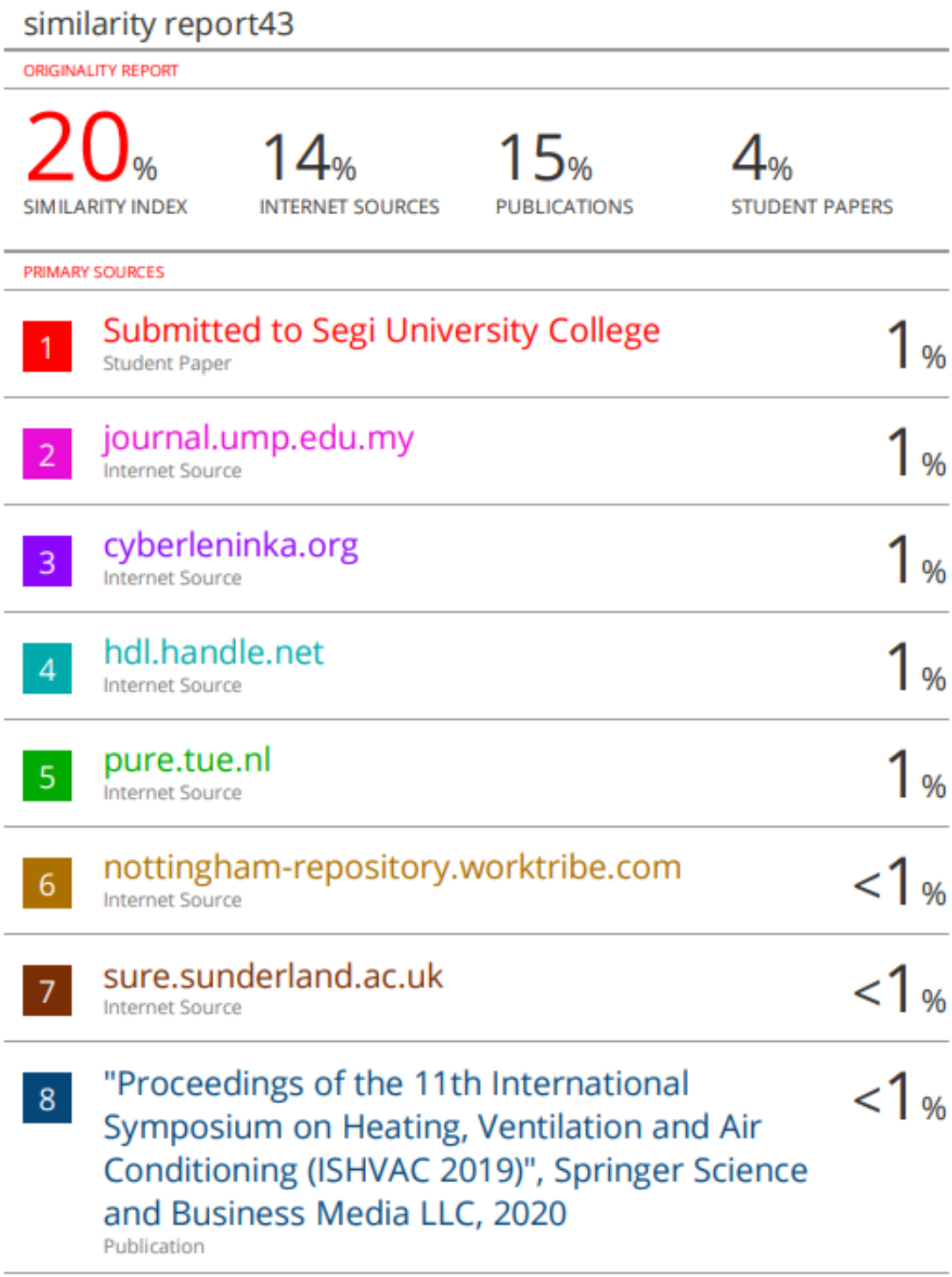

similarity report43

ORIGINALITY REPORT

20%	14%	15%	4%
SIMILARITY INDEX	INTERNET SOURCES	PUBLICATIONS	STUDENT PAPERS

PRIMARY SOURCES

1	Submitted to Segi University College Student Paper	1%
2	journal.ump.edu.my Internet Source	1%
3	cyberleninka.org Internet Source	1%
4	hdl.handle.net Internet Source	1%
5	pure.tue.nl Internet Source	1%
6	nottingham-repository.worktribe.com Internet Source	<1%
7	sure.sunderland.ac.uk Internet Source	<1%
8	"Proceedings of the 11th International Symposium on Heating, Ventilation and Air Conditioning (ISHVAC 2019)", Springer Science and Business Media LLC, 2020 Publication	<1%